



Cite this: *Chem. Soc. Rev.*, 2024, 53, 11165

Received 22nd May 2023

DOI: 10.1039/d3cs00238a

rsc.li/chem-soc-rev

## Enantioselective synthesis of molecules with multiple stereogenic elements

Arthur Gaucherand, Expédite Yen-Pon, Antoine Domain, Alix Bourhis, Jean Rodriguez and Damien Bonne \*

This review explores the fascinating world of molecules featuring multiple stereogenic elements, unraveling the different strategies designed over the years for their enantioselective synthesis. Specifically, (dynamic) kinetic resolutions, desymmetrisations and simultaneous installation of stereogenic elements exploiting either metal- or organo-catalysis are the principal approaches to efficiently create and control the three-dimensional shapes of these attractive molecules. Although most molecules presented in this review possess a stereogenic carbon atom in combination with a stereogenic axis, other combinations with helices or planes of chirality have started to emerge, as well as molecules displaying more than two different stereogenic elements.

## Introduction

In the complex field of three-dimensional molecular architectures, the presence of multiple stereogenic elements in a molecule significantly influences its biological and physical properties. Molecules adorned with multiple stereogenic elements have attracted attention from chemists for exploiting their specific three-dimensional form in several domains. A broad range of natural products bearing multiple stereogenic

elements,<sup>1</sup> such as diconophylline A,<sup>2</sup> vescalin,<sup>3</sup> cordypyridone A,<sup>4</sup> chaetochromin A,<sup>5</sup> and TMC-95 D,<sup>6</sup> often possess a stereogenic C–C bond and one or several stereogenic carbon atoms (Fig. 1). This structural feature is also found in synthetic pharmaceutical ingredients, for example, BI 224436, whose antiviral activity was greatly enhanced by the introduction of two stereogenic elements<sup>7</sup> or diazocanone **1** exhibiting excellent NK<sub>1</sub> antagonistic activities.<sup>8</sup> Sotorasib represents the first FDA-approved monotherapy to be manufactured and marketed as a configurationally stable C–N atropisomerically pure

Aix Marseille Univ, CNRS, Centrale Med, Marseille, ISM2, France



**Arthur Gaucherand**

Arthur Gaucherand studied general chemistry at CPE Lyon Engineering School (France). After spending a year as an exchange student at the Université de Montréal (Canada), where he specialised in organic chemistry, he obtained his master's degree in 2020. He then pursued a PhD at Aix-Marseille University (France), focusing on organocatalytic enantiocontrol of multiple stereogenic elements under the supervision of Prof.

Damien Bonne and Prof. Jean Rodriguez. Upon completing his PhD in 2023, he joined Prof. Jérôme Lacour's group at the University of Geneva (Switzerland) for postdoctoral training, where he is currently based. His research interests centre on the stereocontrol of novel chiral molecules.



**Expédite Yen-Pon**

Expédite Yen-Pon obtained her PhD in chemistry in 2016 working on kinase inhibitors with Dr Huixiong Chen (University Paris Cité). After her first postdoctoral experience in medicinal chemistry with Dr Samir Messaoudi (University Paris Saclay), she joined Dr Davide Audisio's group (CEA Saclay) to work on helicene synthesis. She then worked with Prof. Gary A. Molander (University of Pennsylvania) on photoredox chemistry. In 2022, she joined Aix-Marseille University to work with Prof. Damien Bonne and Prof. Jean Rodriguez on helicene enantioselective synthesis and, afterward, with Dr Yoann Coquerel on PAH preparation. Since 2023, she has been appointed as a CNRS researcher in the same team.

compound,<sup>9</sup> which demonstrated a ten-fold difference in potency against non-small-cell lung cancer.

These intriguing molecules are not only found in nature, but have also been designed for other applications such as ligands<sup>10</sup> and organocatalysts<sup>11</sup> for enantioselective catalysis or in materials science (Fig. 2).<sup>12</sup> In these applications, other combinations of stereogenic elements are found, notably with the incorporation of planar or helical systems.

For years, the most common methods for accessing these attractive molecules bearing multiple stereogenic elements have relied on diastereoselective synthesis, including cyclisation,<sup>13</sup> coupling,<sup>14</sup> rearrangement,<sup>15</sup> and C–H functionalisation,<sup>16</sup> but alternative methods have also been developed,<sup>17</sup> as well as post-functionalisations of optically active substrates.<sup>18</sup> The enantioselective synthesis of these molecules has remained a formidable challenge for several

years with sporadic examples,<sup>19</sup> but renewed interest has been witnessed in the last five years, which justifies this review.<sup>20,21</sup> Hence, we present the history of the development in this field based on the classification of strategies for the direct catalytic enantioselective construction of molecules containing multiple stereogenic elements in the atropoisomeric, planar, helicoidal, and allenic series. To access these attractive systems, various complementary strategies have been developed to date and are presented in five sections: (1) kinetic resolution, (2) dynamic kinetic resolution, (3) desymmetrisation, (4) simultaneous installation of stereogenic elements, and (5) enantioselective synthesis of axially chiral allenes bearing one additional stereogenic centre. Each section is organised based on the nature of the stereogenic elements present in the molecule and the catalytic activation involved in stereocontrol.



**Antoine Domain**

*Antoine Domain studied chemistry for his bachelor's degree at the University of Rennes and a master's degree in organic chemistry at Nantes-Université. After completing his studies, he began his PhD at Aix-Marseille Université under the direction of Pr. Damien Bonne and Pr. Jean Rodriguez. His research focuses on the development of new synthetic methodologies for the control of multiple stereogenic elements.*



**Alix Bourhis**

*Alix Bourhis studied general chemistry at ECPM Strasbourg Engineering School (France). During her final year at ECPM, she had the opportunity to participate in an exchange program at the Université de Sherbrooke (Canada), where she obtained a master's degree in 2022, specialising in organic and pharmaceutical chemistry. She is currently pursuing her academic studies as a PhD student at Aix-Marseille University (France), within the Stereo team of the ISM2 under Prof. Damien Bonne and Prof. Jean Rodriguez's supervision. Her research focuses on the atroposelective synthesis of benzopyrans.*



**Jean Rodriguez**

*Jean Rodriguez was born in Cieza (Spain) in 1958 and studied chemistry at the University of Aix-Marseille (France), he completed his PhD in 1987, and his Habilitation in 1992. He is currently Professor and was appointed Director of the UMR-CNRS-7313-iSm2 until December 2023. His research interests include the development of multiple bond-forming transformations and their application in stereoselective organo-*

*catalysed synthesis. In 2021 he was awarded the "Grand Prix Emile Jungfleisch" from the French Academy of Sciences.*



**Damien Bonne**

*Damien Bonne obtained his PhD in 2006 from the 'Institut de Chimie des Substances Naturelles' (ICSN) under the direction of Prof. Jieping Zhu working on multicomponent reactions. After a postdoc in the group of Prof. Varinder Aggarwal (Bristol), he was appointed Lecturer at Aix-Marseille University in 2007. He was promoted to Full Professor in 2022 and in 2023, he became "Junior Distinguished Member" of the French Chemical Society. His research focuses on the development of enantioselective methodologies for the control of axial and helical chiralities.*



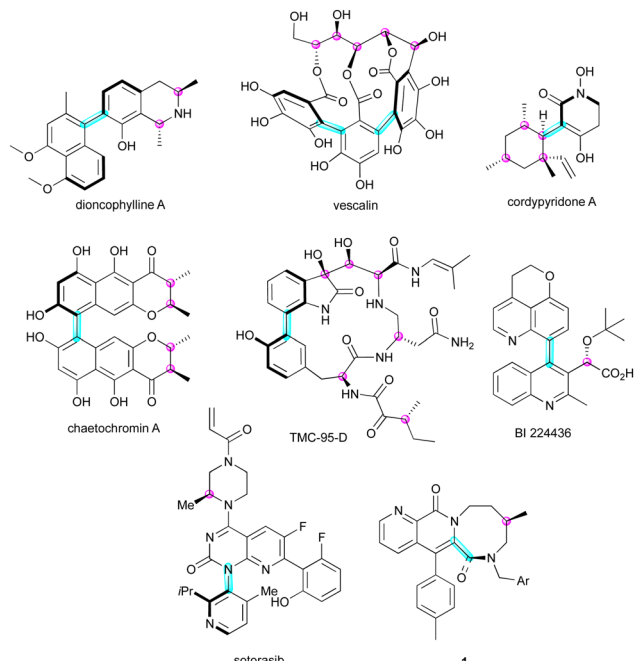


Fig. 1 Natural and non-natural products bearing multiple stereogenic elements.

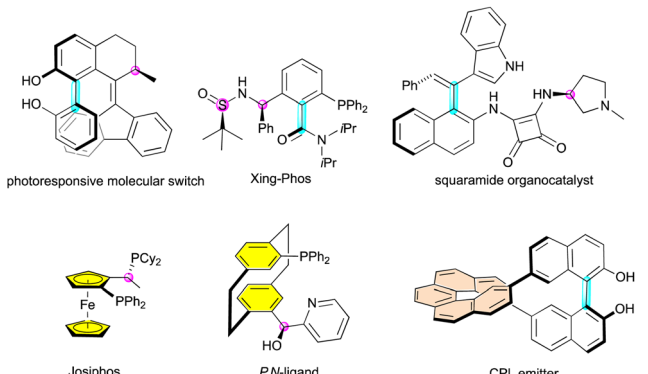


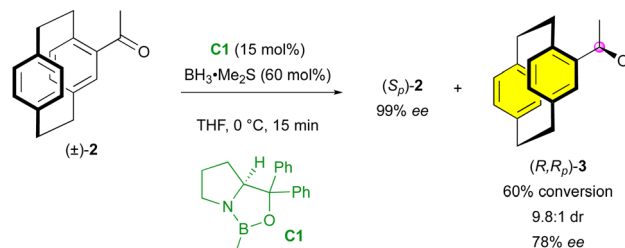
Fig. 2 Applications of multiple stereogenic element-containing molecules.

## Kinetic resolution

### Planar/central stereogenic elements

Among the possible strategies enabling the enantioselective synthesis of molecules bearing different stereogenic elements, kinetic resolution (KR) was the first to be used. Indeed, this technique allows for efficient deracemisation<sup>22</sup> and sometimes results in the formation of an additional stereogenic element with good diastereo- and enantioselectivities.

Interestingly, one of the first reported enantiocontrol of multiple stereogenic elements was done on a planar chiral paracyclophane using a kinetic resolution strategy. In 2001, Kagan and colleagues applied the Corey–Bakshi–Shibata reduction with **C1** as the catalyst to a racemic sample



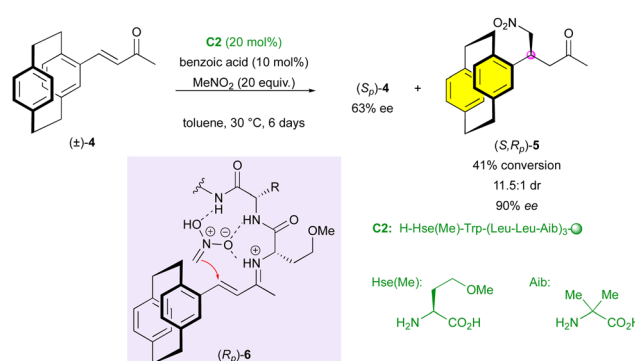
Scheme 1 KR of racemic 4-acetyl[2.2]paracyclophane.

of 4-acetyl[2.2]paracyclophane ( $\pm$ )-2, leading to the formation of the secondary benzylic alcohol ( $R,R_p$ )-3 with good stereoselectivity (9.8:1 dr and 78% ee), together with unreacted substrate ( $S$ )-2 in very high enantiopurity (Scheme 1).<sup>23</sup>

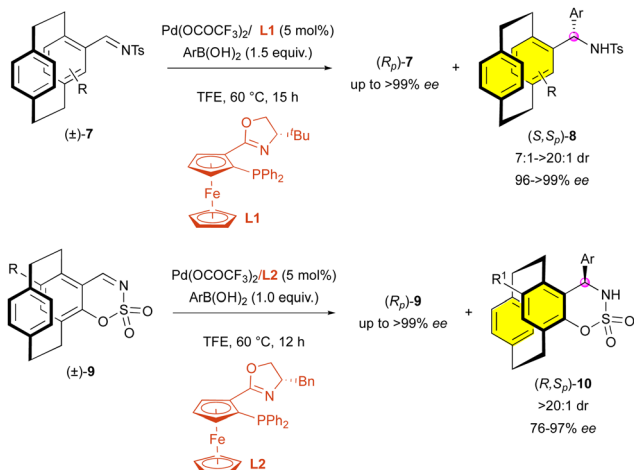
Fourteen years later, the Kudo group proposed the use of an artificial peptide for the enantioselective addition of nitromethane to conjugated ketone ( $\pm$ )-4 (Scheme 2).<sup>24</sup> The formation of a chiral iminium intermediate ( $R_p$ )-6 after the condensation of the catalyst on the ketone guided the addition of nitromethane *via* a hydrogen-bonding network. The stereo-defined structure of peptide catalyst **C2** resulted in the faster formation of ( $S,R_p$ )-5 with very good diastereoselectivity (11.5:1 dr) and high enantiomeric excess (90% ee).

Likewise, enantioselective addition has also been used recently by Zhou and collaborators for the KR of paracyclopheanes. In 2019, they developed the palladium-catalysed addition of arylboronic acids onto *N*-sulfonyl imines ( $\pm$ )-7 bearing planar chirality (Scheme 3).<sup>25</sup> The use of the planarly and centrally chiral ligand **L1** allows the synthesis of ( $S,S_p$ )-8 with good to high diastereoselectivity (7:1 to >20:1 dr) and excellent enantiocontrol (96% to 99% ee). Two years later, they applied their method to cyclic *N*-sulfonyl imines ( $\pm$ )-9 using a similar ligand **L2**.<sup>26</sup> Interestingly, when applied to these substrates, the reaction led to the formation of ( $R,S_p$ )-10 with always perfect diastereoselectivity (>20:1 dr), which is probably due to the rigid cyclic structure of the imine function, although the enantiomeric excess was slightly impacted (76% to 97% ee).

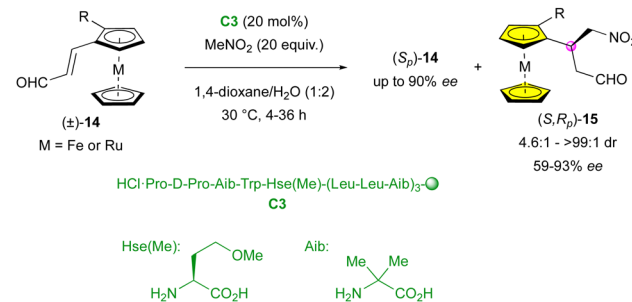
Although less examples exist, the enantioselective formation of a stereocentre for the KR of planar-chiral compounds has been applied to metallocenes as well. As early as 2009, Rios,



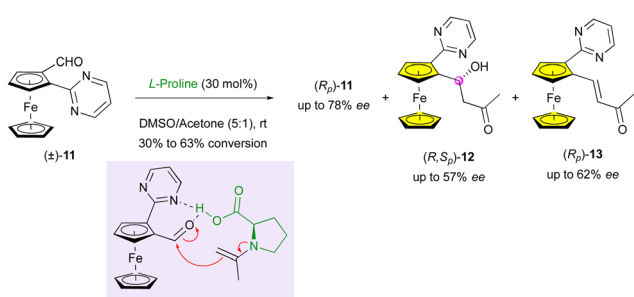
Scheme 2 KR via enantioselective Michael addition.



Scheme 3 Pd-Catalysed addition of arylboronic acids on planarly chiral N-sulfonyl imines.



Scheme 5 KR of metallocenes via organocatalysed enantioselective Michael addition.



Scheme 4 KR of ferrocenecarbaldehyde via aldolisation.

Moyano and coworkers performed the KR of ferrocenecarbaldehyde ( $\pm$ )-11 bearing a pyrimidine substituent (Scheme 4).<sup>27</sup> The L-proline-catalysed aldolisation with acetone resulted in the isolation of three different products, enantioenriched unreacted substrate ( $R_p$ )-11, target aldol adduct ( $R, S_p$ )-12 featuring planar and central chirality, and the corresponding dehydrated compound ( $R_p$ )-13. Although only moderate enantioselective excess and low yield (up to 57% ee with 15% yield and down to 38% ee with 26% yield) could be obtained, this simple approach constitutes the first remarkable example of this stereochemical combination.

In 2014, the Kudo group applied their peptide-catalysed enantioselective addition of nitromethane to planar-chiral metallocenes ( $\pm$ )-14, achieving efficient KR (Scheme 5).<sup>28</sup> Products ( $S, R_p$ )-15 displayed good to perfect diastereoselectivity (4.6:1 to  $>99:1$  dr) and modest to excellent enantiomeric excess (59% to 93% ee). As expected, the stereoselectivity was closely related to the conversion, where higher yields led to a decrease in the diastereo- and enantioselectivity. Interestingly, ruthenocene reacted faster than its ferrocene analogue, leading to a lower stereocontrol (49:1 dr, 92% ee and 36% yield for  $M = Fe$ ,  $R = I$  vs. 4.6:1 dr, 66% ee and 38% yield for  $M = Ru$ ,  $R = I$ ).

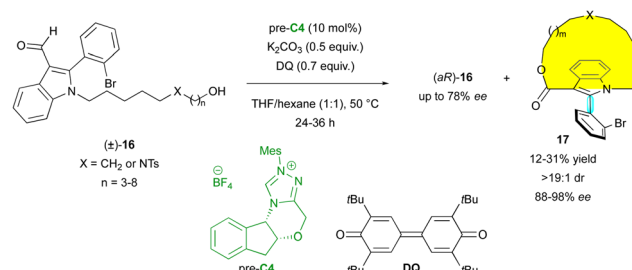
## Planar/axial stereogenic elements

Besides paracyclophanes and metallocenes, planar chirality can be observed in macrocycles. Thus, very recently, the Wang group proposed the original KR of axially chiral indoles ( $\pm$ )-16 via NHC-catalysed oxidative macrocyclisation with pre-catalyst C4 (Scheme 6).<sup>29</sup> Various sizes of macrocycles 17 could be obtained, always with excellent diastereoselectivity ( $>19:1$  dr) and enantioselectivity (88% to 98% ee), endowing ( $aR$ )-16 with moderate enantioselectivities. The planar configuration of the macrocycle was confirmed by X-ray diffraction analysis of a similar non-axially chiral compound, but the absolute configuration of the stereogenic axis was not determined.

## Central/axial stereogenic elements

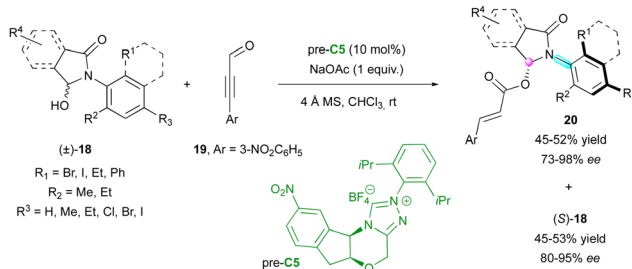
Among the methodologies developed for the enantioselective synthesis of molecules containing multiple stereogenic elements, the combination of a stereogenic centre with an axis is the most common. In this regard, in 2018, the Wang group described the catalytic KR of racemic anilide hemiaminals ( $\pm$ )-18 by an enantioselective NHC-catalysed acylation with propargylic aldehydes 19 involving pre-catalyst C5 (Scheme 7).<sup>30</sup> The resulting catalytic C–O bond formation provided C–N axially chiral isoindolinones 20 and allowed the separation of the two enantiomers of anilides giving ( $S$ )-18 efficiently in high yield with excellent enantioselectivity.

More recently, chiral NHC-catalysed (3+3) annulation was proposed by the Biju group for the KR of racemic *N*-aryl aminomaleimides 21 with 2-bromoaldehydes 22 to furnish C–N axially chiral fused-dihydropyridinones ( $M, S$ )-23 bearing a stereogenic centre and leaving the enantioenriched starting



Scheme 6 KR of axially chiral indoles via NHC-catalysed macrocyclisation.



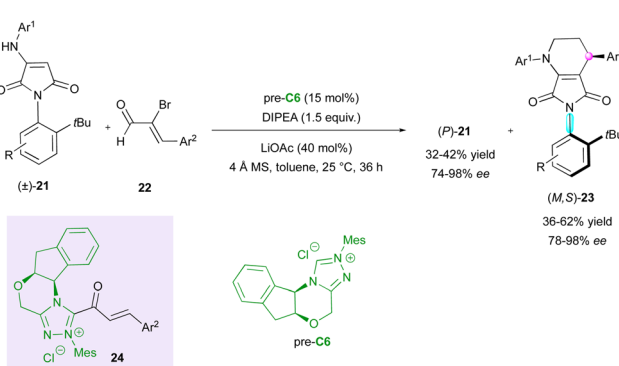


Scheme 7 KR of axially chiral anilides via enantioselective NHC-catalysed acylation.

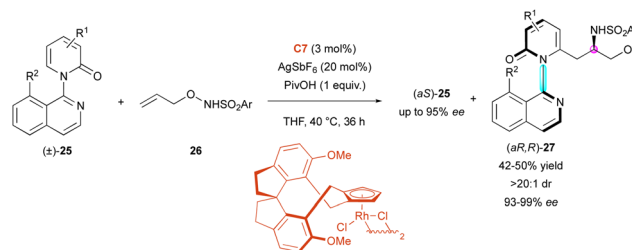
material (*P*)-21 (Scheme 8).<sup>31</sup> The observed remote chirality induction provided by pre-catalyst C6 was governed by the crucial bulky *t*-Bu group and the aminoindanol moiety of the  $\alpha,\beta$ -acylazolium intermediate 24, both imposing good facial diastereoselectivity, which resulted in good to excellent enantioselectivities but moderate diastereoselectivities.

Very recently, the Li group exploited the rhodium-catalysed C–H activation of pyridone rings for the KR of C–N axially chiral isoquinolines ( $\pm$ )-25. In this process, *N*-protected *O*-allylhydroxyamines 26, with Rh-catalyst C7, underwent enantio- and diastereoselective C–H carboamidation directed by the large 8-substituted isoquinolyl motif (Scheme 9).<sup>32</sup> The starting 2-pyridones 25 were efficiently resolved and the centrally and axially chiral amino alcohols (*aR,R*)-27 were obtained as one diastereomer with excellent enantiomeric excess (93% to 99% ee) and *s*-factor of up to >600, allowing the recovery of (*aS*)-25 with high enantiomeric excesses. Several sulfonyl substituents were tolerated; however, a bulky enough R<sup>2</sup> substituent was necessary to prevent free rotation around the C–N axis ( $\Delta G^\ddagger = 118$  kJ mol<sup>-1</sup> for R<sup>1</sup> = H, R<sup>2</sup> = Cl).

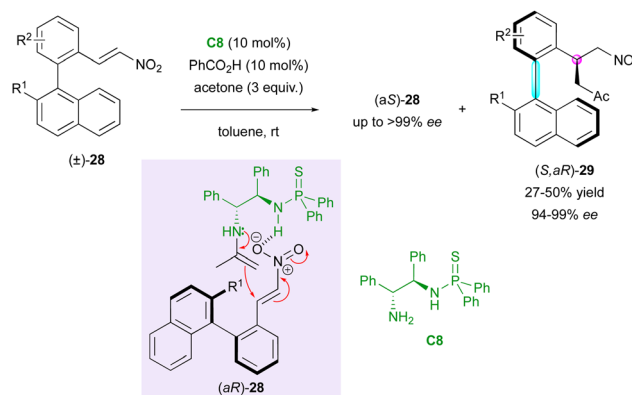
Concerning access to C–C axially chiral biaryls bearing a stereogenic centre, in 2019, the Li and Zhou group described the catalytic KR of axially chiral biaryl nitroalkenes ( $\pm$ )-28 via an enantioselective Michael addition upon enamine activation of acetone (Scheme 10).<sup>33</sup> This method relies on the hydrogen bond network established between the substrate and bifunctional thiophosphinamide catalyst C8 bearing a primary amine, which guides the addition of the chiral enamine intermediate. The reaction delivered molecules (*S,aR*)- (ok) with very high



Scheme 8 NHC-Catalysed (3+3) annulation.



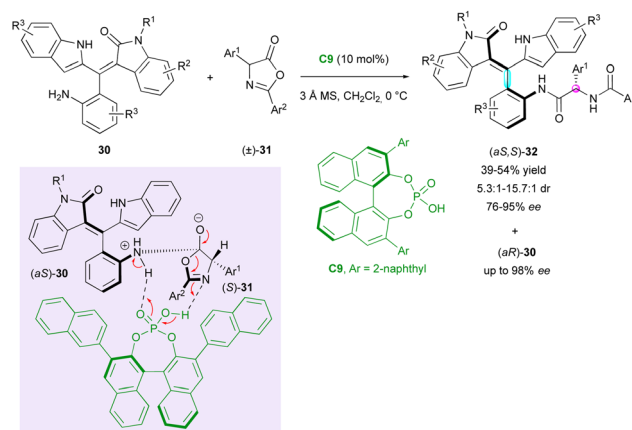
Scheme 9 Access to chiral amino alcohols via enantioselective carboamidation.



Scheme 10 Organocatalysed KR of axially chiral 2-nitrovinyl biaryls.

enantiomeric excess but poor diastereomeric ratio in most cases and enantioenriched starting material (*aS*)-28 was recovered with good selectivity. However, the diastereoselectivity of (*S,aR*)-29 could be enhanced in the presence of bulky R<sup>2</sup> substituents in the *ortho* position.

One year later, Zhang, Tan and Shi attempted the KR of the original non-biaryl atropisomers using chiral phosphoric acid catalyst (CPA) C9 (Scheme 11).<sup>34</sup> The CPA-catalysed enantioselective nucleophilic substitution of axially chiral anilines



Scheme 11 Atroposelective access to oxindole-based chiral styrenes via KR.

( $\pm$ )-30 on centrally chiral azalactones ( $\pm$ )-31 resulted in the formation of rare tetrasubstituted axially chiral styrene-type atropisomers (*as,S*)-32 bearing an additional stereocentre with good diastereoselectivity (5.3 : 1 to 15.7 : 1 dr) and high enantioselective excess (76% to 95% ee). Besides leaving highly enantioenriched starting anilines (*aR*)-30, the method resulted in the concomitant dynamic kinetic resolution of centrally chiral azalactones ( $\pm$ )-31, whose racemisation was fast under these reaction conditions.

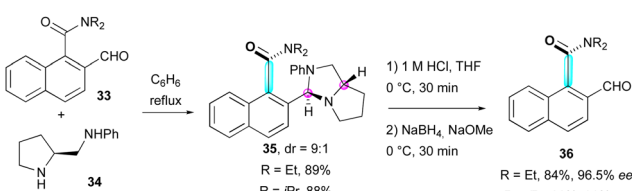
## Dynamic kinetic resolution

### Organocatalysed activation

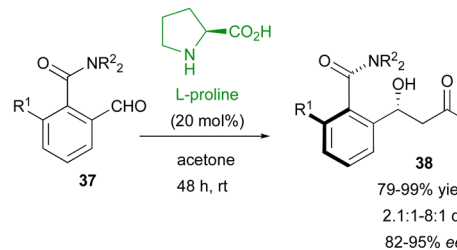
The inherent conformational flexibility of atropisomers makes them ideal substrates for dynamic kinetic resolution (DKR).<sup>35</sup> This was first exploited by Clayden and co-workers in 1999 for the synthesis of atropisomeric amides 36 by the dynamic resolution of *ortho*-formyl naphthamides 33<sup>36</sup> using enantio-pure proline-derived diamine 34 as a resolving agent *via* thermodynamic control during the formation of aminal intermediates 35 in a 9 : 1 diastereomeric ratio (Scheme 12).

Following this pioneer result, in 2004, the Walsh group reported the first example of the DKR strategy using an organocatalyst for the control of two different stereogenic elements (Scheme 13).<sup>37</sup> They proposed an efficient way to afford molecules 38 bearing both a stereodefined secondary alcohol and a stereogenic axis starting from 2-formylbenzamides 37 and using L-proline as the catalyst. Initially conducted in DMSO/acetone as the solvent, the reaction gave higher enantio- and diastereoselectivities using neat acetone. This strategy gave very good yields (up to >99%) and high enantiomeric excesses (up to 95%) but moderate diastereoselectivity (1.6 : 1 to 8 : 1). To account for the observed stereochemistry, transition state 40 should be less favorable than 39 as a result of the unfavorable interaction between the amide moiety and the axial hydrogen atom in the Zimmerman-Traxler six-membered chair-like transition state model.

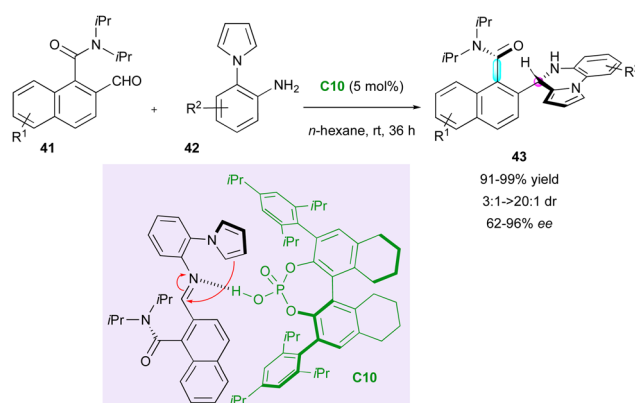
In 2020, capitalising on Clayden's aminal formation,<sup>35</sup> Hang, Zhang and Jiang performed an elegant enantioselective CPA-(C10)-catalysed aminocyclisation involving *ortho*-formyl 1-naphthamides 41 and pyrrolylanilines 42 (Scheme 14).<sup>38</sup> The control experiments showed that the catalyst plays a crucial role in the chiral recognition for each step of the sequence to organise a postulated transition state, which reasonably explains the observed stereoselectivity after the addition of the pyrrole to the intermediate imine. This putative synergy



Scheme 12 Dynamic resolution of atropisomeric amides.



Scheme 13 DKR of atropisomeric amides via enantioselective aldolisation.



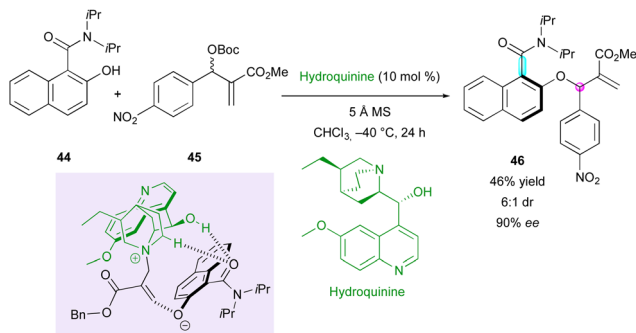
Scheme 14 CPA-Catalysed DKR of atropisomeric *o*-formyl naphthamides.

results in the efficient formation of axially and centrally chiral pyrrolopyrazines 43 in very good yield, excellent diastereoselectivity and enantiomeric excess in most cases.

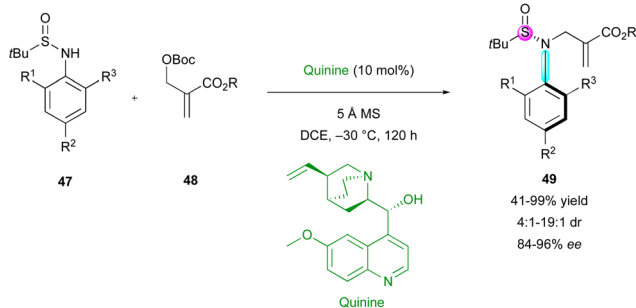
Shortly after, Li's group was interested in the atroposelective *O*-allylation of related *ortho*-hydroxy naphthamide 44 with Morita-Baylis-Hillman (MBH) adduct 45, employing hydroquinine as the catalyst and reported a single example of DKR with modest yield and diastereoselectivity with a decent enantioselective excess of 90% for product 46 (Scheme 15).<sup>39</sup> The catalyst interacts with the deprotonated naphthol through hydrogen bonding interactions and controls the stereoselectivity of the reaction.

The incorporation of a stereogenic atom other than carbon in the final structure is not a common feature and still constitutes a real synthetic challenge. In 2021, the same group proposed the related *N*-allylation of *N*-aryl sulfinamides 47 with MBH-adducts 48, employing quinine as the catalyst (Scheme 16).<sup>40</sup> They showed an unusual simultaneous control of a stereogenic sulfur atom and a C–N stereogenic axis. Although most of the examples exhibited moderate diastereoselectivity (4 : 1 to 9 : 1 dr), a few allylated sulfinamides 49 were





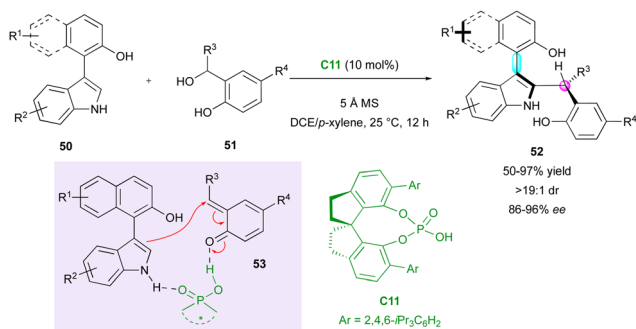
Scheme 15 DKR of *o*-hydroxy 1-naphthamide via atroposelective allylation.



Scheme 16 DKR of sulfinamides via atroposelective *N*-allylation.

obtained with very good diastereomeric ratio (dr > 19:1), always with excellent enantiocontrol.

The functionalisation of 3-substituted arylindoles has allowed the design of several organocatalysed DKR for the enantioselective synthesis of axially and centrally chiral indole-based heterocycles. The pioneering work was disclosed by Shi's group in 2019 who proposed the interesting enantioselective synthesis of naphthyl-indole atropisomers bearing a stereogenic centre (Scheme 17).<sup>41</sup> They achieved control of both stereogenic elements employing SPINOL-derivative catalyst C11. Initially, phosphoric acid reacts with the phenol derivatives 51, forming *ortho*-quinone methide (*o*-QM) intermediate 53. Subsequently, the CPA efficiently



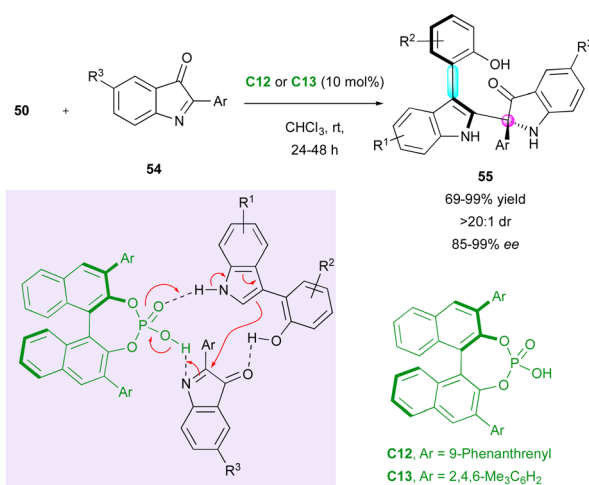
Scheme 17 DKR of naphthyl-indoles via atroposelective functionalisation with *o*-QM.

controls the stereoselectivity of the nucleophilic addition through hydrogen bond interactions with naphthyl-indole substrates 50 and delivers centrally chiral indole atropisomers 52 in high efficiency. Recently, this strategy was applied by the same group for the enantioselective diastereodivergent synthesis of 2-alkenylindoles bearing both axial and central stereogenic elements.<sup>42</sup>

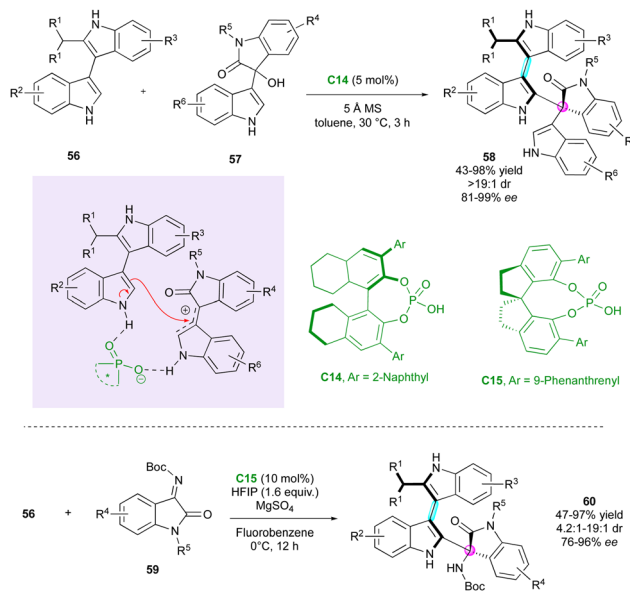
Following the pioneer work by Shi, Fu and co-workers applied the same strategy with 2-aryl-3*H*-indol-3-ones 54 as electrophiles for the direct synthesis of arylindolyl indolin-3-ones 55 with the creation and control of both a stereogenic axis and a quaternary stereogenic centre with good to excellent enantiomeric excess (Scheme 18).<sup>43</sup> The experimental evidence indicated the slight influence of the naphthyl-indole hydroxyl group of the starting 3-substituted arylindoles 50 on the enantioselectivity.

Concurrently, Shi's research group developed the first example of simultaneous control of a stereogenic axis between two indole nuclei and a stereogenic quaternary centre through the DKR strategy of 2-substituted 3,3'-bisindoles 56 (Scheme 19).<sup>44</sup> They selected BINOL-derivative C14 as the catalyst, enabling interaction with both substrates 56 and 57, while governing the reactivity and selectivity of the reaction. The diastereo- and enantioselectivity were excellent, affording complex tris-indole scaffolds 58, representing a rare example of two five-membered ring atropisomers. In 2020, the same group demonstrated the feasibility of the reaction with isatin-derived imines as electrophiles utilising SPINOL-derivative catalyst C15, which led to related atropisomeric bis-indoles 60 featuring a C–N stereogenic centre with very high stereoselectivities.<sup>45</sup>

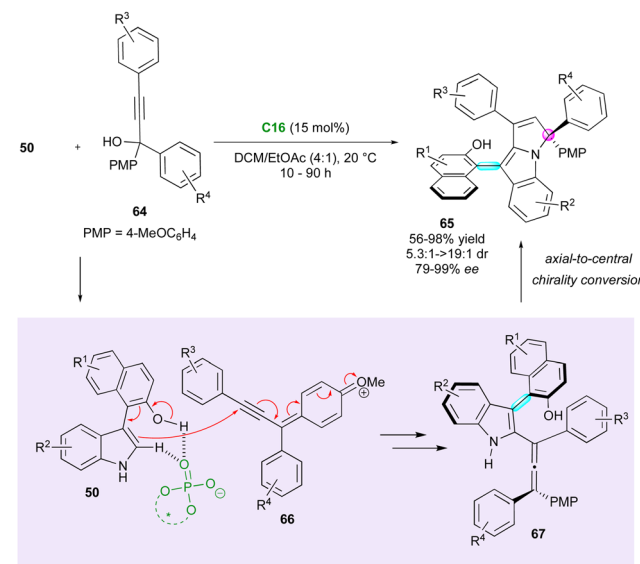
Shi, Tan and Ni applied their previous methodology for the enantioselective and diastereoselective synthesis of furan atropisomers 63 bearing an additional stereogenic carbon atom *via* the formal (4+2) cycloaddition between pro-atropisomeric 3-furan-indole scaffolds 61 and 2,3-indolylmethanols 62 (Scheme 20).<sup>46</sup> Under CPA organocatalysis with C16, the regioselective functionalisation of both nitrogen and C2 atoms of the



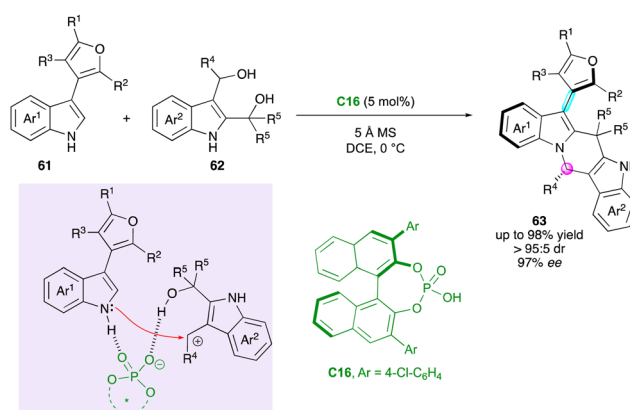
Scheme 18 Synthesis of arylindolyl indolin-3-ones with axial/central chiralities.



**Scheme 19** Enantioselective construction of axially chiral 3,3'-bisindole scaffolds.



**Scheme 21** Organocatalytic enantioselective (2+3) cyclisation for the synthesis of axially chiral arylpyrroloindoles.



**Scheme 20** Enantioselective synthesis of 3-furan-indoles with central and axial chirality.

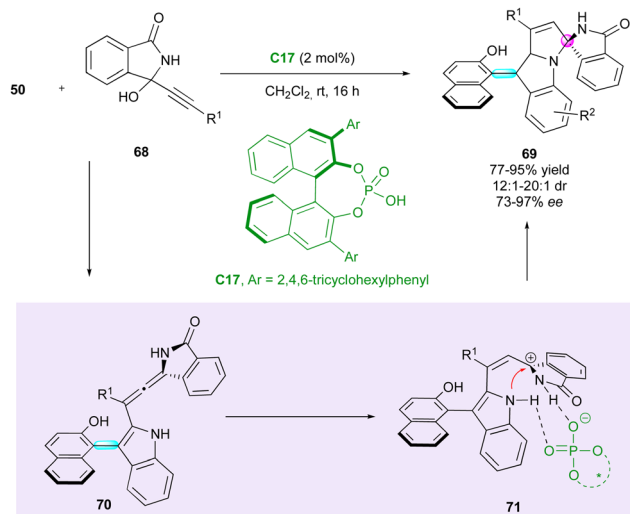
indole moiety resulted in a significant increase in the rotational barrier around the C–C bond, giving rise to desired products **63** with high barriers to diastereomerisation *via* the DKR process. The synthesis of furan atropisomers is a great challenge, as attested by the availability of only a few methods,<sup>47</sup> which makes the present work significant. Many examples have been realised with constant good enantio- and diastereoselectivities. In addition, several useful post-functionalisations and deep study on the reaction mechanism were provided, allowing a clear explanation of the enantioselectivity as well as the uncommon regioselectivity observed for this type of cycloaddition.

Axially chiral allenes can be considered as crucial intermediates controlling the diastereo- and enantioselectivity during the formation of centrally and axially chiral compounds. In 2023,

Jiao, Tan and Shi presented a notable example of this strategy, wherein an elegant DKR approach was employed to create arylpyrroloindoles **65** bearing both a stereogenic axis and a quaternary stereocentre (Scheme 21).<sup>48</sup> CPA **C16** involved in the reaction governs both the stereochemistry and regioselectivity. The catalyst activates the OH and NH groups of arylindoles **50** and triggers the formation of key *p*-quinone methide cations **66**, resulting in the generation of reactive chiral allene intermediates **67**. Subsequent protonation of the allene function by the CPA and trapping by the nitrogen atom of indole, with axial-to-central conversion of chirality, finalised the overall (2+3) cycloaddition to fused tricyclic atropisomers **65**. This methodology afforded good to excellent diastereoselectivity and moderate to excellent enantioselectivity. However, a slight limitation reported is the required presence of a *p*-methoxyphenyl substituent (PMP) to generate the key *p*-quinone methide cation intermediate.

Shortly after, Li, Dong and Li reported a related approach for enantioselective access to indolyl-pyrroloindoles **69** bearing both axial and spiro-central chirality (Scheme 22).<sup>49</sup> This (3+2) cycloaddition between arylindoles **50** and propargylic alcohols **68** was catalysed by CPA **C17**, albeit requiring a lower catalytic loading (2 mol%). Notably, the diastereoselectivity exhibited moderate improvements for specific products compared with previous work. It is imperative to note that the presence of an *R*<sup>1</sup> aryl group plays a crucial role in governing the enantioselectivity. Indeed, the introduction of a cyclopropyl group resulted in the formation of racemic product **69**. From a mechanistic point of view, dehydration of **68** gave a *N*-acyl propargylic imine, which underwent enantioselective 1,4-addition with **50**, giving rise to enantioenriched chiral allene intermediate **70**. Protonation of the latter led to cationic intermediate **71** and subsequent diastereoselective intramolecular annulation furnished the desired product **69**.

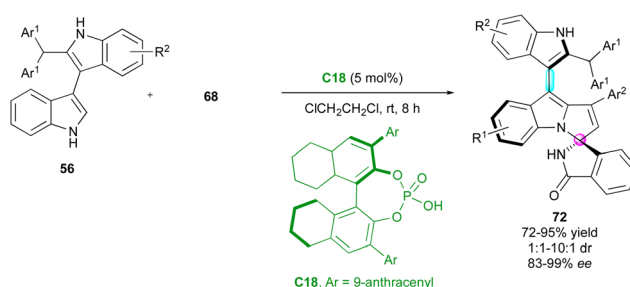




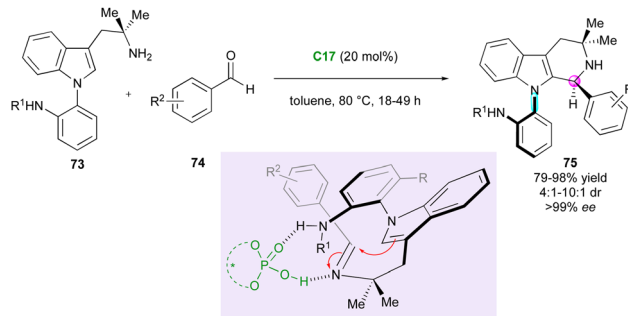
Scheme 22 Enantioselective synthesis of axially/centrally chiral indolyl-pyrroloindoles.

The last closely related example of this spiroannulation strategy was published by Zhang, Shi and co-workers (Scheme 23).<sup>50</sup> This challenging regio-, diastereo- and enantioselective cycloaddition involved 2-substituted 3,3'-bisindoles 56 and isoindolinone-based propargylic alcohols 68 catalysed by CPA C18. In comparison with the precedent examples, the final bisindolyl-pyrroloindoles 72 exhibited lower diastereomeric ratios but with consistently excellent enantiomeric excesses.

Axially chiral C–N atropisomers featuring a five-membered ring are not commonly encountered in the literature and still constitute a challenging synthetic target. In 2021, Kwon's group published the first enantio- and atroposelective Pictet–Spengler reaction of pro-atropisomeric amino-functionalised *N*-aryl indoles 73 and benzaldehydes 74 involving a CPA-(C17)-organocatalysed DKR strategy (Scheme 24).<sup>51</sup> Although the diastereoselectivity was moderate to good, the enantiomeric excesses were excellent despite the high temperature of the condensation, highlighting the strong configurational stability of the obtained axially and centrally chiral *N*-aryl-tetra-hydro- $\beta$ -carbolines 75. The presence of a secondary amine in the *ortho* position of the *N*-aryl substituent of 73 was crucial for the stereocontrol due to the hydrogen-bond interactions with the CPA catalyst. Moreover, reactivity was only observed when electron-withdrawing groups were introduced on



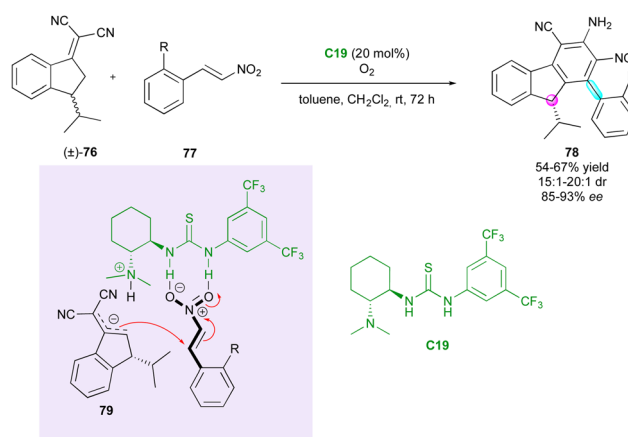
Scheme 23 Enantioselective synthesis of bisindolyl-pyrroloindoles.



Scheme 24 CPA-Catalysed atroposelective Pictet–Spengler reaction.

benzaldehydes 74 ( $\text{R}^2 = \text{CN, CF}_3, \text{NO}_2$ ). The same group exploited this approach using related indoles bearing an *o*-amidoaryl group on the N-1, C-2 or C-3 positions, which underwent efficient DKR under CPA catalysis with bulky electrophiles, yielding valuable C–N indole atropisomers with central chirality.<sup>52</sup>

To date, all the DKR strategies reported in this review were centred on the resolution of pro-axially chiral substrates with low barriers to enantiomerisation. However, in 2020, Chen and Chen demonstrated an interesting complementary extension to racemic centrally chiral compounds *via* remote vinylogous DKR. They reported an original cascade catalysed by Takemoto thiourea C19 between chiral indenylidene malononitrile ( $\pm$ )-76 and *ortho*-substituted  $\beta$ -nitrostyrenes 77, simultaneously governing the configuration of a stereogenic axis and a stereocentre (Scheme 25).<sup>53</sup> The racemisation of ( $\pm$ )-76 relies on a fast reversible deprotonation–protonation process at the benzylic position, and both the diastereomeric ratio and the enantiomeric excess are controlled during the Michael addition of chiral vinylogous nucleophilic intermediate 79. Subsequently, the stereogenic axis is formed in the final oxidative aromatisation under an oxygen atmosphere through a central-to-axial chirality conversion. However, although this strategy is efficient in terms of diastereo- and enantiocontrol and elegant in the construction of diverse stereogenic elements, the presence of



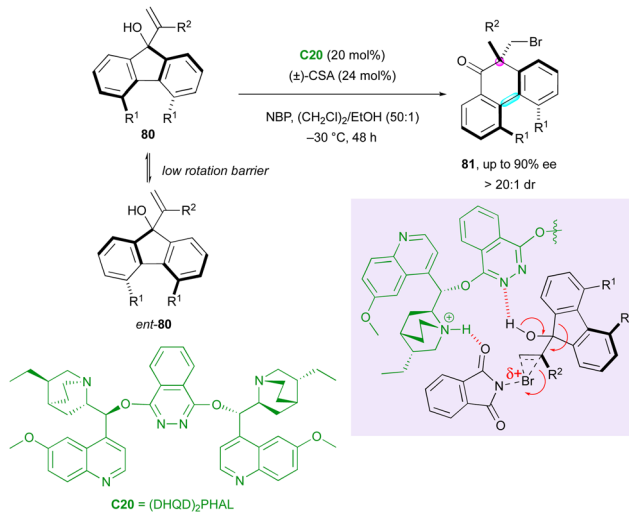
Scheme 25 Synthesis of enantioenriched 9H-fluorenes scaffolds *via* vinylogous DKR.

the strongly electron-withdrawing  $\alpha,\alpha$ -dicyanoolefin motif is required to perform the DKR strategy.

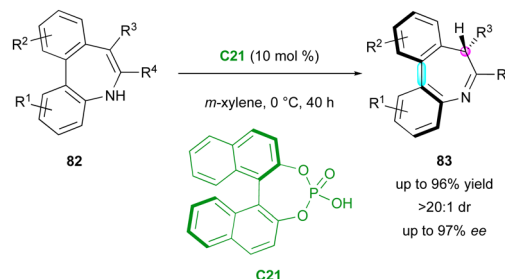
Recently, chiral bridged biaryls have attracted interest from synthetic chemists due to their numerous applications<sup>54</sup> but their enantioselective synthesis is a still significant challenge. An initial contribution in this direction was reported by the Yeung group in 2017, describing access to a rare family of axially and centrally chiral six-membered ring fused biaryls *via* an organocatalytic enantioselective DKR-semipinacol rearrangement (Scheme 26).<sup>55</sup> Racemic fluorenols **80** underwent ring expansion to form brominated axially and centrally chiral 9,10-dihydrophenanthrenes **81** with a central-to-axial conversion of chirality triggered by *N*-bromophthalimide (NBP) in the presence of  $(DHQD)_2PHAL$  **C20** as a chiral catalyst. The addition of racemic camphor sulfonic acid provided an appreciable improvement in the enantioselectivity and excellent diastereoselectivity.

The plausible mechanism based on the configurationally labile starting fluorenols with a low barrier to racemisation relies on the possible activation of NBP by the protonated quinuclidine core during the formation of the bromonium intermediate, while the basic nitrogen of the phthalazine can deprotonate the tertiary alcohol of the substrate, triggering the semipinacol rearrangement.

Another pioneering contribution was reported by the Luan group in 2018, with the first example of the catalytic enantioselective tautomerisation of structurally labile but isolable enamines to access to chiral imines (Scheme 27).<sup>56</sup> Kinetically stable pro-axially chiral enamine-based dibenz[b,d]azepines **82** were tautomerised by simple chiral BINOL-phosphoric acid **C21**, which offered a range of seven-membered imine products **83** featuring both central and axial stereogenic elements, achieving good yields (up to 96%) with excellent enantioselectivity and diastereoselectivity (up to 97% ee,  $>20:1$  dr). This highly atom-economical process is a rare example of converting one class of kinetically stable enols or enols equivalents into



Scheme 26 Semipinacol rearrangement to centrally and axially chiral biaryls.

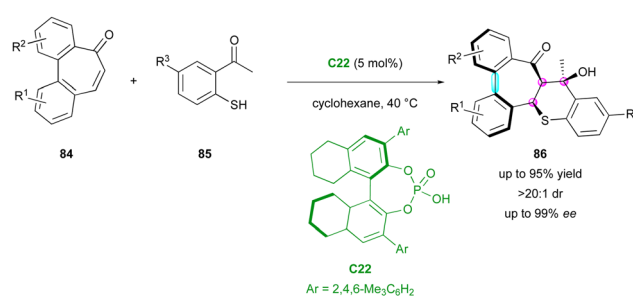


Scheme 27 Catalytic enantioselective tautomerisation of enamines.

their enantioenriched keto tautomers through an enantioselective tautomerisation strategy.

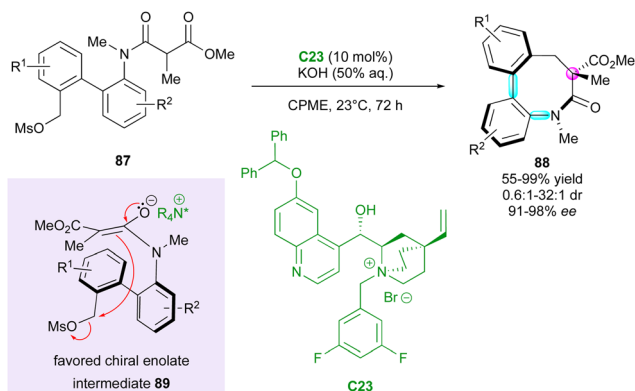
More recently, the Luo and Zhao group reported an example of enantioselective domino thia-Michael/aldol reaction, simultaneously controlling the formation of three stereogenic centres and one stereogenic axis starting from pro-axially chiral seven-membered ring bridged biaryl ketones **84** as Michael acceptors and 2-mercaptoacetophenones **85** as thia-nucleophiles (Scheme 28).<sup>57</sup> Among the different catalysts, the optimal conditions were found with CPA **C22** in cyclohexane, directing both the enantio-determining thia-Michael addition and the following diastereoselective aldol reaction by its dual ability to be a hydrogen bond donor and acceptor. The resulting multi-chiral thiochromene-fused dibenzoannuleneone derivatives **86** were obtained with excellent yield, enantio- and diastereoselectivity (up to 95% yield, up to 99% ee,  $>20:1$  dr). DFT calculations gave an energy difference of 9.1 kcal mol<sup>-1</sup> between the two possible atropodiastereomers, in perfect agreement with the constantly high diastereoselectivity observed.

Smith and coworkers reported the unique and elegant enantioconvergent counterion-directed cyclisation of racemic biaryl anilides **87** under phase-transfer catalysis (PTC), allowing the formation of multi-chiral eight-membered ring lactams **88** (Scheme 29).<sup>58</sup> Although starting anilides **87** existed as a complex mixture of enantiomers and diastereomeric conformers due to the presence of multiple axes of restricted rotation and a stereogenic centre, chiral ammonium salt catalyst **C23** could differentiate between a complex and rapidly equilibrating *in situ*-formed mixture of enolates and rotational isomers. The overall dynamic and enantioconvergent process allowed the highly enantioselective alkylative ring closure from favored



Scheme 28 Enantioselective thia-Michael/aldol for simultaneous stereogenic centres and chiral axis formation.



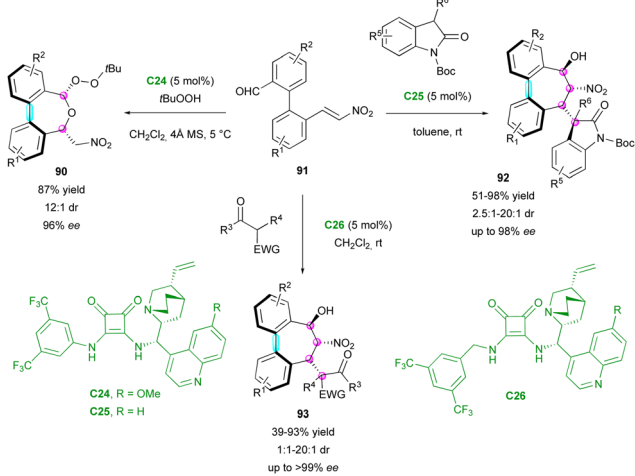


**Scheme 29** PTC for enantioconvergent synthesis of bis-axially and centrally chiral medium-sized lactams.

chiral enolates **89**, with efficient control of three stereogenic elements including an all-carbon quaternary centre and a two-axis (C–C and C–N) system by virtue of the *N*-aryl and biaryl bonds.

Interestingly, the fused biaryl lactam products **88** adopt a deep bowl-like arrangement with a torsion angle of about 60° and a measured barrier to diastereomerisation (bowl inversion) of 124.1 kJ mol<sup>-1</sup>, meaning that the bowl inversion does not occur at room temperature.

In complement, the Chauhan group simultaneously reported an enantioselective organocatalytic process to obtain various seven-membered ring bridged biaryls, containing one chiral axis and up to four stereogenic centres (Scheme 30).<sup>59</sup> This challenging process is based on a stereoselective domino 1,4/1,2 addition or 1,2/oxa-Michael addition, depending on the nucleophile class. Due to squaramide catalysts **C24**–**C26**, simple pro-stereogenic biaryl substrates **91** could react with different nucleophiles, such as *tert*-butylhydroperoxyde, 3-substituted 2-oxindoles and substituted 1,3-dicarbonyls, giving the corresponding products **90**, **92** and **93**, respectively. After the optimisation of the conditions for these three classes of



**Scheme 30** Enantioselective synthesis of seven-membered ring bridged biaryls via nucleophile-dependent switchable domino process.

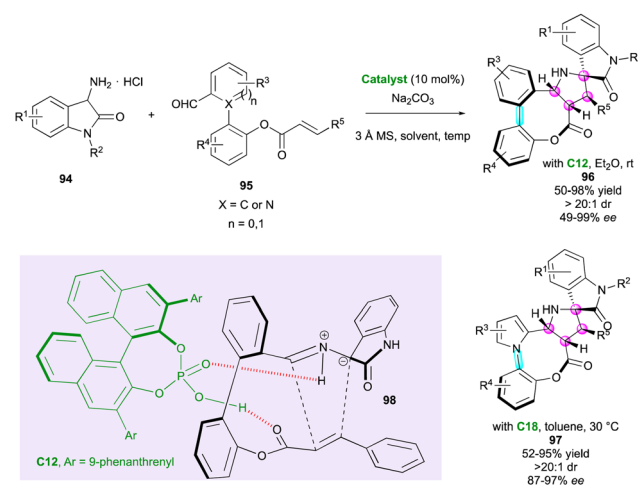
nucleophiles, the reaction scope was investigated. Only rare examples did not provide the corresponding product with good stereoselectivity, while a broad range of substrates could be employed, giving good yield (39–98%) with high enantio- and diastereoselectivity (1:1 to 20:1 dr, up to >99% ee).

Very recently, pro-stereogenic biaryl aldehydes **95** were ingeniously used by Wang and co-workers in combination with amino oxindoles **94** for the *atropo*- and highly diastereoselective synthesis of eight-membered bridged (hetero)biaryl lactones fused to spiro pyrrolidine-oxindole derivatives **96** and **97** (Scheme 31).<sup>60</sup> Depending on the structure of starting substrate **95** (X = C or N), these complex molecular architectures displayed either a C–C and C–N stereogenic axis and four contiguous stereocentres. The high degree of diastereococontrol was due to the stereospecificity and stereoselectivity of intramolecular (3+2) cycloaddition involving azomethine intermediate **98** together with the tendency of eight-membered bridged biaryls to form a stable boat conformation. In addition, CPA catalyst **C12** or **C18** activated both the ester moiety and the 1,3-dipole through hydrogen-bonds, delivering the final products **96** or **97**, respectively, with high levels of stereocontrol.

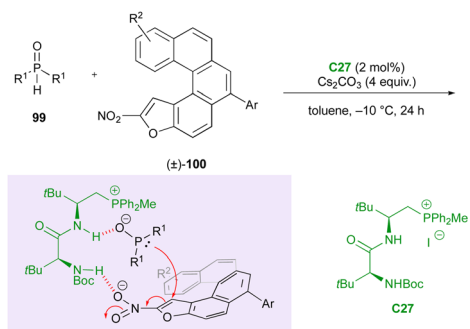
Finally, in 2023, Wang's group published an interesting approach for the simultaneous control of central and helicoidal stereogenic elements through a DKR strategy involving conformationally labile oxa[5]nitro helicenes ( $\pm$ )-**100** as Michael acceptors towards various phosphine oxides **99** (Scheme 32).<sup>61</sup> The phospha-Michael addition was catalysed by peptide phosphonium salt **C27** interacting with both substrates through a hydrogen bonding network and ionic interactions. This innovative methodology enabled the synthesis of various phosphorus-containing hetero helicenoid structures **101** with excellent diastereoselectivity and good to excellent enantioselective excess.

### Metal-catalysed activation

Besides organocatalysed methodologies, the DKR strategy for accessing molecules bearing multiple stereogenic elements can



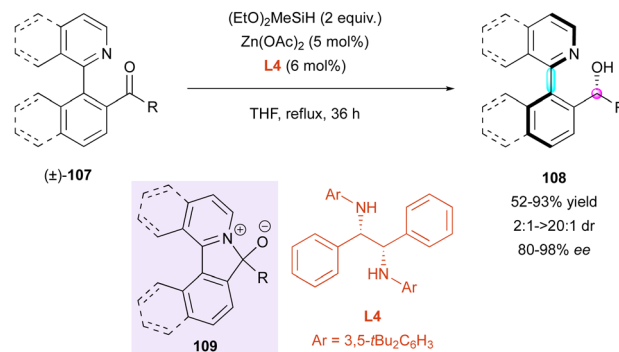
**Scheme 31** Atroposelective intramolecular (3+2) cycloaddition to eight-membered bridged (hetero)biaryls.



Scheme 32 DKR for the enantioselective synthesis of *P*-containing helicenoids.

also be efficient using transition metal catalysis. In this regard, in 2018, the Fernández and Lassaletta group published a series of works on the DKR of N-heterobiaryls. Their first proposal dealt with a palladium-catalysed atroposelective Heck reaction with chiral BINAP-type ligand **L3** of a variety of quinoline, quinazoline, phthalazine, and picoline sulfonate derivatives **102** with 2,3-dihydrofuran **103** ( $Z = O$ ) and N-Boc protected 2,3-dihydropyrrole **103** ( $Z = \text{NBoc}$ ) (Scheme 33).<sup>62</sup> From a mechanistic point of view corroborated by experimental observations and DFT studies, after oxidative addition, the formation of five-membered cationic palladacycle **106** is essential for reactivity. Then, the following insertion/β-elimination sequence leads to the major axially and centrally chiral olefins **104** together with the corresponding isomerised olefins **105** with good selectivity ratios, ranging from 6:1 to >20:1, for dihydrofurans **104/105** ( $Z = O$ ), while dihydropyrroles **104/105** ( $Z = \text{NBoc}$ ) were obtained with slightly lower selectivity from 3:1 to 6:1.

Another complementary DKR approach by the same group concerns the enantioselective reduction of racemic configurationally labile heterobiaryl ketones  $(\pm)$ -**107** (Scheme 34). Thus, they developed a zinc-catalysed enantioselective hydro-silylation with chiral diamine ligand **L4**, leading to axially and centrally chiral N-heterocycles **108** with moderate to excellent

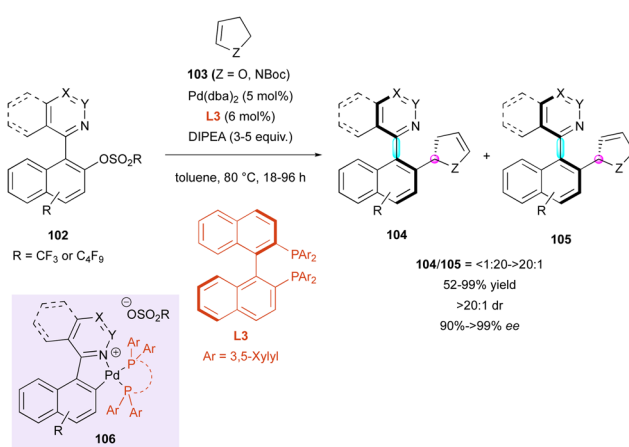


Scheme 34 Zn-Catalysed enantioselective hydro-silylation.

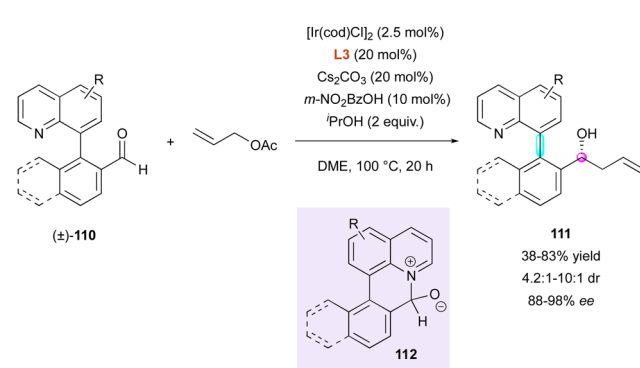
diastereoselectivity (2:1 to >20:1 dr) and very good enantioselectivity (80% to 98% ee).<sup>63</sup> This strategy is based on racemisation by a ring-closing/ring-opening event through a transient intramolecular Lewis acid–base interaction, resulting in five-membered ring cyclic intermediate **109**. Intriguingly, perfect diastereoselectivity was observed in the case of the sterically challenging ketone (dr >20:1 for  $R = \text{CH}_2t\text{Bu}$ ), albeit with lower enantioselectivity (80% ee) and yield (52%). Unfortunately, beside this example, the diastereoselectivities were moderate (up to 8.5:1 dr), but with consistently high enantioselectivities (>90% ee).

Recently, this group applied their precedent ring-closing/ring-opening strategy<sup>61</sup> through transient Lewis acid–base interaction to very similar substrates  $(\pm)$ -**110**, forming six-membered ring intermediate **112** (Scheme 35). In that respect, aldehydes **110** could undergo enantioselective iridium-catalysed transfer hydrogenative allylation, leading to the formation of centrally and axially chiral homoallylic alcohols **111** with good diastereoselectivity (4.2:1 to 10:1 dr) and excellent enantioselectivity (88% to 98% ee).<sup>64</sup> Although no value was given, supposedly high rotational barrier of products **111** allowed the reaction to be performed at high temperature (100 °C, 20 h) without any reduction in the stereoselectivity.

Simultaneously, the same group proposed a closely related transient Lewis acid–base interaction for the DKR of configurationally labile 3-thioaryl indole-2-carbaldehydes  $(\pm)$ -**113** (Scheme 36).<sup>65</sup> This method exploited the reactivity of chiral

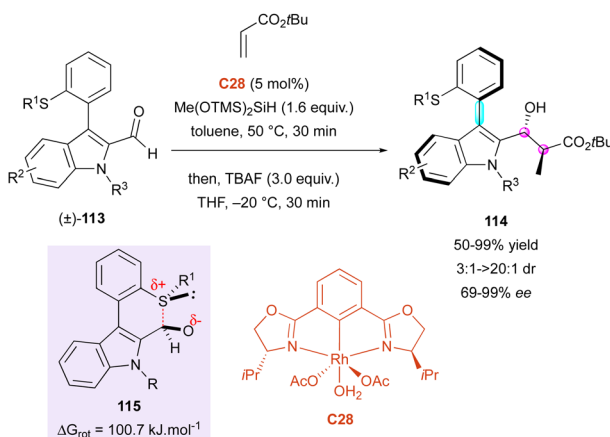


Scheme 33 DKR via Pd-catalysed atroposelective Heck reaction.



Scheme 35 Ir-Catalysed transfer hydrogenative allylation.



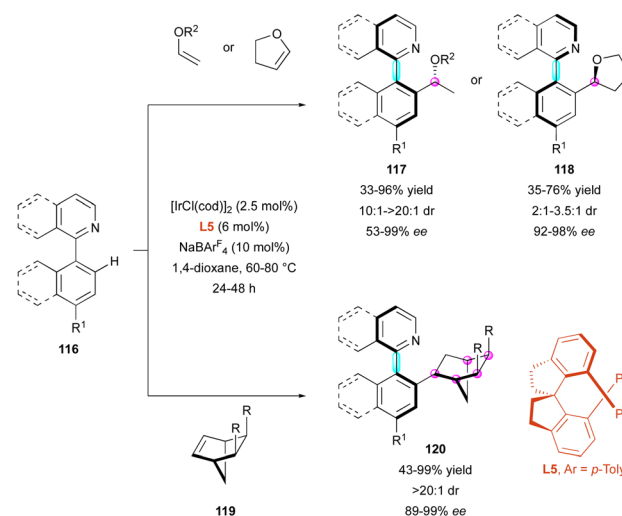


Scheme 36 Rh-Catalysed reductive aldol reaction.

bis-oxazoline rhodium-complex **C29** as the catalyst in a reductive aldol reaction with simple acrylates, simultaneously creating two adjacent stereocentres together with the stereogenic axis on products **114** with uniformly very high enantiomeric excesses (87% to 99% ee). In this case, the DFT computational studies were consistent with a racemisation process involving 2*H*-thiopyran transition-state **115** with a barrier to enantiomerisation of 100.7 kJ mol<sup>-1</sup>, in total agreement with a possible DKR at ambient temperature and above. It is worth noting that good diastereoselectivity was observed for R<sup>1</sup> = Me (3 : 1 to > 20 : 1 dr), whereas perfect diastereoselectivity was achieved for R<sup>1</sup> = Et or Bn (> 20 : 1 dr). Interestingly, *n*-butyl acrylate could be used instead of *tert*-butyl acrylate, albeit with moderate enantioselectivity (69% ee for R<sup>1</sup> = Me, R<sup>2</sup> = H, R<sup>3</sup> = Bn).

Another strategy to functionalize pro-axially chiral substrates is to develop C–H functionalisation close to the stereogenic axis, which delivers atropostable products *via* DKR. In this case, the Fernández and Lassaletta group developed the Ir-catalysed atroposelective C–H functionalisation of pro-axially chiral heterobiaryls **116** *via* the hydroarylation of acyclic vinyl ethers and bicycloalkenes **119** (Scheme 37).<sup>66</sup> In the presence of chiral diphosphine ligand **L5**, simple vinyl ethers gave complete branched/linear selectivity, leading to axially and centrally chiral heterobiaryls **117** with excellent diastereomeric ratio and high enantioselectivity. In contrast, 2,3-dihydrofuran gave the opposite configuration and the corresponding hydroarylated derivatives **118** were obtained with high enantioselectivity but moderate diastereoselectivity (dr from 2 : 1 to 3.5 : 1). In fact, the diastereoselectivity seemed to be closely related to the steric hindrance of the ether, as also shown by the relatively lower diastereomeric ratio of ethyl vinyl ether (dr < 15 : 1 for R<sup>2</sup> = Et) compared to all others (dr > 20 : 1). Alternatively, the use of prochiral norbornene substrates **119** led to a double desymmetrisation process, leading to hydroarylated heterocyclic systems **120** with perfect control of up to five stereogenic carbon atoms and a stereogenic axis in high yields with excellent enantioselectivity.

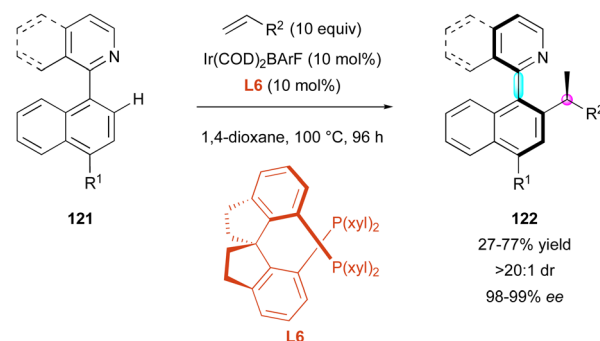
Similarly, the Xing group exploited the aforementioned Ir-catalysed atroposelective C–H functionalisation to broaden



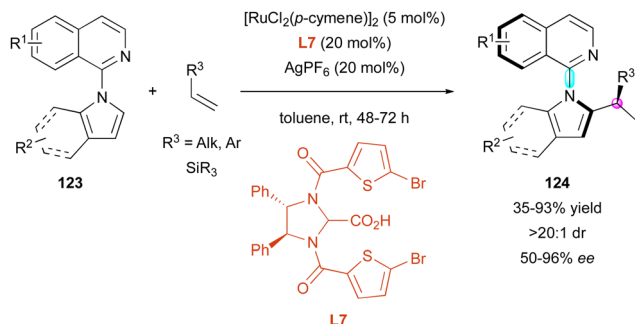
Scheme 37 DKR of heterobiaryls via Ir-catalysed atroposelective hydroarylation.

the DKR of pro-axially chiral **121** using aliphatic alkenes (Scheme 38).<sup>67</sup> Slight modifications of the reaction conditions involving diphosphine ligand **L6** allowed the construction of nine new examples of heterobiaryls **122** with perfect diastereomeric and enantioselectivities.

Recently, the Ackermann group also exploited ruthenium catalysis for the enantioselective C–H activation of pro-axially chiral *N*-isoquinoline-indoles **123** with functionalised terminal alkenes **124** in the presence of chiral carboxylic acid ligand **L7** (Scheme 39).<sup>68</sup> In this case, the authors could isolate a wide range of branched products **124** bearing a C–N stereogenic axis and a stereocentre as single diastereomers (> 20 : 1 dr). The large number of examples highlighted the beneficial effect of an aromatic ring on the olefin partners given that alkyl-substituted alkenes (R<sup>3</sup> = Alk) proceeded with lower enantioselectivity compared to vinylarenes (R<sup>3</sup> = Ar). These results are consistent with a probable π-chelating interaction between ligand **L7** and alkenes, playing a pivotal role in the enantiocontrol. Also, vinyl silanes (R<sup>3</sup> = SiR<sub>3</sub>) were well supported by this method to produce valuable chiral organosilanes **124**



Scheme 38 Ir-Catalysed atroposelective hydroarylation with aliphatic alkenes.

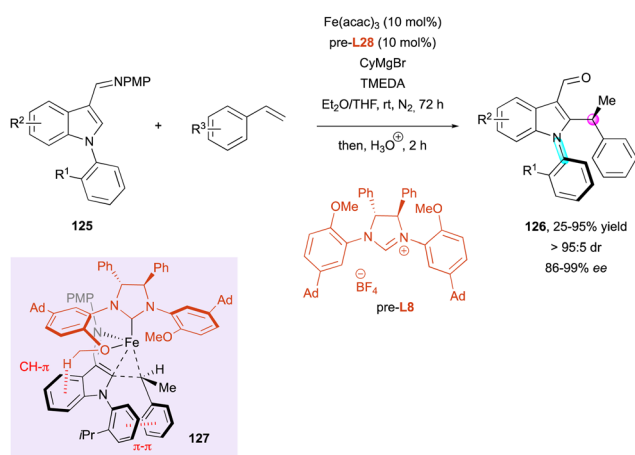


Scheme 39 DKR of *N*-isoquinoline-indoles via Ru-catalysed C–H activation.

( $R^3 = SiR_3$ ) with good enantioselectivities (68% to 95% ee), albeit with a small drop in (35% to 75% yield).

An impressive iron-catalysed C–H alkylation of indoles 125 with alkenes was recently disclosed by Neidig, Wencel-Delord and Ackermann for the simultaneous introduction and control of central and axial chirality in substituted indoles 126 (Scheme 40).<sup>69</sup> The careful design of NHC ligand pre-L8 allowed excellent diastereocontrol and very high enantioselectivities to be achieved in final products 126. Deuterium-labelling experiments and DFT calculations shed light on the reaction mechanism, which occurs by ligand-to-ligand hydrogen transfer (LLHT) rather than the classical C–H bond oxidative addition. In addition, the stereocontrol of both stereogenic elements is supposed to occur *via* transition state 127, which displays favorable CH–π and π–π interactions and determines both the configuration of the stereogenic axis and the carbon atom. These findings highlight the crucial role of the methoxy group of the NHC ligand in the stereochemical outcome of the reaction.

In their work on Ni/Al-catalysed atroposelective C–H alkylation using heteroatom-substituted secondary phosphine oxide (HASPO) preligands, Hong and Ackermann described two examples of benzimidazole C–N atropisomers bearing an

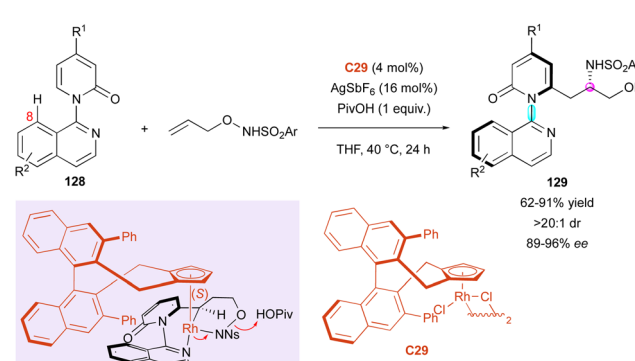


Scheme 40 Fe-Catalysed C–H alkylation of indoles.

additional stereocentre with very high diastereo- and enantioselectivities.<sup>70</sup>

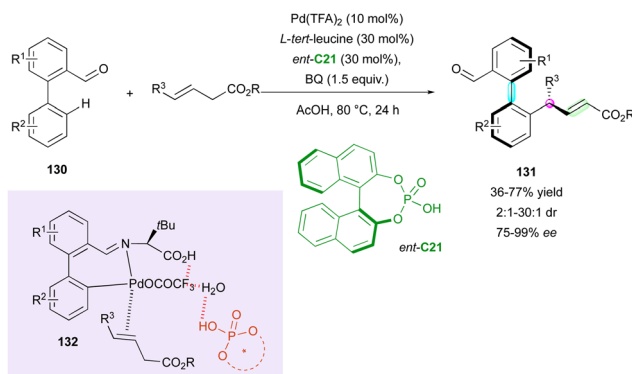
The Li group capitalised on their work on rhodium-catalysed C–H activation for the kinetic resolution of racemic axially chiral pyridone rings (±)-25 (Scheme 9).<sup>31</sup> In continuation, the authors proposed a complementary DKR process involving pro-axially chiral pyridones 128 lacking substitution at the 8 position (Scheme 41). The resulting carboamidation with *N*-protected *O*-allylhydroxyamines proceeded with perfect diastereoselectivities (>20:1 dr) and high enantiomeric excesses (89% to 96% ee). Nevertheless, modification of the substrates mostly concerned the *N*-protected *O*-allylhydroxyamine substrate with a large panel of sulfonyl groups but only one variation of  $R^1$  in 128 ( $R^1 = H$  or  $R^1 = CO_2Me$ ). The proposed transition state with Rh-complex C29 coordinated with the pyridine ring and the sulfonyl amide accounts for the excellent enantioselectivity. Due to the relatively free rotation around the C–N axis, which allows substrate 128 to react in its *aS* configuration, atropisomeric amino alcohols (*aS,S*)-129 are selectively obtained.

The aldehyde function can also be used as a directing group for the C–H functionalisation of biaryls. Recently, the Ge, Sunoj and Maiti groups proposed the palladium-catalysed C–H allylation of pro-axially chiral biaryl aldehydes 130 with *trans*-3-alkeneoates proceeding *via* a DKR process with control of three stereogenic elements, *i.e.*, one C–C axis, one central chirality and the alkene configuration (Scheme 42).<sup>71</sup> Cooperative assistance by CPA *ent*-C21 and *L*-*tert*-leucine provided a highly stereoselective transformation with good enantioselectivity and perfect regio- and (*E*)-selectivity. The DKR pathway was supported by the low barrier to interconversion of the starting racemic aryl aldehydes 130, calculated at 80.6 kJ mol<sup>-1</sup>, in agreement with rapid racemisation and indicating the faster reactivity of (*R<sub>a</sub>*)-130. In-depth DFT calculations unveiled the mechanistic pathway, indicating that the axial chirality is controlled by the formation of chiral transient imine 132 as a directing function, while the central chirality and stereochemistry of the alkene are controlled by the migratory insertion of [Pd]. The *Re* prochiral face is energetically favored, leading to (*S<sub>a</sub>,R*) products 131.



Scheme 41 Rh-Catalysed C–H activation of pyridone rings towards amino alcohol atropisomers.

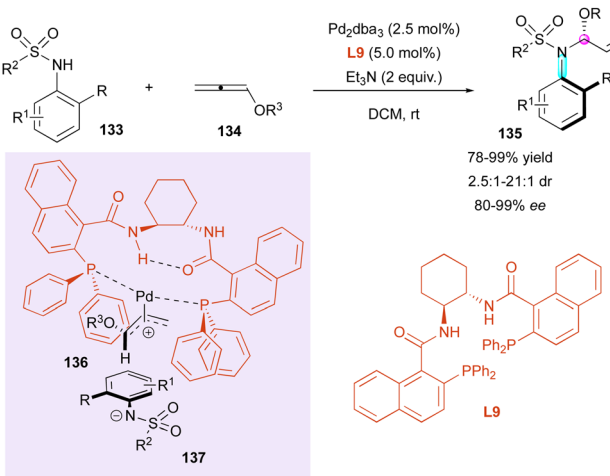




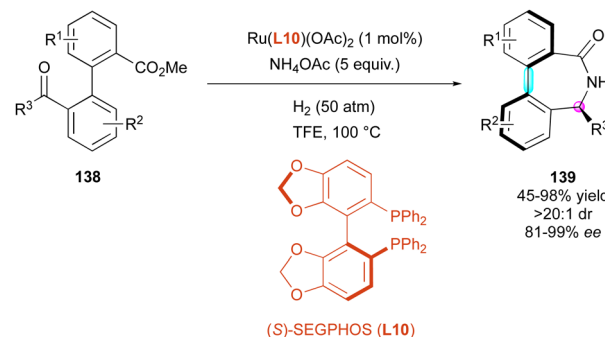
Scheme 42 Pd-Catalysed DKR C–H allylation.

Inspired by the work reported by Rhee on the hydroamination of allenes **134** to construct *N,O*-acetals with one stereogenic centre,<sup>72</sup> in 2021, Zhou and Zhang developed an hydroamination of allenes with pro-axially chiral sulfonamides to implement a C–N axis as an additional stereogenic element (Scheme 43).<sup>73</sup> Using bidentate chiral ligand **L9** with  $\text{Pd}_2\text{dba}_3$  as the catalyst, high enantio- and diastereoselectivities were obtained with aryl sulfonamides **133** as the starting material, while alkyl sulfonamides led to a reduction in the diastereomeric ratio (dr = 2.5 : 1). The origin of the stereoselectivity was rationalised by DFT calculations, with a more favorable transition state involving palladium  $\pi$ -allyl intermediate **136**, which underwent nucleophilic addition of sulfonamide anion **137**.

The formation of axially chiral bridged molecules *via* DKR of pro-stereogenic substrates can be an efficient approach for the introduction and control of multiple stereogenic elements. In 2020, Zhang and Yin reported a reductive amination/ring closing cascade to afford enantioenriched bridged atropisomers **139** of the dibenzo[*c,e*]azepin-5-one family, catalysed by a ruthenium complex (Scheme 44).<sup>74</sup> The reaction was optimised starting from biaryl keto esters **138** using  $\text{Ru}(\text{L10})(\text{OAc})_2$  as the catalyst, excess of  $\text{NH}_4\text{OAc}$  as the ammonia source under a high-pressure hydrogen atmosphere (50 bar)



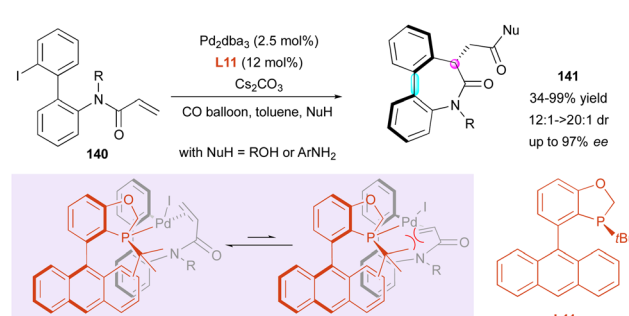
Scheme 43 Pd-Catalysed hydroamination of allenes.



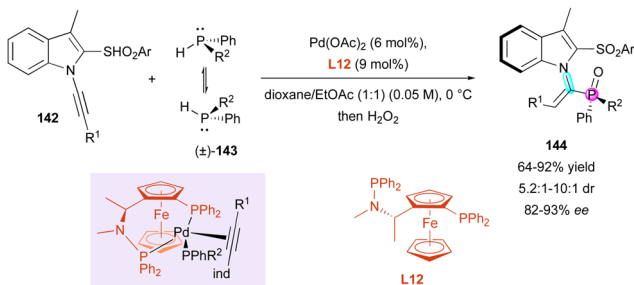
Scheme 44 Ru-Catalysed reductive amination/ring closing cascade.

in trifluoromethanol at high temperature (100 °C). These very harsh conditions gave the best results in terms of yield and enantioselectivity (up to 99% ee). Methyl or ethyl ketones performed the best, while phenyl ketones required the stoichiometric use of  $\text{Ti}(\text{O}i\text{Pr})_4$  and only afforded the products in low yield and lower enantioselectivity (45% yield, 81% ee). They proposed that the configuration of the stereogenic axis, which is created and controlled in the initial reductive amination step.

In 2021, the Luo and Zhu groups reported the enantioselective synthesis of related dibenzo[*b,d*]azepin-6-ones **141** *via* a carbopalladation/carbonylation cascade (Scheme 45).<sup>75</sup> The prepared heterocyclic seven-membered ring lactams contain both central and axial stereogenic elements. This palladium-catalysed reaction was optimised with 2'-iodo-[1,1'-biphenyl]-2-yl-*N*-methylacrylamides **140** under a CO atmosphere and various nucleophiles. As predicted by DFT calculations, excellent diastereo- and enantioselectivity were obtained using (S)-AntPhos **L11** as a chiral ligand after 10 h of reaction in toluene. Although a high ligand loading is required  $\{[\text{Pd}]/[\text{L}] = 1:9.6\}$ , different nucleophiles such as anilines and alcohols were successfully engaged in this reaction. The observed configuration was explained by the strong steric repulsion after the oxidative addition of the aryl iodide to the  $[\text{Pd}(0)]$  species, which forces the terminal alkene to approach  $[\text{Pd}(II)]$  away from the ligand. As suggested by  $^1\text{H}$  NMR, where only one product was detected, the atropisomerism is thermodynamically controlled by the newly formed stereogenic centre.



Scheme 45 Pd-Catalysed carbopalladation/carbonylation cascade.



Scheme 46 Pd-Catalysed hydrophosphination of 1-alkynyl indoles.

Finally, Wang and Li reported the original atroposelective hydrophosphination of 1-alkynyl indoles **142** with simple non-symmetrical configurationally labile diarylphosphines  $(\pm)$ -**143** as nucleophiles catalysed by a chiral palladium complex for the synthesis of *P*-stereogenic substituted alkenes **144** (Scheme 46).<sup>76</sup> Their initial efforts at optimising the chiral ligand allowed *(S)*-Me-Bophoz **L12** to be selected as optimal to give, after *in situ* hydrogen peroxide oxidation, configurationally stable vinylphosphine oxides **144** featuring a C–N axially chiral trisubstituted olefin and a *P*-stereogenic centre with perfect regio- and *(E)*-selectivity, moderate to good diastereoselectivity (5.2:1 to 10:1 dr) and enantioselectivity above 81%. Supported by DFT calculations, only the observed axial chirality was rationalised, and the migratory insertion was identified as the enantio-determining step with two essential arguments, where firstly, the more hindered indole moiety tends to be placed downward with minimal repulsion between  $R^1$  and  $PPh_2$  groups as the depicted intermediate. Secondly, the  $\pi$ -acidic alkyne is *trans* to the more donating arylphosphino group, favoring the *(S)* configuration of the product.

Another recent DKR for the atroposelective synthesis of C–N axially chiral compounds featuring a stereogenic centre was proposed by Wang, Ren and colleagues.<sup>77</sup> They envisaged a unique Rh(II)-catalysed carbene N–H insertion strategy of diazonaphthoquinones **146** to racemic 3-indolinone spiroacetals  $(\pm)$ -**145** in the presence of chiral amino acid **L13** as the ligand (Scheme 47). Although the mechanism was not explained, ring-opening/ring-closing of spiro-acetal may occur to enable the observed diastereoselective DKR, leading to a new family of

C–N atropisomers **147** with excellent enantioselectivity (72% to 99% ee). Although the diastereoselectivity was generally moderate (mostly 1.5:1 to 2:1 dr), a better result was observed for  $R^3 = 3$ -OnPr (8:1 dr). Interestingly, increased yields were obtained in the case of electron-donating substituents as  $R^1$  and  $R^3$ . Remarkably, the authors proposed an efficient one-pot protocol for the formation of **147** ( $R^1 = R^2 = R^3 = H$ ) directly from isatin **148**, triggering both N–H and C–O carbene insertion with concomitant *N*-arylation and spirocyclisation with the same efficient creation of the two different stereogenic elements (45% yield, 3:1 dr, 96% ee).

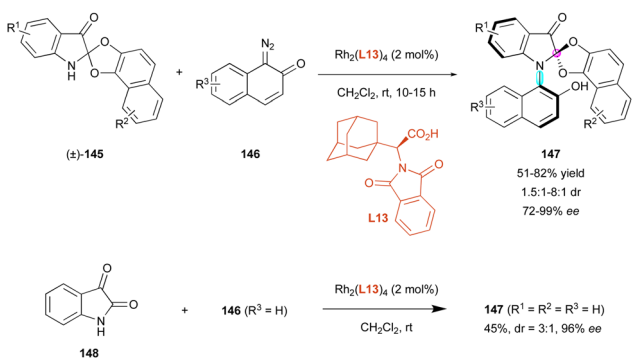
## Desymmetrisation

### Maleimide/succinimide substrates

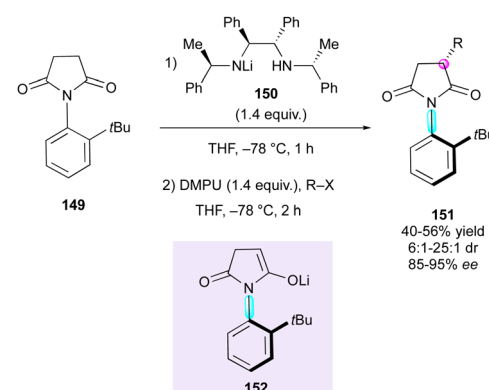
Enantioselective desymmetrisation is a well-established and powerful method to reveal multiple stereogenic elements from simple achiral, prochiral or *meso* substrates by breaking one or more elements of symmetry involving either enzymatic<sup>78</sup> or non-enzymatic<sup>79</sup> catalytic transformations. In this context, the last two decades have witnessed the emergence of new strategies for the synthesis of compounds featuring both central and axial chirality.

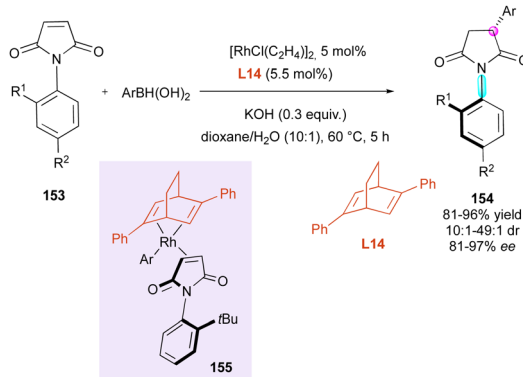
The initial contribution in this direction was from Simpkins and collaborators,<sup>80</sup> who proposed the desymmetrisation of *N*-(2-*tert*-butylphenyl)succinimide **149** involving chiral lithium amide **150** (Scheme 48). The enantiotopic deprotonation of **149** by mono-lithiated base **150** generated atropisomeric enolate intermediate **152**, which reacted diastereoselectively with various electrophiles, leading to enantioenriched succinimides **151** featuring both central and axial chirality. The reaction proceeded with moderate yields (40–56%), good to high diastereoselectivity (6:1–25:1 dr) and high enantiomeric excess (85–95% ee).

Another stereoselective approach to centrally and axially chiral succinimides **154** relies on the desymmetrisation of maleimides **153** triggered by stereoselective 1,4-additions largely inspired by the pioneer Curran's diastereoselective Giese reaction.<sup>81</sup> The first report by the Hayashi and Shintani group deals with the rhodium-catalysed enantio- and



Scheme 47 Rh-Catalysed enantioselective N–H bond insertion of indolinone-spiroacetals.

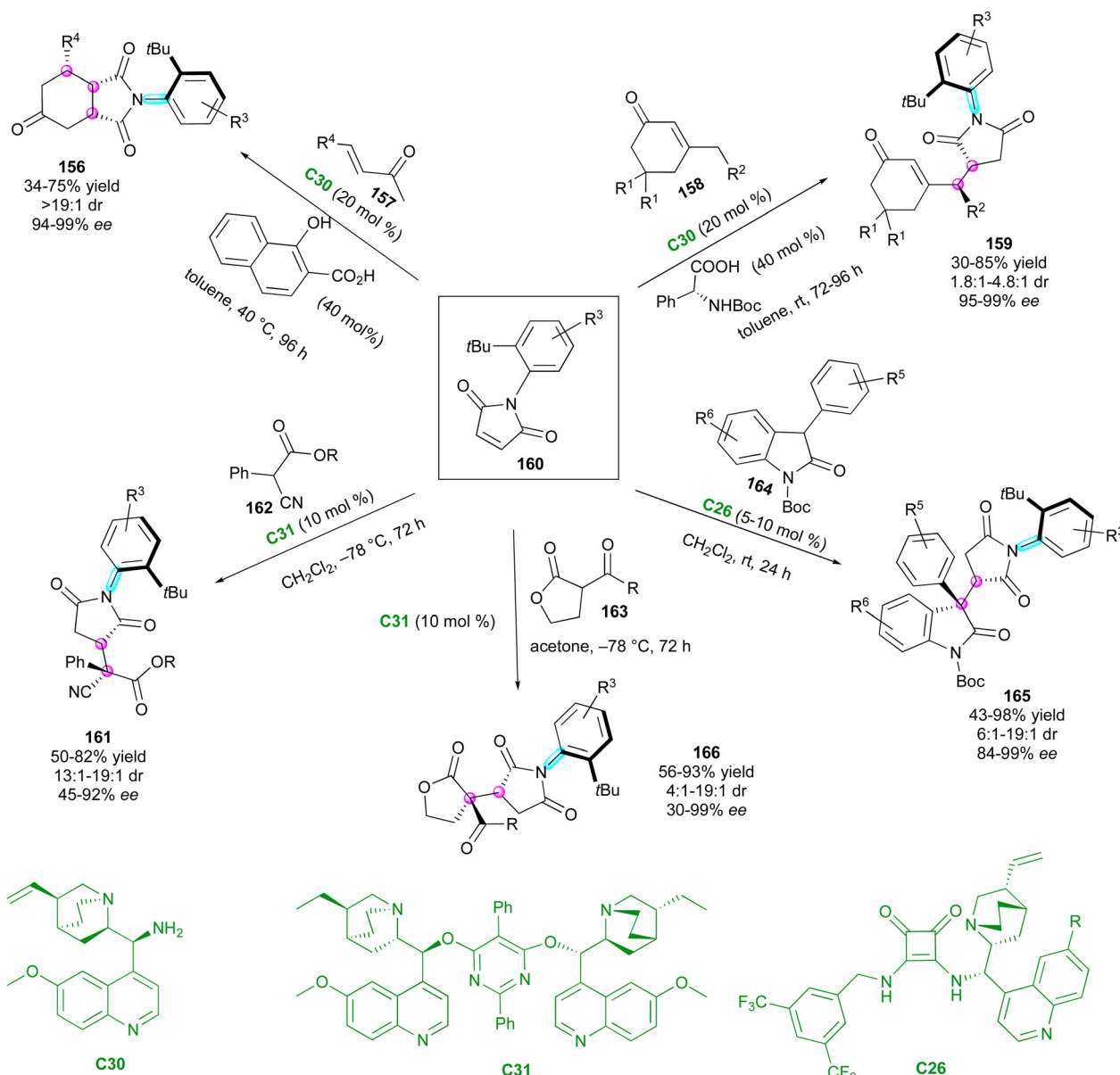
Scheme 48 Enantiotopic desymmetrisation of *N*-(2-*tert*-butylphenyl)succinimide.



Scheme 49 Rh-Catalysed conjugate addition of arylboronic acids.

diastereoselective conjugate addition of arylboronic acids controlled by the commercially available chiral 2,5-diphenyl bicyclo[2.2.2]octadiene ligand **L14** (Scheme 49).<sup>82</sup> Square planar Rh-coordinated transition state **155** minimising the steric repulsion between the *t*Bu-substituent of maleimide and the phenyl groups of the ligand was proposed to support the very high stereoselectivities observed.

After these seminal contributions, the powerful Michael acceptor reactivity of maleimides for desymmetrisation leading to multi-chiral succinimides was advanced in 2014 by the Bencivenni group.<sup>83</sup> Their methodology deals with the amino-catalytic desymmetrisation of *N*-arylmaleimides **160** *via* the vinyllogous Michael addition of 3-substituted cyclohexenones **158** to *N*-(2-*tert*-butylphenyl) succinimides **159** with remote control of the axial chirality (Scheme 50, up right).<sup>84</sup> The salt

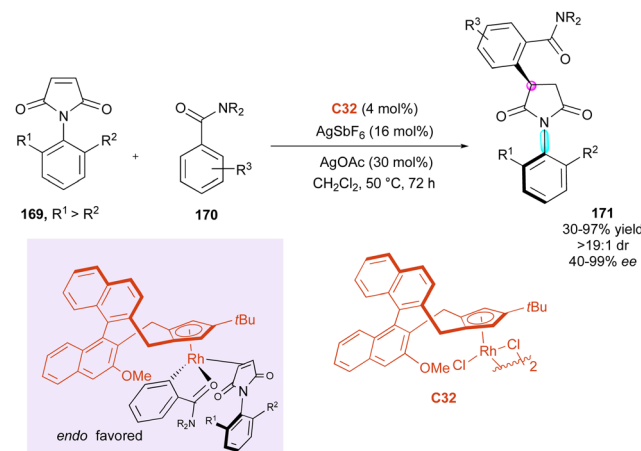


Scheme 50 Amino-catalytic desymmetrisation for remote control of axial chirality.

made of 9-amino(9-deoxy)epi-quinine **C30** and N-Boc phenylglycine catalysed the enantioselective desymmetrisation *via* dienamine activation, leading to atropisomeric succinimides **159** with two adjacent stereocentres. Primary amine catalysis was crucial for achieving enantioselective desymmetrisation, enabling simultaneous and exclusive remote control of both the stereogenic axis and newly formed stereocentres. This process resulted in moderate diastereoselectivity but consistently high enantioselectivity. Following these promising results, the same group developed complementary organocatalysed desymmetrisations of *N*-(2-*tert*-butylphenyl)maleimides **160** *via* either Michael addition of  $\alpha$ -activated carbonyl compounds **162–164**<sup>85</sup> catalysed by **C31** and **C26** (Scheme 50, bottom left, centre and right) or formal Diels–Alder cycloaddition with  $\alpha,\beta$ -unsaturated ketones **157**<sup>86</sup> promoted by catalyst **C30** (Scheme 50, up left). In the first case, activated carbonyl compounds, such as cyanomalonates **162** or 3-aryloxindoles **164**, allowed the control of two stereogenic centres and one C–N axis,<sup>87</sup> while with the last approach, control of three stereogenic centres and one C–N axis in **156** could be reached *via* dienamine activation.

Contemporaneously, Feng and collaborators<sup>88</sup> applied their chiral *N,N'*-dioxide metal complexes for the desymmetrisation of *N*-(2-*tert*-butylphenyl)maleimide **160** ( $R^3 = H$ ) by Michael addition with NH-free 3-benzyl-2-oxindoles **167** (Scheme 51). Among the various combinations, with the **L14-Sc(OTf)<sub>3</sub>** complex, the yields and stereoselectivities of **168** remained consistently high, tolerating a wide array of 3-benzyl groups, while 3-phenyl- or 3-methyl analogues gave poorer results with 89% ee, 9:1 dr and 88% ee, 3:1 dr, respectively. A tetradentate coordination of the Sc(III) by chiral ligand **L15** was proposed as the active catalytic species, allowing to organise an hexacoordinated transition state accounting for the observed stereoselectivities.

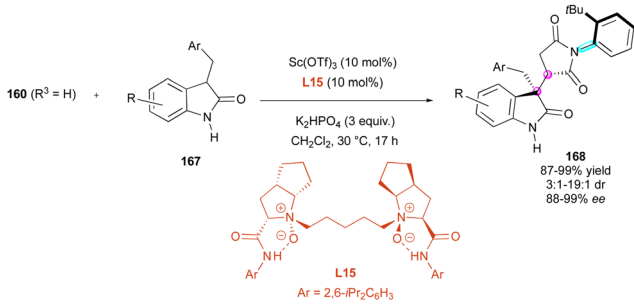
Correspondingly, six years later, Li and collaborators<sup>89</sup> proposed the elegant C–H alkylation of benzamides **170** with Cramer's chiral CpxRh-(III)-catalysts **C32** for the efficient desymmetrisation of a large series of *N*-aryl maleimides **169** as electrophilic Michael acceptor partners (Scheme 52). The coupling system features a broad substrate scope, including *N*-naphthylmaleimides, and proceeds with excellent enantio- and diastereoselectivity for simultaneous control of the axial and



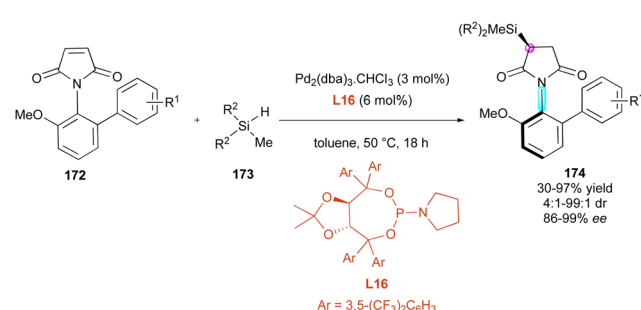
Scheme 52 Rh-Catalysed C–H enantioselective alkylation of benzamides.

central chirality in **171**. The experimental mechanistic studies clearly indicated the reversibility of the C–H bond activation, whose cleavage significantly contributes to the overall kinetic barrier. Moreover, the excellent stereoselectivities were rationalised based on Cramer's stereocontrol model *via* the *endo* coordination of the substrates to Rh with the relatively bulky tertiary amide directing group pointing frontward to minimize the steric repulsions.

Enantioselective metal-catalysed hydrofunctionalisation of olefins has attracted significant attention for the control of central chirality,<sup>90</sup> and more recently found some interesting applications for the desymmetrisation of functionalised maleimides. In 2020, the Xu<sup>91</sup> group developed a stereospecific Si–C coupling with remote control of the axial chirality upon the enantioselective palladium-catalysed hydrosilylation of maleimides **172** (Scheme 53). Among the various chiral ligands, TADDOL-derived phosphoramidites of type **L16** bearing aromatic bulky groups were revealed to be the most efficient, inhibiting both the competitive *O*-hydrosilylation and reductive hydrosilylation. Therefore, the chemo- and enantioselective desymmetrisation tolerated many functional variations including different silanes **173** and proceeded with generally high yields and excellent stereoselectivities for the simultaneous remote control of the stereogenic axis and the newly formed silylated stereocentre in products **174**.

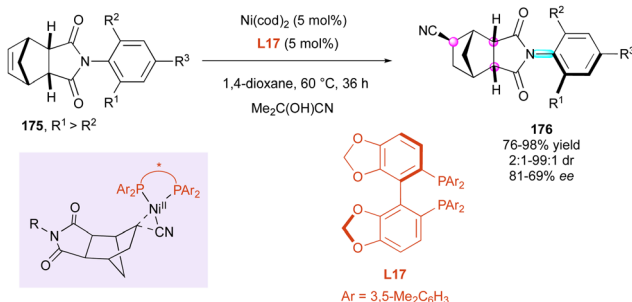


Scheme 51 Sc(III)-Catalysed desymmetrisation of *N*-(2-*tert*-butylphenyl)maleimide.



Scheme 53 Pd-Catalysed enantioselective hydrosilylation of maleimides.

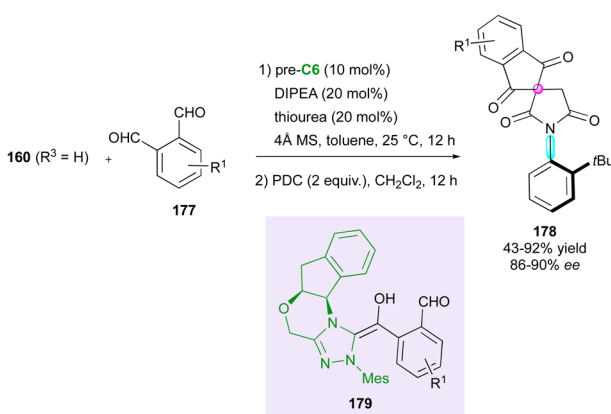




**Scheme 54** Ni-Catalysed enantioselective hydrocyanation of norbornenes.

Similarly, the following year, the Fang and Chen group<sup>92</sup> reported the efficient enantioselective nickel-catalysed hydrocyanative desymmetrisation of *N*-aryl-norbornene-2,3-dicarboximide derivatives 175 (Scheme 54). Acetone cyanohydrin as the *in situ* source of HCN and Ni(cod)<sub>2</sub> as the catalyst in the presence of SegPhos bidentate ligand L17 were selected as the benchmark combination, giving high yields and excellent stereoselectivities even at relatively elevated temperature (60 °C to 100 °C). Consequently, a large series of functionalised succinimides 176 featuring three stereogenic centres and a C–N axially chiral bond was easily available by a remarkable remote control. The complementary experiments combined with DFT calculations clearly indicated that the rigid structure of the cyclic imide was essential to control the enantioselectivity determined during the reductive elimination step through a more favorable transition state ( $\Delta\Delta G^0 = 2.3$  kcal mol<sup>-1</sup>), which is consistent with the high ee values obtained experimentally.

More recently, the Michael acceptor character of maleimides was exploited by the Jindal, Mukherjee and Biju group<sup>93</sup> in an efficient N-heterocyclic carbene-(NHC)-catalysed Stetter-aldol domino sequence involving aromatic dialdehydes **177** and prochiral *N*-(2-*tert*-butylphenyl)maleimide **160** ( $R^3 = H$ ), followed by subsequent oxidation (Scheme 55). This two-step approach afforded atropisomeric *N*-aryl succinimides **178** combining an axially chiral C–N bond and a spirocyclic stereogenic centre in good yields and ee values. The reaction is mostly

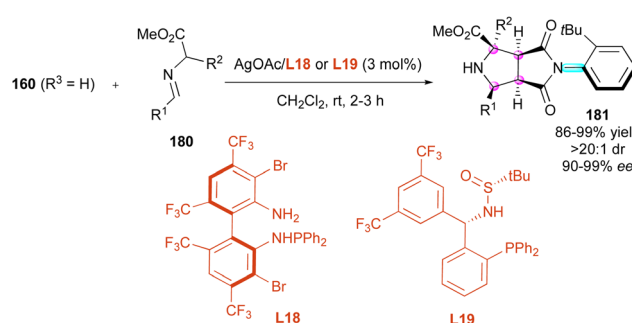


**Scheme 55** NHC-Catalysed enantioselective spiro-desymmetrisation of maleimides.

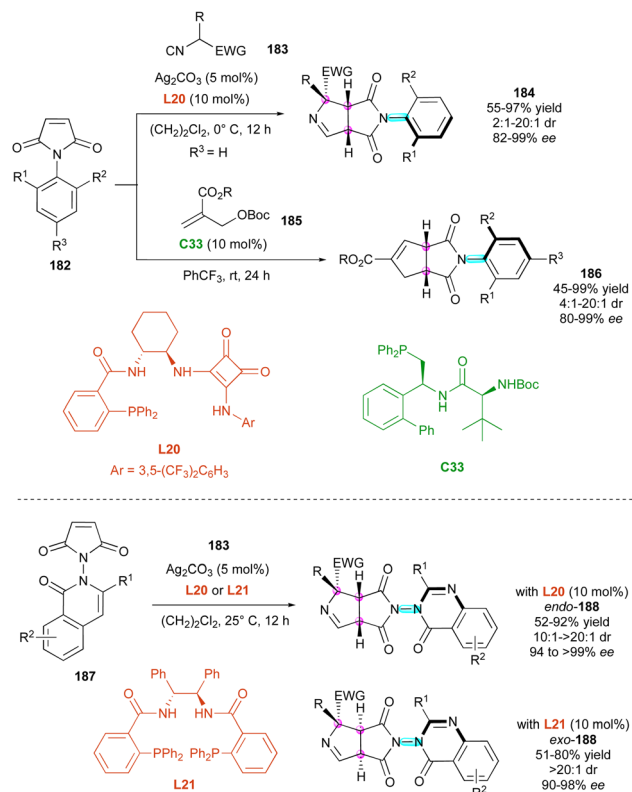
limited to *o*-*t*Bu-*N*-aryl derivatives and proceeds with 10 mol% loading of the N-heterocyclic carbene generated *in situ* by deprotonation of chiral triazolium salt pre-C6 with DIPEA. DFT calculation indicated that the Michael addition of transient Breslow intermediate **179** is the enantio-determining step.

Maleimides have also been known for a long time as excellent dipolarophiles and dienophiles in enantioselective cycloadditions, and recently have emerged as an interesting tool to control both central and axial chirality by desymmetrisation of prochiral maleimides. One of the first contributions was by Wang and collaborators in 2016,<sup>94</sup> who proposed the 1,3-dipolar cycloaddition of azomethine ylides to *N*-(2-*tert*-butylphenyl)maleimide **160** ( $R^3 = H$ ) as a dipolarophile (Scheme 56). The reaction proceeded smoothly with only 3 mol% loading of silver(i)/**L18** catalytic system formed *in situ* and various imino esters **180**. Interestingly, no additional base was required to generate the reactive azomethine ylides, affording enantioenriched octahydropyrrolo[3,4-*c*]pyrrole derivatives **181** bearing four adjacent stereocentres and one C–N stereogenic axis with very high yields and stereoselectivities even when a quaternary stereogenic centre is created ( $R^2 = Me, Et, tBu\dots$ ). Following these pioneer results, Zhang and collaborators<sup>95</sup> proposed alternative trifluoromethylated sulfonyl amide phosphine ligand **L19**, providing similar results but in the presence of the mineral base  $Cs_2CO_3$ .

More recently, two complementary approaches for the simultaneous control of C–N axial and central chirality *via* the (3+2) cycloaddition of prochiral maleimides **182** were reported (Scheme 57). Based on the silver-catalysed 1,3-dipolar cycloaddition, the Qian and Liao group<sup>96</sup> reported the first utilisation of activated isocyanides **183** as 1,3-dipolarophiles for the synthesis of C–N atropisomers in the presence of chiral diamine ligand **L20** (Scheme 57, up). Simultaneously, Wang, Lin and collaborators<sup>97</sup> disclosed the new atroposelective (3+2) annulation of Morita–Baylis–Hillman carbonates **185** catalysed by chiral phosphine **C33**. The first approach gave fused bicyclic 1-pyrrolines **184** featuring a distal C–N stereogenic axis and three adjacent stereogenic centres in high yields and stereo-selectivities, while C–N axially chiral cyclopentannulated *N*-aryl succinimides **186** having two stereogenic centres were obtained by the alternative method with comparable efficiencies. In addition, a closely related protocol of silver-catalysed



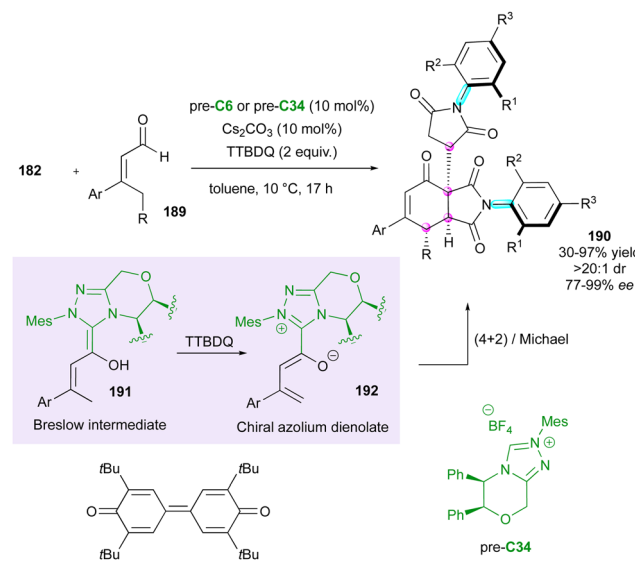
**Scheme 56** Ag(I)-Catalysed enantioselective (3+2) cycloaddition of azo-methine ylides.



Scheme 57 Phosphine- and silver-catalysed (3+2) atroposelective annulations.

1,3-dipolar cycloaddition with isocyanides **183** was applied by Qian and Liao's group for the desymmetrisation of quinazolone maleimides **187**, delivering bicyclic heterocycles **188** displaying a stereogenic N–N axis and three contiguous stereogenic carbon atoms (Scheme 57, bottom).<sup>98</sup> Interestingly, a simple ligand switch allowed the development of a diastereodivergent approach with facile and efficient access to both *endo* and *exo* diastereomers of **188** in excellent dia- and enantioselectivities. This protocol was also applicable to *N*-indole maleimide starting materials.

Concerning the dienophilic reactivity of maleimides, to the best of our knowledge, two pioneer examples by Corey and Yamamoto, in 1994 and 2001, respectively, were reported on the Diels–Alder enantioselective desymmetrisation of *N*-aryl maleimides but the authors did not discuss the possible control of the axial chirality.<sup>99</sup> Since then, besides Bencivenni's formal (4+2) annulation in 2015 (*vide supra*),<sup>83</sup> this approach remained without development until the recent contribution by our group (Scheme 58).<sup>100</sup> We illustrated an unprecedented chiral NHC-catalysed pseudo-three component reaction between enal **182** and two equivalents of a prochiral *N*-aryl maleimide **182** under oxidative conditions, resulting in the formation of bis-succinimide adducts **190** with high stereocontrol of up to four consecutive stereogenic centres and two remote C–N stereogenic axes. The best conditions involved an inorganic base to generate the reactive NHC precursor of Breslow intermediate

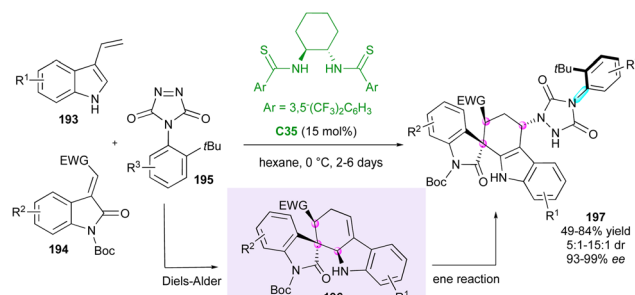


Scheme 58 NHC-Catalysed formal (4+2) oxidative desymmetrisation of maleimides.

**191**, which upon *in situ* oxidation by 3,3'-5,5'-tetra-*tert*-butyl-4,4'-diphenoxquinone (TTBDQ) provided the key chiral azolium dienolate **192**, triggering the formal (4+2) cycloaddition, followed by a completely diastereoselective conjugate addition to a second equivalent of *N*-aryl maleimide **182**. Products **190** featuring multiple stereogenic elements, including two challenging C–N axes in the pentatomic series, were obtained as only one diastereomer out of 64 possible stereoisomers and with excellent enantioselectivity.

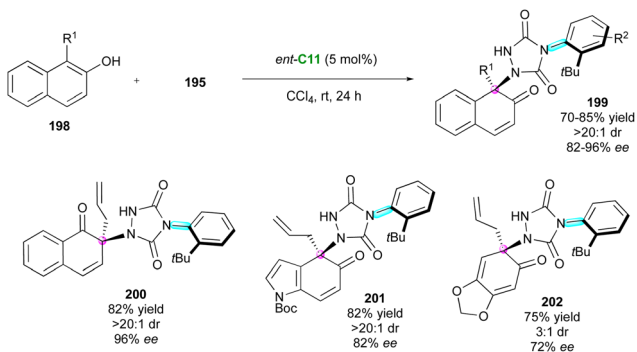
### Non maleimide/succinimide substrates

Closely related to maleimides, 4-aryl-1,2,4-triazole-3,5-dione (ATAD) derivatives can also be interesting candidates for atroposelective desymmetrisations, as shown by Tan's group in 2016.<sup>101</sup> Capitalising on this discovery, the same group<sup>102</sup> proposed an elegant consecutive three-component synthesis of complex axially chiral spiroindole-urazole derivatives **197** bearing three stereogenic centres including a spirocyclic one (Scheme 59). This unique transformation involves, as the first step, the chiral bishthiourea **C35**-catalysed domino Diels–Alder cycloaddition between 3-vinylindoles **193** and



Scheme 59 Three-component desymmetrisation of ATAD derivatives.



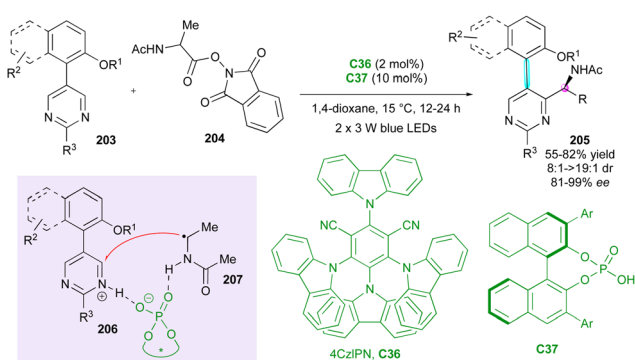


Scheme 60 CPA-Catalysed dearomatative desymmetrisation of urazoles.

methyleneindolinones **194** to afford spirooxindole intermediates **196**, followed by a diastereoselective ene reaction with ATADs **195**. Notwithstanding the long reaction times and the usually moderate chemical yields, good diastereoselectivities and excellent enantiopurities were obtained when an *ortho*-*tert*-butyl group is present on the ATAD.

Very recently, inspired by the peculiar reactivity of ATADs, Pan and collaborators<sup>103</sup> proposed the original CPA-catalysed enantioselective dearomatisation of 1-substituted-2-naphthols **198** for the atroposelective desymmetrisation of 4-(2-*t*-butylphenyl)-1,2,4-triazole-3,5-dione derivatives **195** to give functionalised chiral urazole embedded naphthalenones **199** having both axial and central stereogenic elements in good to high yields with high diastereo- and enantioselectivities (Scheme 60). Both the free OH of the naphthol and the *ortho*-*tert*-Bu substituent of the ATAD are crucial to ensure good efficiency but other phenolic partners are also tolerated, leading to the corresponding 1-naphthalenone **200**, indole derivative **201**, and sesamol **202**.

Concerning the atroposelective construction of axially and centrally chiral C-C heterobiaryls, in 2022, Xiao's group<sup>104</sup> developed the first catalytic Minisci reaction of symmetric 5-arylpyrimidines **203** with  $\alpha$ -amino acid-derived redox-active esters **204** (Scheme 61). This unprecedented metal-free radical desymmetrisation was possible using commercially available carbazolyl isophthalonitrile photoredox catalyst 4CzIPN **C36** in

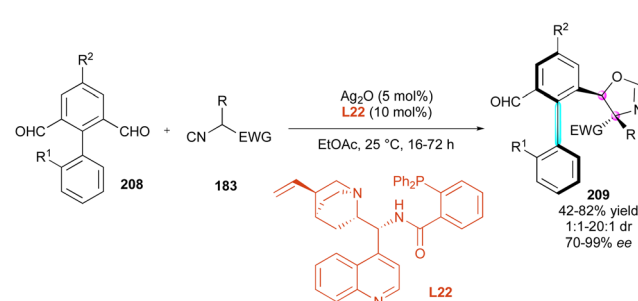


Scheme 61 Photoinduced atroposelective radical Minisci reaction.

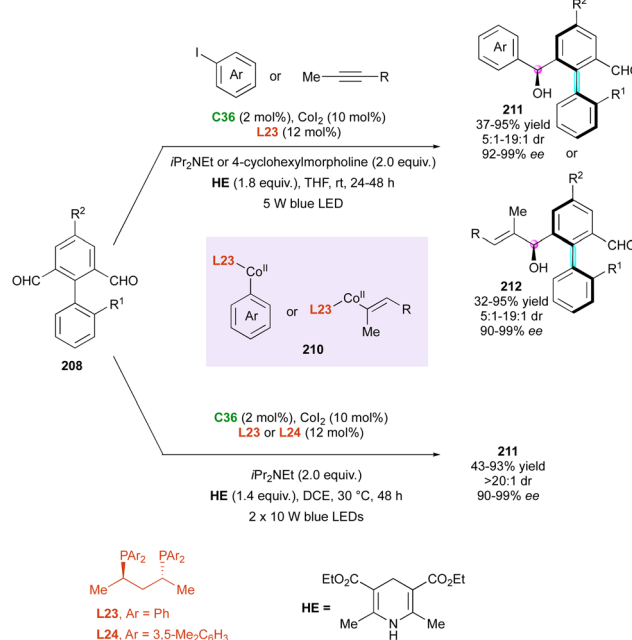
conjunction with CPA organocatalyst **C37** under blue LEDs irradiation. The resulting axially chiral heterobiaryl and centrally chiral  $\alpha$ -branched amines **205** were generally obtained with excellent regio-, diastereo-, and enantioselectivity. The key to the success of this reaction is the photocatalyst-controlled formation of radical intermediate **207** and the efficient transfer of stereochemical information from CPA-pyrimidine salt **206**. Interestingly, the reaction could be scaled up to 4.0 mmol with comparable results, and under sunlight irradiation, the cross-coupled amino pyrimidines were also smoothly obtained without deleterious effects on the efficiency and stereoselectivity.

Another interesting strategy for simultaneously controlling both the central and C-C axial chirality involves metal-catalysed enantioselective desymmetrising additions of various nucleophiles to axially prochiral dialdehydes. This approach emerged recently and concurrently by three different groups. Firstly, Liao's and Qian's groups<sup>105</sup> proposed the intriguing silver-catalysed diastereo- and enantioselective (3+2) cycloaddition of activated isocyanides **183** to prochiral biaryl aldehydes **208** (Scheme 62). Employment of diphenyl phosphine-derived cinchonine chiral ligand **L22** gave the best results in terms of yields and stereoselectivities, producing a wide range of atropisomeric biaryl aldehydes **209** containing a stereogenic C-C axis and two adjacent stereogenic centres in moderate to excellent diastereoselectivities and uniformly excellent enantioselectivities.

Correspondingly, two closely related photoinduced cobalt-catalysed enantioselective reductive couplings were reported independently by the Cheng, Xiao<sup>106</sup> and Zheng, Zhang groups,<sup>107</sup> respectively (Scheme 63, top). The first metallaphotoredox approach combines visible light-induced cobalt-catalysed enantioselective reductive couplings with either aryl iodides or alkynes. The commercially available carbazolyl isophthalonitrile photocatalyst 4CzIPN **C36** in the presence of (*R,R*)-BDPP chiral diphosphine ligand **L23** and Hantzsch ester (**HE**) as the reducing agent gave the best results under blue LED irradiation. A broad substrate scope was achieved, leading to a large panel of atropisomeric biphenyl hydroxy aldehydes **211** or **212** in good yields with excellent stereocontrol of axial and central chirality. The origin of the stereoselectivity was corroborated based on DFT calculations for the stereo-determining transition state during Grignard addition of *in situ*-generated Co(II) intermediates **210** to biaryl dialdehyde



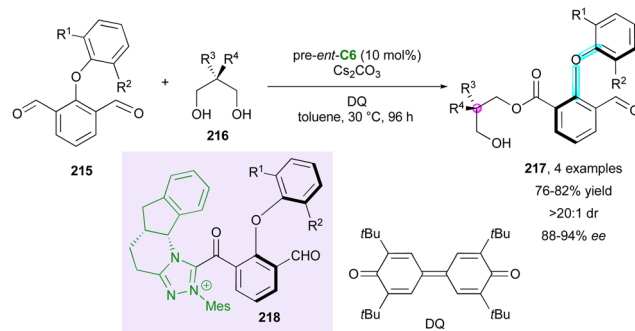
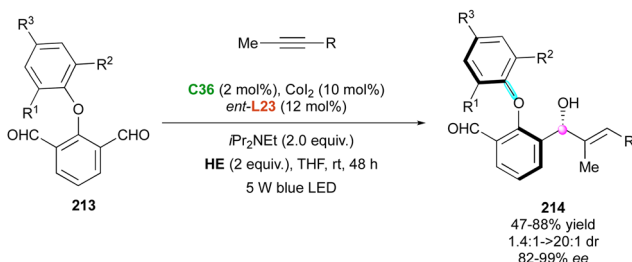
Scheme 62 Ag-Catalysed (3+2) cycloaddition with activated isocyanides.



**208.** Simultaneously, Zheng, Zhang and collaborators proposed the same methodology under similar conditions with comparable results for the desymmetrising reductive arylation of diaryl dialdehydes **208**, leading to benzylic alcohols **211** (Scheme 63, bottom).

More recently, this elegant cobalt-catalysed photo-reductive coupling was extended to the expedient synthesis of axially and centrally chiral more challenging diaryl ethers by the Li and Yu group (Scheme 64).<sup>108</sup> Under the same experimental conditions with an (*S,S*)-BDPP chiral diphosphine ligand (*ent*-**L23**), pro-axially chiral diaryl ethers **213** were efficiently coupled with internal alkynes to give the expected atropisomeric hydroxy diaryl ethers **214** in good yields and usually with good to excellent diastereo- and enantioselectivities.

In their work on the use of NHC organocatalysts for the desymmetrisation of pro-axially chiral dialdehydes **215**,<sup>109</sup> Zeng and coworkers reported the synthesis axially chiral diarylethers, four of which displayed additional central chirality due to the use of prochiral nucleophilic di- or triols **216** (Scheme 65). The

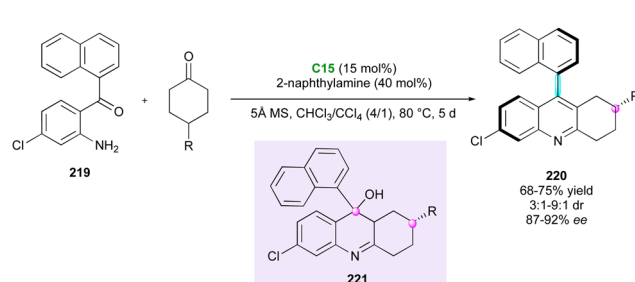


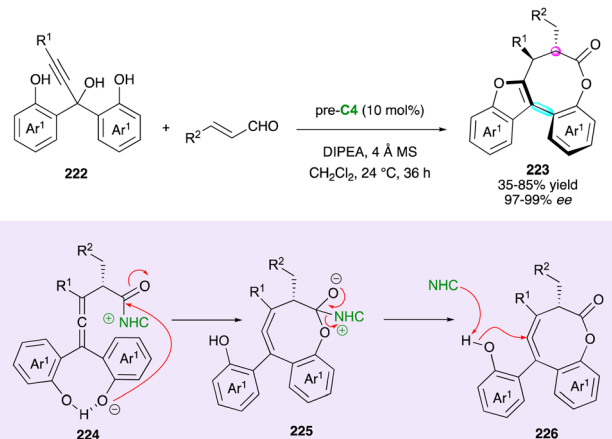
diastereoselectivity in **217** was found to be excellent, and from a mechanistic point of view, the reaction with pre-catalyst *ent*-C6 could generate atropisomerically enriched Breslow acylazolium intermediates **218** under oxidative conditions using bisquinone (DQ) followed by a nucleophilic substitution with various prochiral alcohols.

During their study on the CPA-catalysed atroposelective Friedländer reaction of 2-aminoaryl ketone **219**, Cheng and collaborators<sup>110</sup> revealed its potential for the desymmetrisation of a small series of 4-substituted cyclohexanones (Scheme 66). The overall cyclodehydration process was triggered by catalyst C15, leading to atropisomeric 9-aryltetrahydroacridines **220** and evolved through centrally chiral tertiary alcohol **221**, from which a central-to-axial chirality conversion occurred with relatively modest efficiency in terms of diastereo- and enantioselectivity.

While investigating the NHC-catalysed enantioselective acylation of propargylic triols **222** ( $R^1 = H$ ) (Scheme 67), Wong and Zhao's team unexpectedly discovered the formation of bridged diarylfuranones **223** with an eight-membered lactone when reacted with enals in the presence of azolium pre-catalyst pre-C4 under basic conditions.<sup>111</sup> This unique class of bridged atropisomers, featuring a benzofuran ring and a single stereogenic centre, has a broad scope, but with triol containing an internal alkyne (**222**,  $R^1 = Me$ ), the corresponding axially chiral products with two stereogenic centres were obtained in relatively low yield (32%) and dr (1.5:1 to 3:1).

The mechanistic investigations by DFT calculations suggested the direct propargylic substitution of the *in situ*-generated azolium enolate, resulting in the key centrally chiral allene acylazolium intermediate **224**, which undergoes a



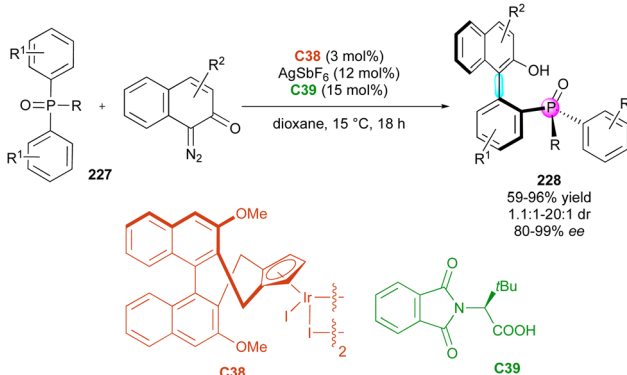


**Scheme 67** Atroposelective synthesis of benzofurans fused with an eight-membered lactone.

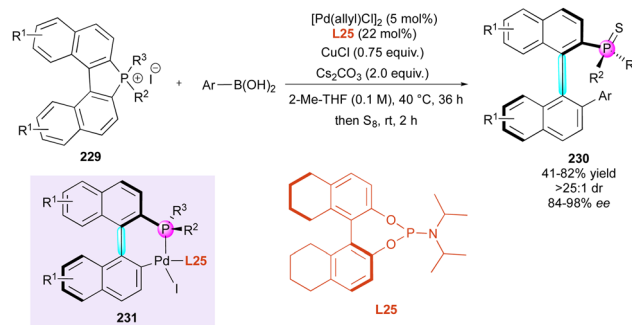
sequential bi-directional heterocyclisation through 225 and 226 to the final products 223 with both axial and central stereogenic elements.

Although much less widespread, the simultaneous control of axial chirality and chirality centred on a heteroelement has recently found some interesting solutions. The first example in 2018 by the Cramer group<sup>112</sup> described the enantioselective desymmetrisation of phosphine oxides 227 by C–H arylation with *o*-quinone diazides catalysed by iridium(III) complex C38 bearing an axially chiral cyclopentadienyl ligand and phthaloyl *tert*-leucine C39 as a co-catalyst (Scheme 68). This method notably enables the selective formation of biaryl C–C atropisomers 228 with a stereogenic phosphorus atom, achieving excellent yields and generally good diastereo- and enantioselectivities. Enantiospecific reductions produce chiral phosphorus(III) compounds, featuring structures and biaryl backbones that are valuable as monodentate ligands in enantioselective catalysis.

More recently, the Yu and Li group<sup>113</sup> proposed the modular assembly of diverse *P*-stereogenic and axially chiral thiophosphine derivatives 230 by the palladium-catalysed enantioselective desymmetrisation of cyclic phosphonium salts 229 in the presence of chiral phosphoramidite ligand L25



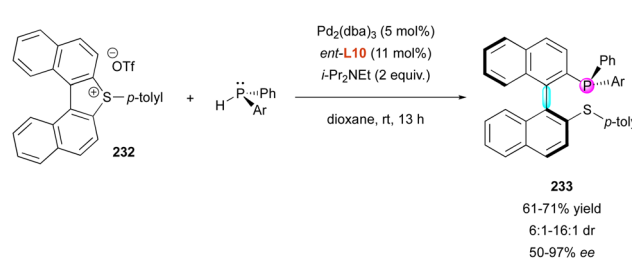
**Scheme 68** Enantioselective C–H arylation of phosphine oxides.



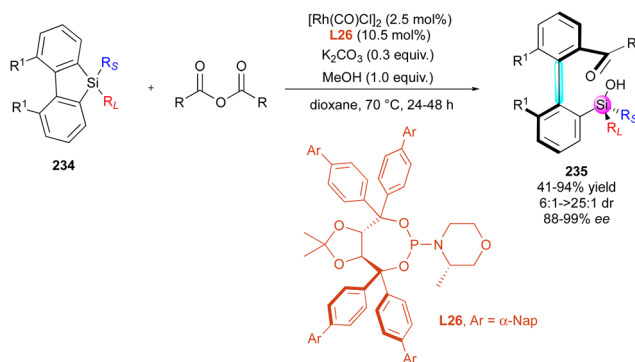
**Scheme 69** Pd-Catalysed assembly of *P*-stereogenic and axially chiral phosphinooxazoles.

(Scheme 69). The overall process involved the cleavage of the C–P bond, followed by concomitant C–H bond functionalisation with diverse aryl boronic acids and final treatment with S<sub>8</sub>. This unprecedented domino sequence was postulated to evolve *via* key chiral phosphapalladacycle 231 and the resulting atropisomeric binaphthyl phosphine sulfides 230, which are usually obtained with high diastereo- and atroposelectivities, can be easily reduced to the corresponding chiral phosphines and used as efficient ligands in the phosphine-catalysed enantioselective (3+2) cycloaddition. The same authors reported an extension of this approach using benzoxazoles/benzothiazoles instead of the boronic acid partners.<sup>114</sup> This palladium-catalysed enantioselective cleavage of C–P bond/intermolecular C–H bond functionalisation allowed related *P*-stereogenic and axially chiral phosphinooxazoles ligands to be obtained after a reduction step.

Another related Pd-catalysed desymmetrisation was recently reported by Huang and coworkers (Scheme 70)<sup>115</sup> *via* ring-opening of the cyclic biarylsulfonium salts 232 with phosphines, which led to the formation of atropisomeric phosphines 233 with a controlled stereogenic axis and phosphorous centre. Interestingly, a methyl was needed at the *ortho* position of the aryl substituent (Ar) of the phosphine, probably for better discrimination regarding the phenyl substituent. Indeed, when a less bulky group was introduced, such as a methoxy, the stereoselectivity dropped remarkably (50% ee and 6:1 dr *vs.* >87% ee and >10:1 dr for *o*-Me substituted aryls). Nevertheless, simple recrystallisation could be performed to improve the enantiopurity of products 233.



**Scheme 70** Pd-Catalysed enantioselective phosphination of cyclic biarylsulfonium salts.

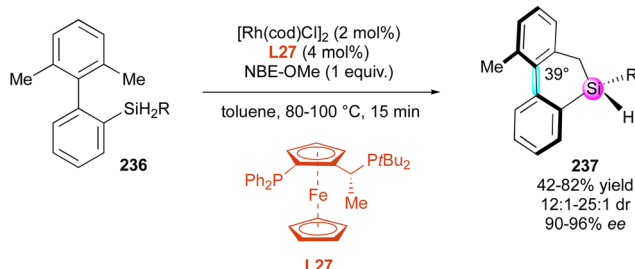


Scheme 71 Rh-Catalysed enantioselective ring-opening of silafluorenes.

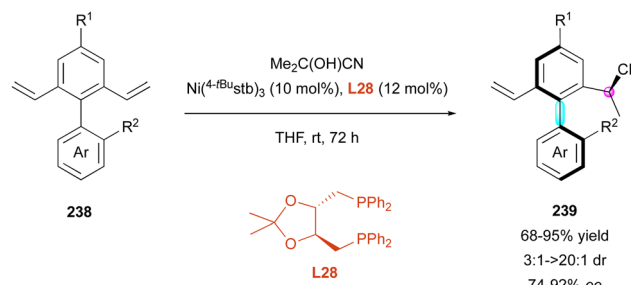
The use of silafluorenes 234 as a substrate by Gu's group allowed access to rare biaryl atropisomers 235, displaying one silicon-stereogenic centre, *via* rhodium-catalysed enantioselective ring-opening (Scheme 71).<sup>116</sup> The use of methanol as an additive allowed excellent diastereoselectivities to be achieved, supposedly acting as a ligand to the rhodium catalyst.

Complementarily, the desymmetrisation of biaryl dihydrosilanes 236 displaying di-*ortho*-substituted methyl groups was realised by the He group<sup>117</sup> based on intramolecular C–H silylation, generating a new type of axially chiral biaryl silicon-stereogenic silanes 237 in moderate yields with high enantioselectivities (Scheme 72). This unprecedented transformation is catalysed by a Rh(i) complex in the presence of Josiphos L27 as a chiral ligand and a norbornene derivative as a hydrogen acceptor (NBE-OMe), giving access to unusual atropisomeric six-membered ring bridged silicon-stereogenic dibenzoxasilines 237, in which the configuration of the stereogenic axis is controlled by the adjacent silicon-stereogenic centre with a large dihedral angle of 39°.

Fang and coworkers demonstrated that biaryl dienes 238 are also suitable substrates for desymmetrisation (Scheme 73).<sup>118</sup> The Ni-catalysed hydrocyanation of 238 using L28 as a chiral diphosphine ligand was reported with good enantio- and diastereoselectivity (one example with 3:1 dr, most of them with >20:1 dr). The authors showed the wide scope of the reaction with intriguing R<sup>1</sup> and R<sup>2</sup> substituents, such as halogens, nitrile, vinyl and heterocycles. Interestingly, a couple of products 239 could be used as the ligand and organocatalyst for enantioselective transformations.



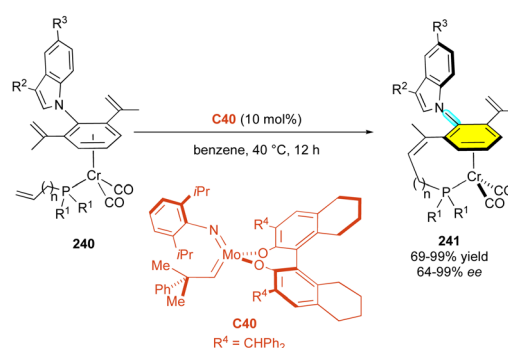
Scheme 72 Rh-Catalysed intramolecular atroposelective C–H silylation.



Scheme 73 Desymmetrisation via Ni-catalysed hydrocyanation of biaryl dienes.

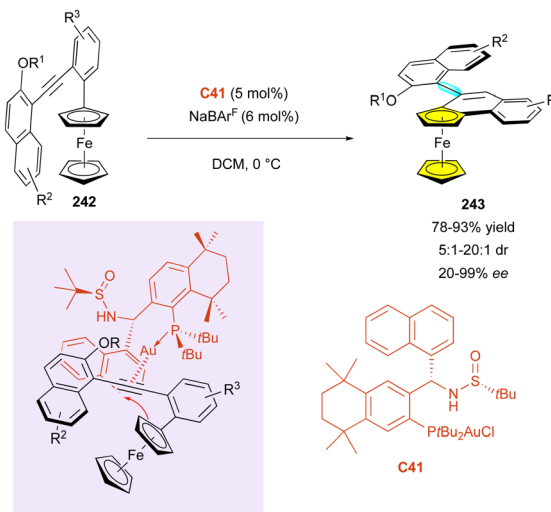
The combination of axial and planar chirality is a rarely encountered scenario, but inspired by the pioneer Uemura's diastereoselective desymmetrisation of planar chiral chromium complexes by enantiotopic *ortho* lithiation,<sup>119</sup> Kamikawa, Takahashi and Ogasawara developed a smart strategy to synthesise axially chiral *N*-aryllindole compounds 241 through enantioselective desymmetrising ring-closing metathesis (RCM) (Scheme 74).<sup>120</sup> They began with functionalised prochiral planar (arene)chromium complexes bearing an indolyl substituent, which is fixed in the *anti*-configuration relative to the chromium atom. The reactions were conducted in benzene at 40 °C with 10 mol% of *in situ*-generated chiral molybdenum catalyst C40. The presence of an electron-rich phosphine coordinated to the chromium was essential for achieving high yields and enantioselectivities. Under these conditions, chiral chromium complexes were efficiently produced, and both axial and planar stereogenic elements were simultaneously generated and controlled during the transformation.

More recent complementary results in this field were reported by the Wu, Li and Zhang group in 2021, with the gold-catalysed enantioselective hydroarylation of *ortho*-alkynylaryl ferrocene derivatives 242, allowing the simultaneous control of axial and planar chirality (Scheme 75).<sup>121</sup> Due to the linear coordination geometry of the Au(i) catalyst, control of the enantioselectivity is more challenging and the bulky chiral sulfoxime ligand is required for this reaction. The optimisation of the key 6-*endo*-dig cyclisation leading to the corresponding ferrocenyl atropisomers 243 resulted in the use of an enantiopure chiral Au(Sadphos)Cl precatalyst C41 and



Scheme 74 Enantioselective ring-closing metathesis.

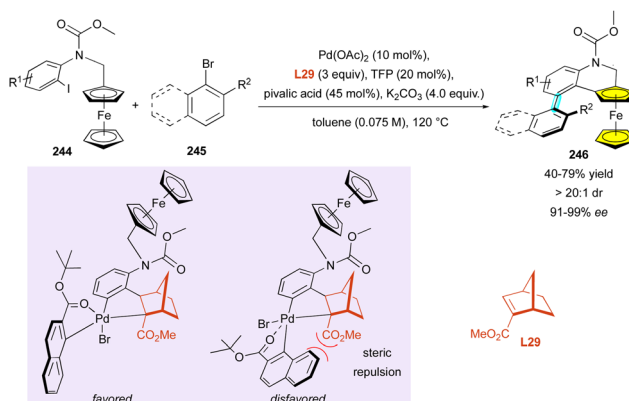




Scheme 75 Au-Catalysed hydroarylation reaction.

$\text{NaBAR}^{\text{F}}$  as an additive in dichloromethane at  $0\text{ }^{\circ}\text{C}$  for 24 h. The diastereoselectivity was improved by using cyclohexylmethyl as a protecting group for naphthol ( $\text{R}^1$ ) but substitution at the *ortho*-position of the aryl alkyne ( $\text{R}^3$ ) was detrimental for the enantioselectivity. The *Re* face of the alkyne is shielded by the naphthyl of the ligand, leading to the addition of the ferrocenyl by the Si face to secure the observed planar chirality, while control of the axial chirality is the result of the impeded rotation of the naphthalene ring provided by the presence of the alkoxy substituent ( $-\text{OR}^1$ ). DFT calculations supported the proposed reaction mechanism, where the enantioselectivity is achieved through  $\pi$ -stacking between the naphthyl groups of the catalyst and the substrate.

Following this first achievement in the desymmetrisation of ferrocene derivatives, the Li, Liu and Liang groups performed the synthesis of a library of ferrocenyl derivatives **246** exhibiting both axial and planar chirality using an enantioselective Catellani reaction (Scheme 76).<sup>122</sup> The catalytic system involved  $\text{Pd}(\text{OAc})_2$  (10 mol%) as the catalyst, tri(2-furyl)phosphine (TFP, 20 mol%) as the ligand and excess of chiral norbornene mediator **L29** (3 equiv.) at reflux in toluene for 24 h to perform

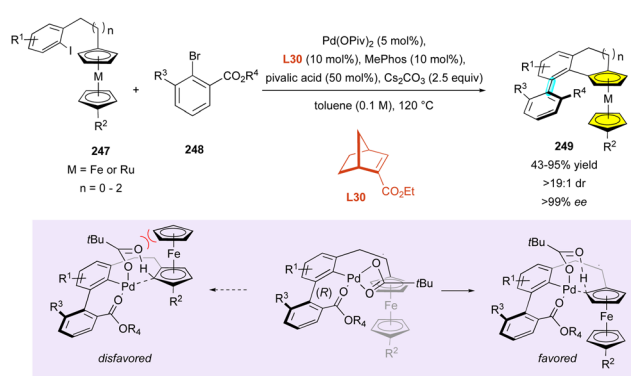


Scheme 76 Pd-Catalysed enantioselective Catellani reaction.

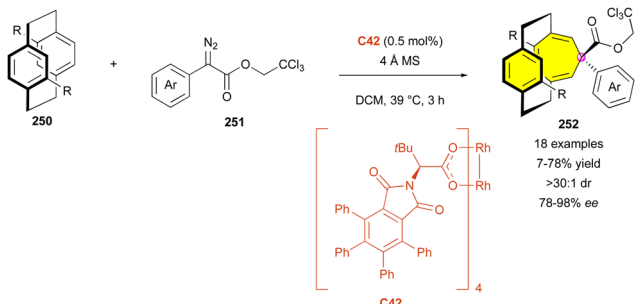
the reaction between 2-iodophenyl(methyl)carbamates **244** and 1-bromonaphthalenes **245**. Axially and planarly chiral products **246** were obtained in high enantio- and diastereoselectivity with a great tolerance for electron-donating and electron-withdrawing groups on the iodo-aryl partner. An axial-to-planar diastereoinduction model was proposed governed by the steric repulsion between the ester moiety of the chiral ligand and the naphthyl, in agreement with the observed diastereoselectivity.

Using a similar Catellani strategy, in 2023, the Zhou group described a domino sequence for the reaction between 2-iodophenethylferrocenes **247** ( $\text{M} = \text{Fe}$ ) and *ortho,ortho'*-disubstituted 2-bromoaryls **248** (Scheme 77).<sup>123</sup> In only 5 h in toluene at  $120\text{ }^{\circ}\text{C}$ , by using  $\text{Pd}(\text{OPiv})_2$ , MePhos and a catalytic amount of chiral enantiopure norbornene derivative **L30** (10 mol%), they obtained a library of fused five- to seven-membered rings **249** combining axial and planar stereogenicity with excellent enantio- and diastereoselectivity and in good to excellent yields. This method was efficiently extended to ruthe-nocenes **247** ( $\text{M} = \text{Ru}$ ), for which a dual cascade was observed and two sets of axial and planar stereogenic elements were obtained, always with high stereoselectivity. An axial-to-planar diastereoinduction model was also proposed for this reaction. Once the chiral axis is formed, the steric repulsion between the pivalic group and the ferrocene ring disfavored the formation of the (*Ra*, *Sp*) product.

Finally, although the desymmetrisation of [2.2]paracyclophanes are rarely encountered in the literature,<sup>124</sup> the Davies group newly reported their work on the reaction of donor/acceptor carbenes **251** with [2.2]paracyclophanes **250** (Scheme 78).<sup>125</sup> The reaction proceeded by rhodium-catalysed enantioselective cyclopropanation, followed by ring opening, leading to the formation of original centrally and planarly chiral [2.2]paracyclophanes **252** bearing a seven-membered ring. A very low catalytic loading (0.5 mol%) of **C42** allowed the construction of 18 examples in varying yields (7–78%) and very good enantioselectivity (78% to 98% ee) always with perfect diastereoselectivity. The reaction tolerated diverse (hetero)aromatic rings with both electron-donating and withdrawing substituents, decorated at the *para*, *meta* and *ortho* positions.



Scheme 77 Pd-Catalysed enantioselective Catellani reaction.



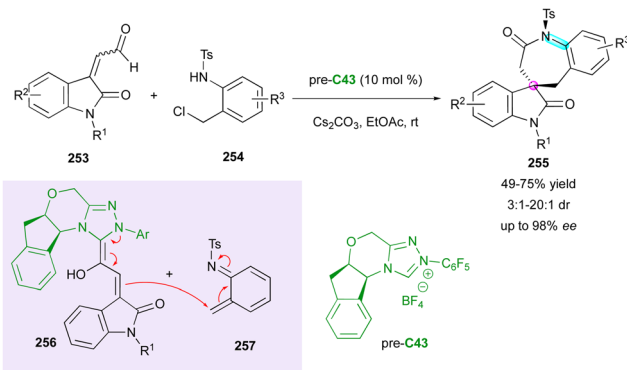
**Scheme 78** Rh(II)-Catalysed enantioselective ring expansion of [2.2]paracyclophanes.

Interestingly, the other enantiomer could be obtained using *ent*-C42 as the catalyst without any loss of efficiency.

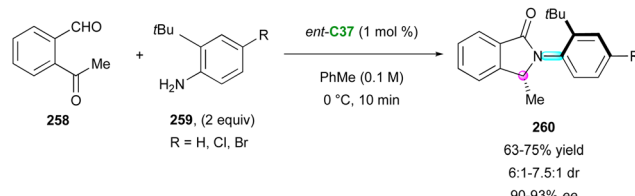
## Simultaneous construction of both stereogenic elements

### Organocatalysed transformations

**Central/axial stereogenic elements.** A pioneer contribution was proposed in 2016 by the Enders group with enantioselective access to original spirobenzazepinones 255 with control of the C–N axial chirality and a spirocyclic stereogenic centre (Scheme 79).<sup>126</sup> This very challenging strategy is based on NHC-catalysed (3+4) spiroannulation reactions using a combination of isatin-derived enals 253 and aza-*o*-quinone methides 257, generated *in situ* from *N*-(*ortho*-chloromethyl)aryl amides 254. Under basic conditions, NHC precatalyst pre-C43 reacts with the enal, leading to chiral Breslow homoenolate intermediate 256. This nucleophilic species can perform an enantioselective Michael-type addition to electrophilic aza-*o*-quinone methides 257, followed by spirocyclisation *via* intramolecular *N*-acylation to form seven-membered lactam 255, featuring a restricted stereogenic C–N axis. Interestingly, these unconventional atropisomers were found to be highly configurationally stable with atropodiastereomerisation at temperatures over 90 °C. The overall original sequence offers a very broad scope and decent yields (49–75%), with good to excellent



**Scheme 79** Enantioselective access to spirobenzazepinones bearing axial and spirocentral chirality.



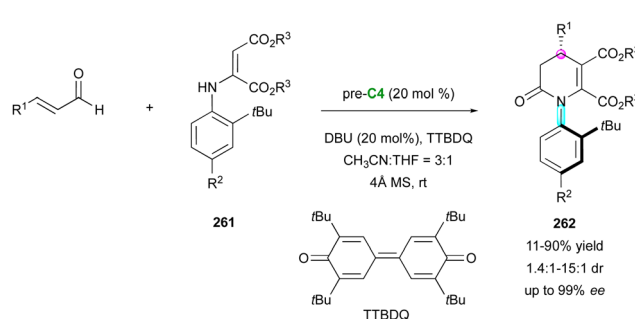
**Scheme 80** Enantioselective condensation between 2-acylbenzaldehydes and *o*-tBu-anilines.

diastereoselectivity (3/1 to >20:1 dr) and uniformly good to high enantioselectivity (76–98% ee).

Closely following these pioneering results, the Seidel group described the efficient catalytic enantioselective synthesis of C–N atropisomeric isoindolinones 260 due to the condensation of 2-acylbenzaldehydes 258 and anilines 259 following a biomimetic pathway (Scheme 80).<sup>127</sup> In the presence of only 1 mol% of CPA catalyst (*S*)-TRIP *ent*-C37, the reactions reached completion within 10 min and provided products with up to 98% enantiomeric excess. Three examples of anilines with an *ortho* *t*-butyl group formed atropisomeric products with decent diastereoselectivity, thereby enabling the simultaneous generation of axial and central stereoelements from achiral substrates by a simple dehydration sequence.

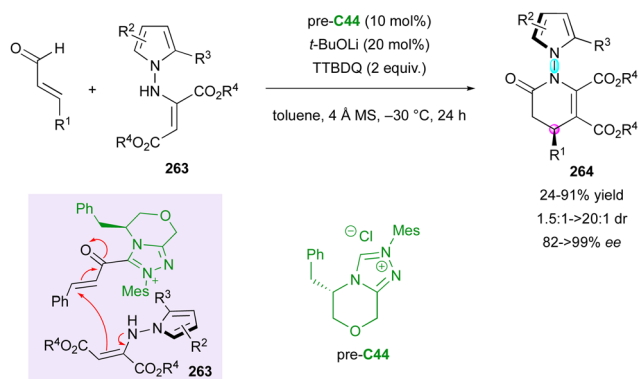
Similarly, in 2023, the Qi group reported a rare example of atroposelective access to dihydropyridinones scaffold 262 with a stereodefined C–N axis and bearing central chirality, starting from achiral 2-aminomaleate derivatives 261 and simple enals (Scheme 81).<sup>128</sup> This transformation uses the reactivity of the NHC catalyst in the presence of base (DBU) and oxidant (TTBDQ) to afford the desired products with high enantiomeric excess (up to 99% ee) in moderate to high yield (11–90%) and diastereoselectivity (1.4:1–15:1 dr). However, a bulky *tert*-butyl substituent is a requirement for high control of the stereoselectivity, which limits its applicability.

Correspondingly, the Biju group harnessed the power NHC catalysis for the creation of a stereogenic N–N axis together with a stereogenic carbon centre (Scheme 82).<sup>129</sup> Here, the presence of the benzyl group in precatalyst C44 was sufficient to dictate the approach of enamine 263 with excellent enantioselectivity and variable diastereoselectivity. Substantial rotational barriers were calculated ( $\approx 250$  kJ mol<sup>-1</sup>), justifying the very high



**Scheme 81** Enantioselective synthesis of dihydropyridinones bearing a stereogenic C–N axis.



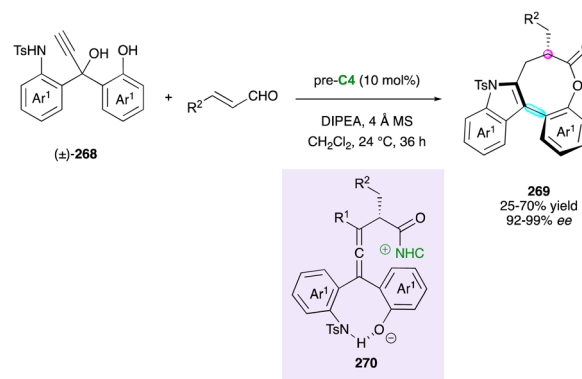


Scheme 82 NHC-Catalysed diastereoselective (3+3) annulation.

configurational stability of **264** and leading to a large range of products (51 examples) with moderate to very good yields.

Very recently, a related strategy involving oxidative NHC-organocatalysis was disclosed by Wong and Lu for the atroposelective synthesis of rare N–N axially and centrally chiral indoles and pyrroles **266** (Scheme 83).<sup>130</sup> This concept is based on the enantioselective construction of the 5,6-dihydro-pyrimidine ring using chiral  $\alpha,\beta$ -unsaturated acylazoliums from enals as C3-synthons towards the aza-Michael addition of readily available isothioureas **265**, leading to the key centrally chiral acylazolium intermediate **267**, which evolved by intramolecular *N*-acylation to the final N–N atropisomers **266**. The reaction is efficient in terms of yield and enantioselectivity even if only moderate to good diastereoselectivities were generally observed. The experimental evidence corroborated by DFT calculations clearly indicates an interesting negative non-linear effect (NLE), suggesting that a second NHC molecule helps to activate the isothiourea function in the enantio-differentiating transition state. The desired products **266** showed reasonable atropostability with a diastereomerisation barrier of 155 kJ mol<sup>-1</sup> (for R<sup>1</sup> = Ph, R<sup>2</sup> = H, R<sup>3</sup> = Me).

The Wong and Zhao group successfully applied their NHC-catalysed atropoenantioselective benzofurannulation (see Scheme 67) to the synthesis of related indole-derived bridged biaryls **269** (Scheme 84).<sup>108</sup> Starting from racemic propargylic tosylamidophenols ( $\pm$ )-**268**, they observed highly



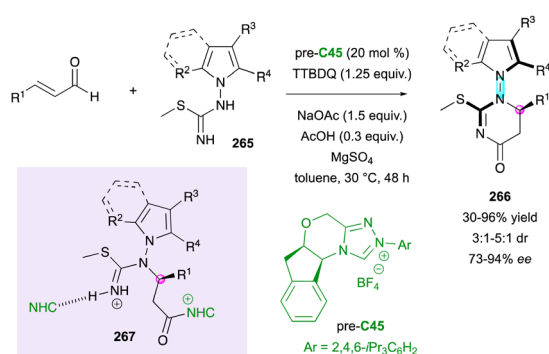
Scheme 84 Atroposelective synthesis of indole-derived bridged biaryls.

chemoselective sequential intramolecular *O*-acylation and *N*-alkylation from key acyl azolium intermediate **270**, producing eight-membered ring bridged lactones **269** featuring central and axial stereogenic elements.

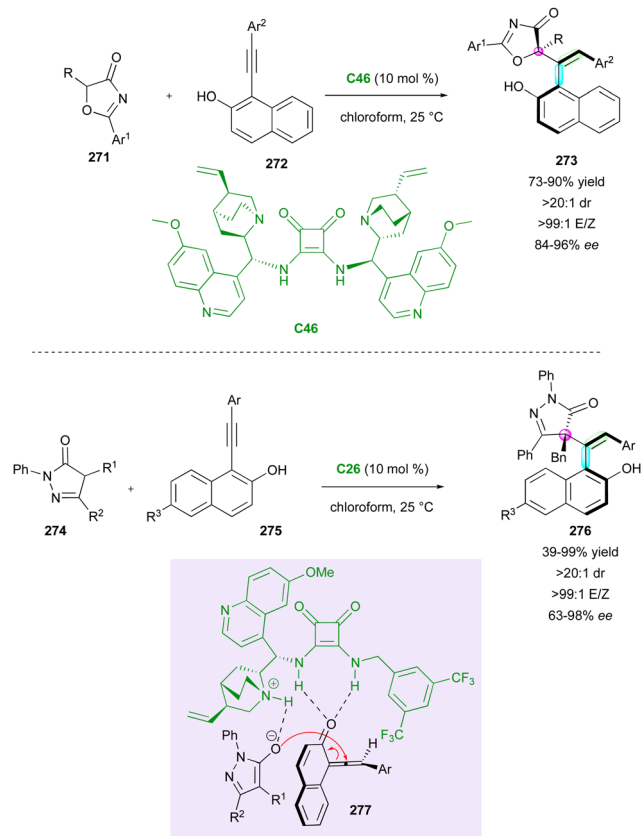
The highly electrophilic reactivity of the allene function combined with its intrinsic axial chirality makes this intriguing structural unit a particularly efficient intermediate for the control of multi-chirality (see Schemes 21–23). Also, the *in situ* generation of chiral vinylidene-quinone methides (VQMs)<sup>131</sup> from 2-alkynylnaphthols by organocatalysis has recently attracted interest for the simultaneous control of multiple stereogenic elements involving cycloadditions or nucleophilic additions with the transfer of chirality.<sup>132</sup>

In this context, in 2019, Liu, Yan and Li described the enantioselective one-pot construction of intriguing molecules **273** bearing a stereogenic carbon atom, an axially chiral styrene with a stereoisomeric double bond (Scheme 85).<sup>133</sup> They employed 5*H*-oxazol-4-ones **271** as nucleophilic partners towards 2-alkynylnaphthols **272**. This method enabled the rapid construction of a series of stereochemically complex products **273** with excellent *E,Z* selectivity, diastereoselectivity (>20:1 dr), and enantioselectivity (up to 96% ee). The reaction proceeds under mild reaction conditions, tolerates a range of functional groups, and is applicable to gram-scale synthesis. Two years later, the same strategy was successfully employed by Wang with pyrazolones **274** as nucleophiles, with *in situ*-generated chiral VQM intermediates **277** under hydrogen-bonding organocatalysis with **C47** yielding fully enantiocontrolled products **276** within a shorter reaction time (5 to 6 h).<sup>134</sup> Benzyl derivatives (R<sup>1</sup>) are preferable in terms of enantioselectivity, but modifications on other positions are very well tolerated. Gram-scale synthesis was performed smoothly without the loss of efficiency or stereoselectivity.

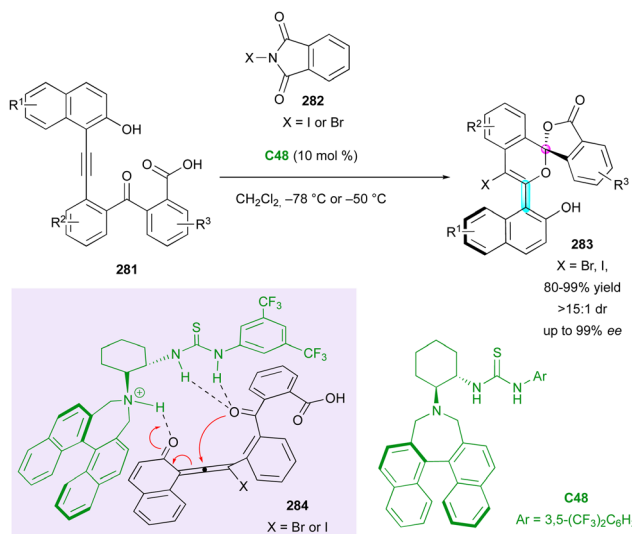
Simultaneously, the Yan group reported an intramolecular nucleophilic addition on transient chiral VQMs as a unique example of the fully controlled enantioselective synthesis of three different stereogenic elements generated simultaneously from properly functionalised achiral substrates using organocatalysis (Scheme 86).<sup>135</sup> They smartly designed 1-(2-(9*H*-carbazol-9-yl)phenyl)naphthalen-2-ols **278**, which undergo concomitant electrophilic bromination, leading to chiral VQM



Scheme 83 Organocatalytic atroposelective synthesis of N–N axially chiral indoles and pyrroles.



Scheme 85 Enantioselective intermolecular nucleophilic addition on VQM intermediates.

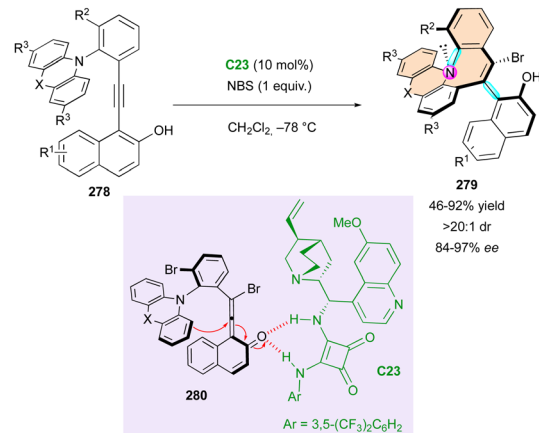


Scheme 87 Enantioselective synthesis of spiroketal lactones with both axial and central chirality.

tolerated both electron-withdrawing and donating groups without the loss of enantioselectivity.

The Hong group was inspired by this intramolecular approach, who reported an alternative enantioselective domino strategy for the construction of spiroketal lactones **283** containing both a C–C stereogenic axis and a spirocyclic quaternary stereogenic centre (Scheme 87).<sup>136</sup> The key chiral VQM intermediates **284** were generated *via* electrophilic halogenation of functionalised 2-alkynyl naphthols **281** using *N*-haloimides **282** in the presence of bifunctional thiourea catalyst **C48**, triggering an intramolecular domino annulation, which resulted in the construction of axial and central chirality by the transfer of axial chirality. This elegant spiroannulation tolerated a broad functional diversity, producing a large new family of atropisomeric and centrally chiral spiroketals **283** in good yields (up to 99%) with high enantio- and diastereoselectivities (up to 98%, >20:1 dr).

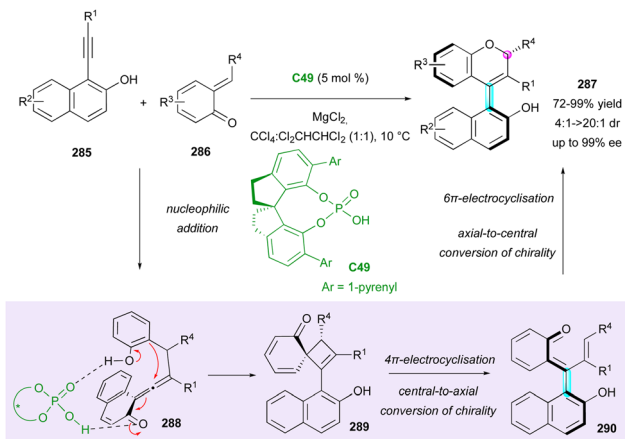
In a related intramolecular trapping of a chiral VQM intermediate, the Zhou group performed the enantioselective synthesis of a new class of naphthyl-2*H*-chromene derivatives **287** bearing both central and axial chirality (Scheme 88).<sup>137</sup> CPA catalyst **C49** was used as a dual hydrogen-bonding activator, performing the enantioselective nucleophilic addition of 2-alkynyl naphthols **285** to *o*-quinone methides **286** (*o*-QMs) as *C*-electrophiles, which resulted in the generation of the corresponding chiral all-carbon tetrasubstituted VQM intermediates **288** instead of the hetero-Diels–Alder reaction with a triple bond. Based on DFT calculations, the reaction seems to evolve by an intramolecular dearomatic Michael-type addition to spirocyclobutene intermediate **289**, suffering 4*π* electrocyclic ring opening, which determines the resulting configuration of the stereogenic axis in **290** by central-to-axial chirality conversion. The last step is an oxa-6*π*-electrocyclisation, providing stable chiral naphthyl-2*H*-chromene derivatives **287** *via* an axial-to-central chirality conversion. This efficient synthesis



Scheme 86 Enantioselective intramolecular nucleophilic addition on chiral VQM intermediates.

intermediates **280**, followed by annulation to yield a new class of chiral azepines **279** displaying two chiral axes (C–C and C–N) and a stereogenic nitrogen atom, which together resulted in an inherent helical shape of the fused heterocyclic moiety. Low temperature (−78 °C) and *N*-bromosuccinimide (NBS) quickly afforded azepines **279** in excellent yields and stereoselectivities. A gram-scale reaction could be achieved and the reaction

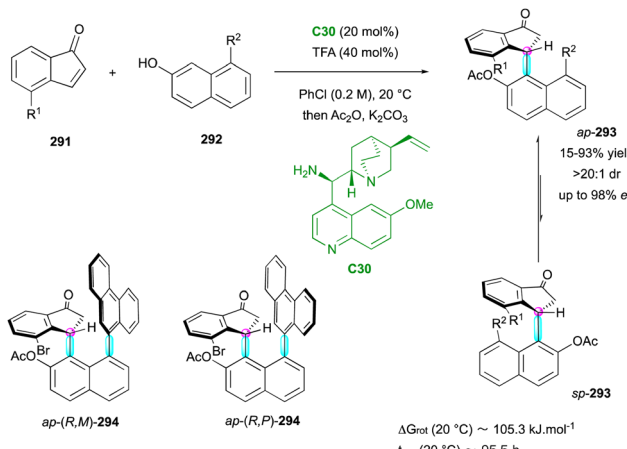




**Scheme 88** Enantioselective synthesis of axially and centrally chiral naphthyl-2H-chromenes.

provided the product in excellent yield (72–99%) with high enantioselectivity (81–99%) and moderate to high diastereoselectivity (4:1 to >20:1 dr).

Recently, a new class of conformationally stable  $C(sp^2)-C(sp^3)$  atropisomers was discovered in some natural products,<sup>138</sup> attracting interest from chemists for the enantioselective synthesis of these unusual molecular frameworks. In 2017, the Bencivenni group reported the first case of thermodynamic control of the  $C(sp^2)-C(sp^3)$  stereogenic axis (Scheme 89).<sup>139</sup> They performed the enantioselective Friedel–Crafts-type alkylation of properly functionalised inden-1-ones 219 with 8-substituted 2-naphthols 292 using chiral quinidine derivative C30 as the catalyst. Interestingly, under these conditions, with bulky  $R^2$  groups, a single antiperiplanar conformational diastereomer *ap*-293 combining axial and central chirality was obtained with very high enantioselectivity (up to 98% ee). This clearly indicates that the barrier for the rotation of the  $C(sp^2)-C(sp^3)$  bond is high enough to prevent atropodiastereomerisation to *sp*-293. This experimental observation was corroborated by DFT calculations, indicating that the

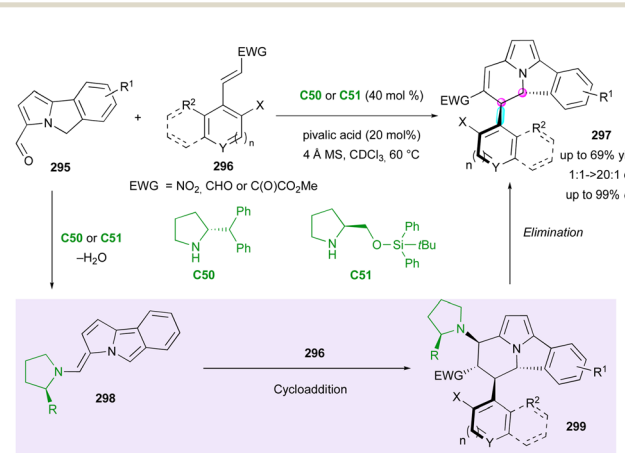


**Scheme 89** Enantioselective synthesis of stable  $C(sp^2)-C(sp^3)$  atropisomers via Friedel–Crafts-type alkylation.

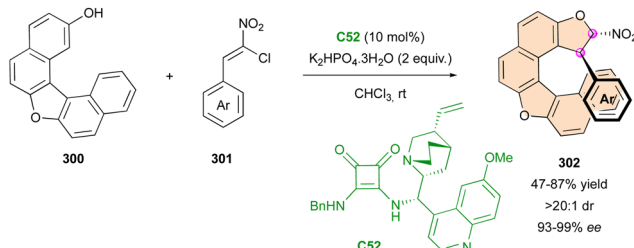
bulkiest are the groups on the 8-position of naphthol 292 and on the 4-position of inden-1-ones 291, making the atropodiastereomerisation barrier higher. A step further was possible when  $R^2$  = phenanthrenyl, albeit in the low yield of 15%, obtaining a 1:1 mixture of two diastereomers *ap*-(*R,M*)-294 and *ap*-(*R,P*)-294 featuring two stereogenic axes and one stereogenic centre in 94% and 65% ee, respectively.

Some years later, the Jørgensen group published one of the first case of multi-stereogenic synthesis including a conformationally stable  $C(sp^2)-C(sp^3)$  bond and two consecutive stereogenic centres (Scheme 90).<sup>140</sup> This new approach was developed with two different chiral pyrrolidine catalysts, C50 or C51, in combination with pivalic acid. This catalytic system provided the addition of 5*H*-benzo[*a*]pyrrolizine-3-carbaldehydes 295 to olefin-bearing electron-withdrawing group 296 as Michael acceptors, leading to the corresponding cyclised product 297 with moderate yield (up to 69%) and moderate to excellent enantio- and diastereoselectivity (up to 99% ee, from 1:1 to >20:1 dr). The plausible mechanism involves enamine intermediate 298 from aldehyde 295 with the pyrrolidine catalyst in acid condition followed by a Michael/Mannich-type cyclisation sequence with the olefin rendering the final chiral atropisomeric heterocycle 297 after regeneration of the catalyst by elimination from intermediate 299.

**Central/helical stereogenic elements.** Although the combination of central and axial stereogenicity has flourished the last few decades, the stereoselective control of helicoidal structures featuring a stereogenic centre is still in its infancy. In 2020, our group reported the first example of organocatalysed access to centrally and helically chiral molecules 302 by a new helicoselective heteroannulation (Scheme 91).<sup>141</sup> The Michael/O-alkylation heteroannulation sequence proved to be robust for the synthesis of axially chiral furan<sup>142</sup> and has been exploited for the control of helical chirality. Hence, the reaction between achiral dinaphthofuranols 300 and chloronitroalkenes 301 in the presence of bisquaramide organocatalyst C52 in chloroform at room temperature afforded dihydronaphthofurans 302, displaying both a helix and two stereogenic carbon atoms in good



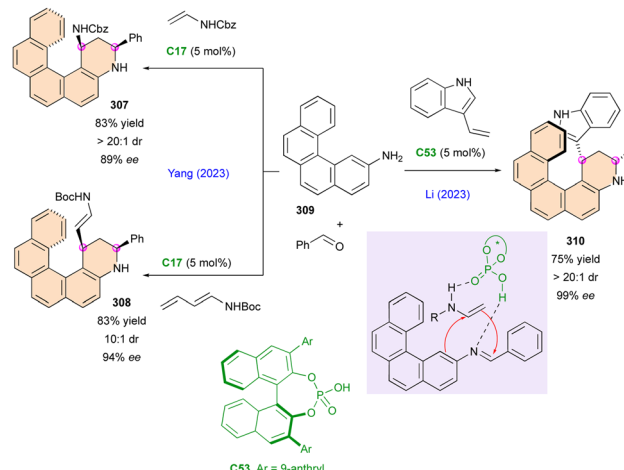
**Scheme 90** Enantioselective organocatalytic synthesis of conformationally stable  $C(sp^2)-C(sp^3)$  atropisomers.



Scheme 91 Helicoselective heteroannulation of naphthol derivatives.

yield and high enantio- and diastereoselectivity. The reaction was performed with a wide range of nitroalkenes without affecting the yield and the stereoselectivity. The configurational stability of dioxa[6]helicenoids **302** was ensured by the remote steric effect of the aryl substituent. Only one diastereomer was observed and a DFT study of the diastereomerisation barrier unveiled that the event is thermodynamically unfavorable due to its low “return barrier” of only 29 kJ mol<sup>-1</sup>.

The synthesis of small molecules with a stable helical shape, particularly when incorporating five-membered rings, presents a significant challenge in organic chemistry. The inherent instability of these configurations complicates their production and necessitates the development of new methodologies. In the following very recent study, our group introduced a padlocking technique employing the enantioselective organocatalytic domino furannulation shown before (Scheme 91). This method allows the controlled synthesis of helically chiral tetracyclic structures **304**, containing one or two five-membered rings, from carefully designed achiral fused-tricyclic precursors **303** (Scheme 92).<sup>143</sup> Through this approach, we achieved simultaneous control of both the central and helical chirality, addressing a crucial need in this field. Moreover, applying this protocol to achiral naphthofuran **305** having a low barrier to rotation of only 55.7 kJ mol<sup>-1</sup>, we were pleased to observe the clean formation of products **306** displaying three different stereogenic elements, in good yield, excellent enantioselectivity

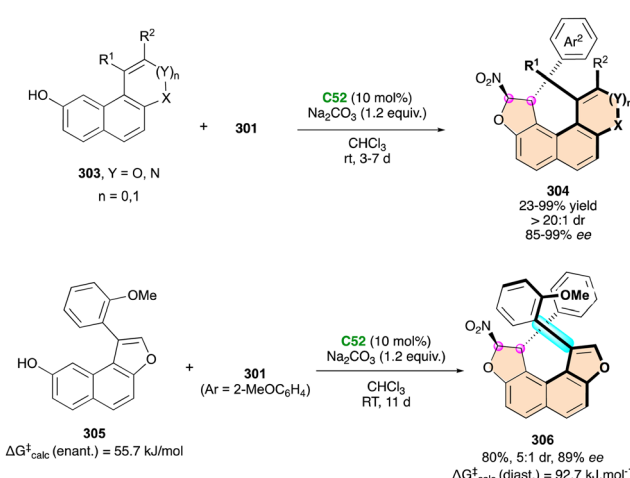


Scheme 93 Helicoselective Povarov reaction.

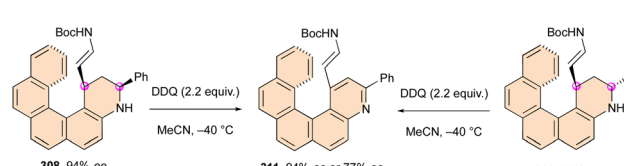
and in a decent 5:1 diastereomeric ratio, relative to the configuration of the stereogenic C-C bond. Noteworthy, the generation of this still rare family of enantioenriched compounds featuring axial, central and helicoidal stereogenic elements was achieved through a one-step synthesis.

A conceptually related sequential oxidative helicoselective heteroannulation was reported in 2023 independently by the Li<sup>144</sup> and Yang<sup>145</sup> groups, who proposed two complementary elegant methods to access azahelicene structures based on a CPA-catalysed three-component Povarov reaction followed by oxidative aromatisation of the transient helicoidal tetrahydroquinolines featuring two stereogenic centres. Although the overall one-pot oxidative process is efficient and general for the preparation of a large series of aza[4]- and aza[5]helicenes, the corresponding multi-chiral helicenoid tetrahydroquinolines were isolated only once by Li (**310**) and twice by Yang (**307** and **308**) (Scheme 93).

In both contributions, the proposed selective functionalisation of benzo[c]phenanthrene-2-amine **309**, in the presence of benzaldehyde and enamides or 3-vinyl-indole gave the expected centrally and helically chiral tetrahydroquinolines **307**, **308** and **310**, respectively, in good yield and high stereocontrol. Alternatively, in the study by Li, the relative 1,3-configuration of **310** was not determined, while Yang was able to separate the two diastereomers of **308** and **312** and showed that their respective DDQ oxidation afforded the same aza[5]helicene **311** (Scheme 94). This result is in agreement with the helical chirality being determined by the formation of the C-1 stereocentre of tetrahydroquinoline **308**. Finally, the mechanistic studies proposed by Yang suggested that the (4+2)

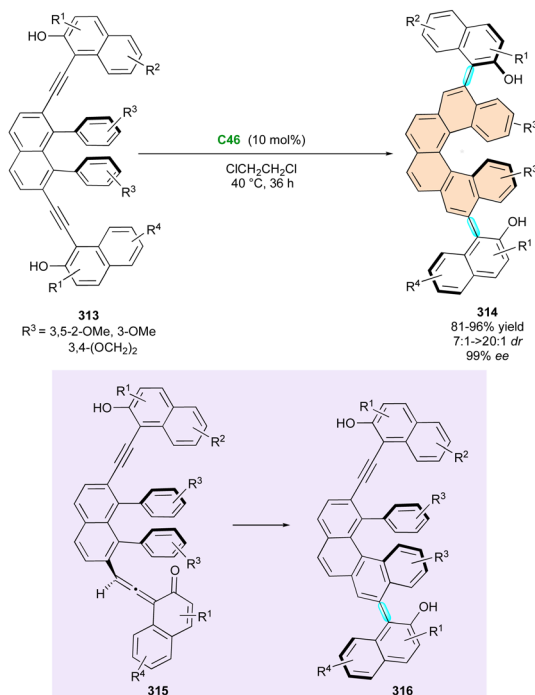


Scheme 92 Enantioselective construction of configurationally locked helically-chiral tetracyclic scaffolds.



Scheme 94 DDQ oxidation of diastereomeric helicoidal tetrahydroquinolines.



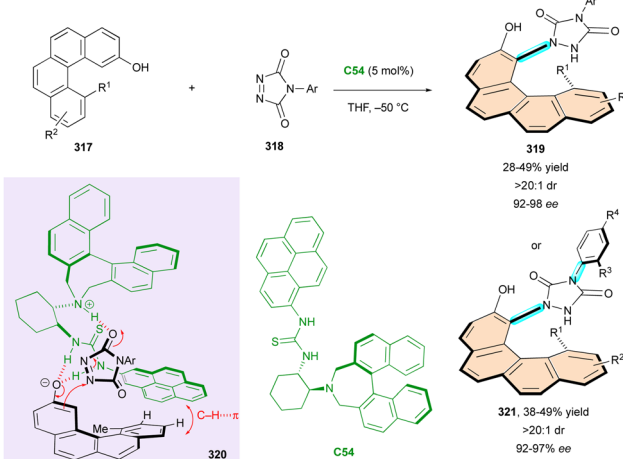


Scheme 95 Enantioselective synthesis of axially chiral carbo[6]helicenes.

cycloaddition reaction could occur in a stepwise manner, fully catalysed by the CPA with perfect stereocontrol.

**Axial/helical stereogenic elements.** In 2019, Yan's group leveraged the reactivity of chiral VQMs to design an innovative method for synthesising optically active carbo[6]helicenes 314, which feature two distant stereogenic axes (Scheme 95).<sup>146</sup> Using the spinol-derived CPA organocatalyst C46, they successfully transformed the carefully designed *ortho*-alkynylphenols 313 into carbo[6]helicenes 314 with high diastereo- and enantioselectivity *via* the corresponding chiral VQM intermediates 315. The mechanistic studies revealed that the initial cyclisation step produced an intermediate with a stereogenic axis, as demonstrated by the isolation of mono-cyclisation products 316 with 99% ee after just 8 h of reaction. The remaining helix and stereogenic axis were formed through a DKR process, enabling a catalyst-controlled stereodivergent approach to access the different diastereomers of this complex structure.

C–H *peri*-functionalisation of 2-hydroxybenzo[*c*]phenanthrene derivatives 317 was reported by Liu and Wang for the efficient assembly of 1,12-disubstituted carbo[4]helicenes (Scheme 96).<sup>147</sup> Hence, organocatalyst C54 promoted the simultaneous *atropo*- and helicoselective C–H amination of 317 with highly electrophilic diazocarboxamide partners 318, delivering the desired carbo[4]helicenes 319 in moderate yield but excellent diastereo- and enantioselectivities. DFT calculations revealed that a dual hydrogen-bonding activation between the thiourea N–H group and phenolate moiety for one part and between the alkylammonium ion and the diazocarboxamide for the other part accounted for the observed stereochemistry. In the major transition state 320, supplementary favorable C–H–π interactions between the pyrenyl substituent of the catalyst and

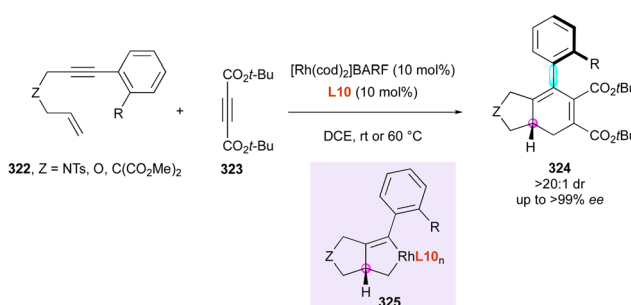


Scheme 96 Atropo- and helicoselective C–H amination of benzophenanthrols.

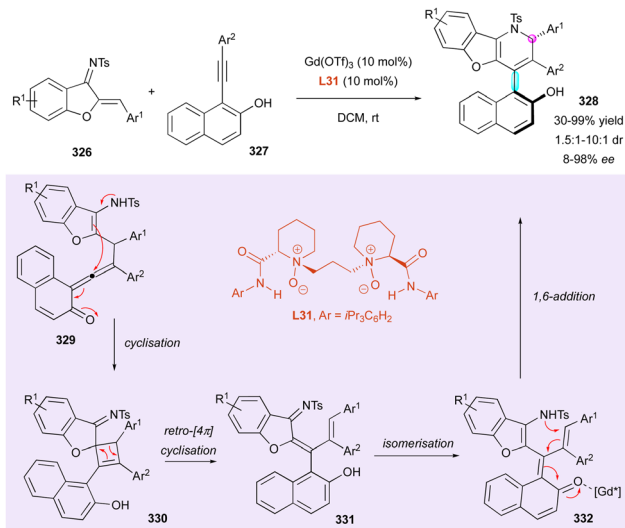
phenanthrenol substrate 317 were postulated. Remarkably, the authors reported the use of prochiral diazocarboxamide 318 as a substrate for the control of an additional stereogenic C–N bond in final structure 321.

**Metal-catalysed transformations.** In 2008, the Shibata group reported the first Rhodium-catalysed [2+2+2] cycloaddition to construct fused aryl-substituted cyclohexadienes 324 bearing central and axial stereogenic elements (Scheme 97).<sup>148</sup> Initially, they optimised the reaction between nitrogen-tethered enynes 322 with a naphthyl group on their terminal alkyne and 1,4-dimethoxybut-2-yne as a model reaction. (S)-SegPhos ligand L10 was found to give the best yield but moderate diastereoselectivity (dr = 2 : 1) within one hour. Subsequently, the reaction conditions were further optimised to enhance diastereoselectivity by increasing the reaction temperature to 60 °C and adding di-*tert*-butyl acetylenedicarboxylate 323 dropwise. Central chirality was introduced at the ring-fused position of bicyclic rhodacyclopentene intermediate 325 through the oxidative coupling of the metal centre with an enyne. The configuration of the stereogenic axis was not controlled at this stage, but during the following reaction with the alkyne.

Functionalised alkynes are also prone to react with electron-deficient alkenes following a [2+2] cycloaddition/retroelectrocyclisation (CA-RE) sequence to synthetically useful 1,3-butadiene



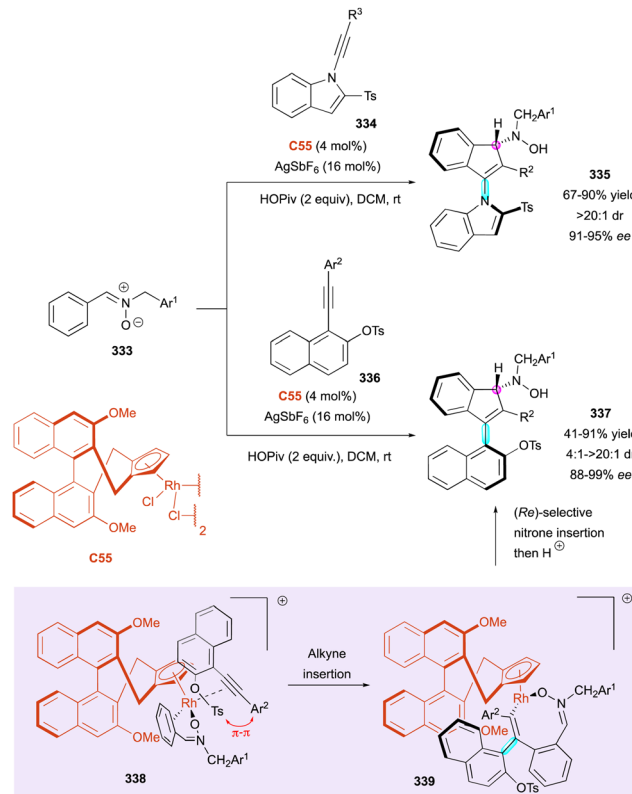
Scheme 97 Rh-Catalysed [2+2+2] atroposelective cycloaddition.



**Scheme 98** Gd-Catalysed [2+2] cycloaddition/retroelectrocyclisation cascade.

intermediates.<sup>149</sup> This attractive strategy was elegantly exploited by Cao and Feng in 2023, starting with *ortho*-alkynyl naphthols 327 and 1-azadienes 326 to obtain axially and centrally chiral 1,2-dihydrobenzofuro[3,2-*b*]pyridines 328 (Scheme 98).<sup>150</sup> The catalytic process was performed using a L31-gadolinium(III) complex as the Lewis acid, triggering the *in situ* formation of reactive vinylidene quinone methides (VQMs) 329 as precursors of [2+2] cycloadduct intermediate 330. In most cases, centrally and axially chiral dihydrobenzofuro-pyridines 328 were obtained with decent to high stereocontrol together with good yields after 1 to 7 days of reaction at room temperature. Lower stereoselectivities were observed when changing the *N*-protecting group to a methyl sulfonyl and the enantiocontrol was negatively affected with *ortho*-substituted aryl (Ar<sup>1</sup> and Ar<sup>2</sup>). The proposed mechanism emphasises the formation of axially chiral intermediate 331, which after tautomerisation gives 331, evolving by a stereoselective 1,6-conjugate addition with an overall axial-to-central conversion of chirality and leading to centrally and axially chiral dihydrobenzofuro-pyridines 328 with decent to high stereocontrol.

1-Alkynyl tosylindoles 334 were identified by Li and collaborators as powerful partners for the development of an efficient enantioselective Rh(III)-catalysed (3+2) annulation, initiated by a C-H activation of an aryl nitrone 333 acting as an electrophilic directing group (Scheme 99, top).<sup>151</sup> The enantiopure bis-methoxy Cramer-type (*R*)-CpxRh(III) catalyst C55 proved to be optimal to give the expected pentatomic C–N atropisomeric cycloadducts 335 bearing a distal C-centred point-chirality with excellent diastereo- and enantioselectivity. Extrapolation to *ortho*-tosyloxy-naphthyl-substituted alkynes 336 proceeded with the same global efficiency when Ar<sup>2</sup> is a bulky aromatic substituent to form the corresponding axially and centrally chiral indene derivatives 337 (Scheme 99, bottom). The experimental observations combined with DFT



**Scheme 99** Rh-Catalysed (3+2) cycloaddition to C–N and C–C axially and centrally chiral indenes.

calculations allowed the identification of two enantio-determining steps under the catalyst control and highlighted the crucial role of the tosyl substituent in 336, given that changing the 2-OTs group to 2-OMs led essentially to no reaction. Firstly, the alkyne insertion in 338 determines the atroposelectivity and the folding of the tosyl group allows a stabilising  $\pi$ – $\pi$  stacking, which reduces steric repulsion with the nitrone group. Secondly, the diastereoselectivity of the reaction is dictated by 339 *via* the migratory insertion of Rh-alkenyl to nitrone driven by the oxygen-tethering effect.

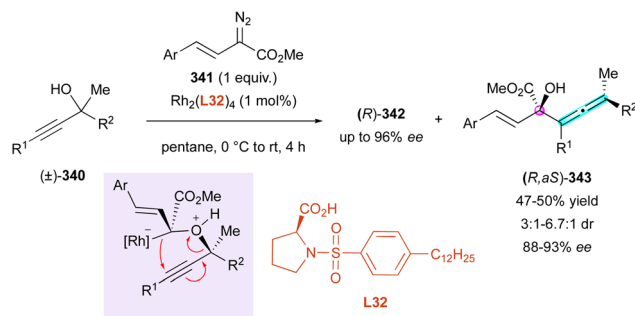
## Enantioselective synthesis of axially chiral allenes bearing central chirality

### Metal-catalysed approaches

In complement with previous strategies for the control of multiple stereogenic elements in the central, axial, planar, and helicoidal series, axially chiral allenes with point chirality also constitute targets of recent interest.

In 2012, Davies and colleagues exploited the well-established transition-metal-catalysed functionalisation of propargylic alcohols<sup>152</sup> for the enantioselective synthesis of a few centrally and axially chiral products (*R,aS*)-343 from racemic propargylic tertiary alcohols ( $\pm$ )-341 with moderate to good diastereoselectivity and high enantiomeric excess (Scheme 100).<sup>153</sup> Mechanistically, the reaction proceeds through a rhodium-catalysed



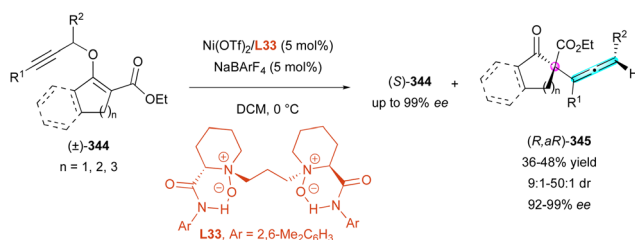


Scheme 100 Enantioselective Rh-catalysed ylide formation/[2,3]-sigmatropic rearrangement.

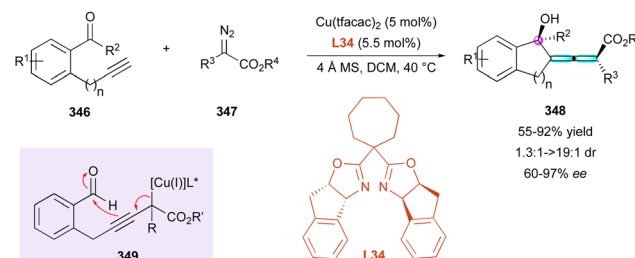
[2,3]-sigmatropic rearrangement in the presence of *N*-sulfonyl (*S*)-proline ligand **L32**, with migration of the tertiary alcohol revealing both stereogenic elements. This method has not been broadly exemplified and the diastereoselectivity seems to be dependent on the substrate, but it represents one rare example of the enantioselective synthesis of centrally and axially chiral allenes.

Similarly, four years later, Liu, Feng, and coworkers designed racemic propargyl vinyl ethers  $(\pm)$ -344 capable of undergoing sigmatropic Claisen rearrangement for the synthesis of centrally and axially chiral allenes (*R,AR*)-345 *via* a KR process, also producing  $(S)$ -344 in up to 99% ee (Scheme 101).<sup>154</sup> The nickel-catalysed reaction in the presence of chiral *N,N'*-dioxide ligand **L33** allowed the isolation of several examples with excellent stereoselectivity (9:1 to 50:1 dr and 92% to 99% ee). Interestingly, the size of the carbocycle in the substrate plays a crucial role in the reactivity of the transformation. Indeed, for  $(\pm)$ -344a ( $n = 1$ ,  $R^1 = \text{Ph}$ ,  $R^2 = \text{Me}$ ), the reaction was completed after one hour at  $-20$  °C, whereas with  $(\pm)$ -344b ( $n = 3$ ,  $R^1 = \text{Ph}$ ,  $R^2 = \text{Me}$ ), almost a day at 35 °C was necessary for complete transformation. Additionally, the diastereoselectivity seemed to be impacted by the presence of bulky  $R^1$  and  $R^2$  substituents.

In 2021, using a copper-catalysed cross-coupling/alkynyllogous aldol sequence, the Sun group displayed access to chiral cyclic  $\alpha$ -allenols 348 containing both central and axial stereogenic elements (Scheme 102).<sup>155</sup> A copper(II) salt combined with BOX ligand **L34** was used to perform this enantioselective transformation starting from 2-prop-2yn-1-ylbenzaldehydes 346 and  $\alpha$ -phenyl diazoacetates 347 to give five-membered



Scheme 101 Enantioselective Claisen rearrangement for the synthesis of chiral allenes.

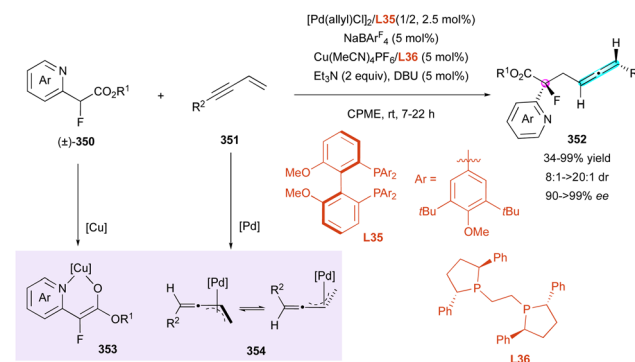


Scheme 102 Cu-Catalysed cross-coupling/alkynyllogous aldol sequence.

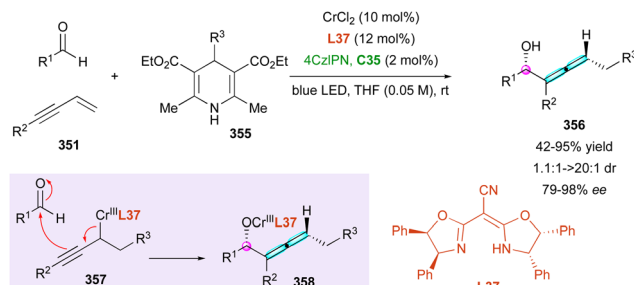
ring products 348 in good to excellent yields, enantiomeric excess and diastereoselectivity. Modifications of the diazo partner were well tolerated, but the utilisation of ketones ( $R^2 = \text{Me}$ ) and the formation six-membered rings ( $n = 2$ ) were far less efficient or even not feasible for four-membered analogues ( $n = 0$ ). The copper–carbene migratory insertion to the alkyne was enantio-determining for the control of both the axial and central chirality.

Capitalising on the stereoselective formation of chiral allenes by the hydrofunctionalisation of conjugated enynes, Lin, He, and collaborators showed that this transformation can be combined with a DKR process when racemic fluorinated esters  $(\pm)$ -350 are used as pronucleophiles (Scheme 103).<sup>156</sup> This method relied on an enantioselective dual Cu/Pd synergistic catalysis with two complementary chiral ligands **L35** and **L36** for palladium and copper, involving the reversible *in situ* formation of nucleophilic copper-enolate intermediate 353 and electrophilic  $\pi$ -allylpalladium complex 354, respectively. Both stereogenic elements could be controlled efficiently, leading to the formation of a large number of tertiary fluoride-tethered allenes 352 with very high stereoselectivity (8:1 to  $>20:1$  dr and 90% to  $>99\%$  ee). Interestingly, the nature of the Ar groups of biaryl diphosphine ligand **L35** was crucial given that a simple phenyl gave almost no diastereoselectivity.

One year later, Wang's group reported the elegant three-component dual photoredox and chromium-catalysed radical 1,4-functionalisation of 1,3-enynes for the preparation of chiral  $\alpha$ -allenols 356 bearing a C-centred stereogenic element (Scheme 104).<sup>157</sup> The conditions were optimised using



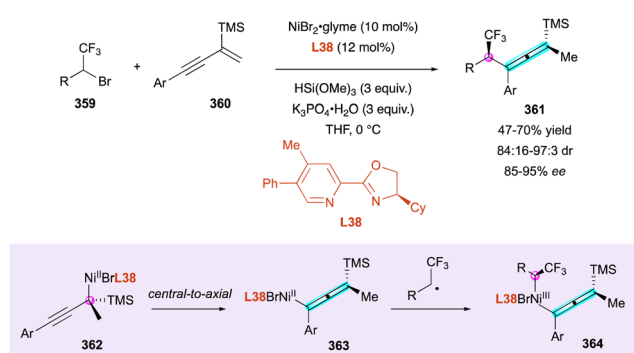
Scheme 103 Dual Cu/Pd-catalysed stereodivergent synthesis of fluoride-containing allenes.



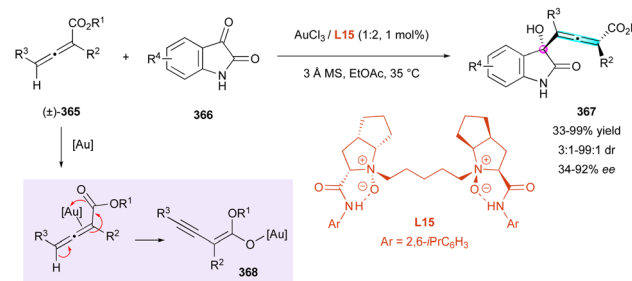
Scheme 104 Photoinduced and Cr dual-catalysed cascade reaction.

benzaldehyde ( $R^1 = \text{Ph}$ ), a slight excess of both TIPS-1,3-ene 351 ( $R^2 = \text{TIPS}$ ) and isopropyl dihydropyridine (DHP) 355 ( $R^3 = \text{iPr}$ ) as a radical precursor. Chromium dichloride and chiral oxazoline ligand L37 with 4-CzIPN C35 as the photocatalyst under blue LED irradiation for 12 h at room temperature afforded  $\alpha$ -allenols 356 in excellent yield, enantio- and diastereoselectivity. This method tolerated both aryl and aliphatic aldehydes but changing the 1,3-ene partner for a less hindered silyl or aryl derivative often resulted in the loss of diastereoselectivity. Finally, other radical sources such as redox active esters and trifluoroborate salts were also successfully investigated but the transfer was limited to secondary and tertiary radicals. The authors suggested that both stereogenic elements are formed simultaneously during the addition of propargyl chromium(III) intermediate 357 to the aldehyde.

Fu and co-workers reported the nickel-catalysed enantioconvergent and diastereoselective cross-coupling between trifluoromethyl alkyl bromides 359 and TMS-substituted 1,3-enynes 360 for the simultaneous installation of central and axial stereogenic elements in allenes 361 (Scheme 105).<sup>158</sup> In addition to not being highly sensitive to moisture or air, this protocol allows the coupling between a variety of  $\text{CF}_3$ -substituted alkyl bromides, including possibly sensitive moieties such as primary alkyl chloride/bromide, secondary carbamate and epoxide. The mechanism is supposed to proceed *via* the formation of chiral nickel complex 362 with controlled central chirality, which is converted to axial chirality upon the formation of complex 363. Then, diastereoselective cross-coupling with  $\text{CF}_3$ -alkyl radical affords 364 as precursors of 361 after a final reductive elimination step (Scheme 106).



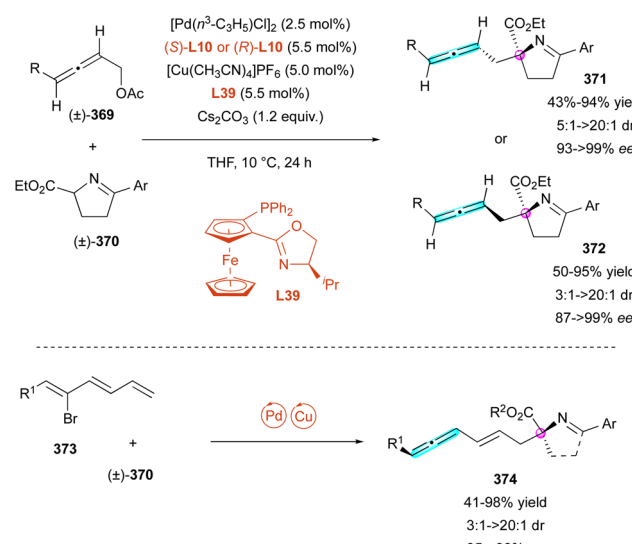
Scheme 105 Ni-Catalysed enantioconvergent allenylation of alkyl electrophiles.



Scheme 106 Au-Catalysed enantioselective allen-aldol reaction of allenotes with isatins.

In complement to the rearrangement of propargylic derivatives, in 2016, the Feng group engaged racemic allenes 365 in an enantioselective gold-catalysed allen-aldol reaction with isatins 366, creating a stereocentre, while controlling the configuration of the allene moiety in 367.<sup>160</sup> The interaction between allenotes and the gold complex allowed epimerisation *via* the formation of key reactive gold-alkenyl enolate intermediate 368 as the precursor of the final allene. Thus, the authors presented a number of allen-oxindoles 367 obtained with mostly excellent yields (up to 99%) although sterically challenging  $R^2$  substituents led to lower yields (33% yield for  $R^1 = \text{Et}$ ,  $R^2 = \text{i-pentyl}$ ,  $R^3 = \text{Me}$ ,  $R^4 = \text{H}$ ) and an aryl  $R^2$  substituent could not be introduced. Variable diastereoselectivity from 3:1 to 99:1 was observed together with decent enantioselectivity not exceeding 90% ee. Lower selectivity was observed in the case of sterically hindered isatins with  $R^4 = 4\text{-Cl}$  or 4-Br.

Finally, Ma, Zhang, and colleagues simultaneously published their work on the DKR of allenic acetates ( $\pm$ )-369 through the synergistic Pd/Cu-catalysed enantioselective allenylation of imines 370 (Scheme 107).<sup>161</sup> Here, the chiral environment of both Pd and Cu complexes combining SegPhos [(S)- or (R)-L10] and Phosferrox (L39) ligands, respectively,



Scheme 107 Pd-Catalysed stereoselective construction of chiral allenes.

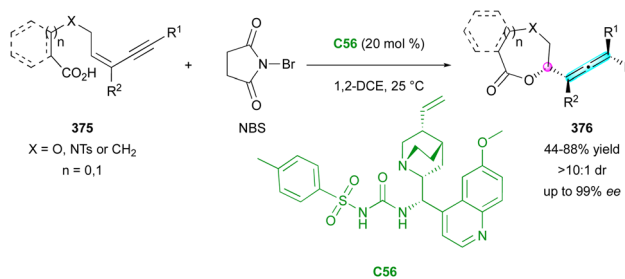


allowed efficient stereocontrol of the reaction *via* racemisation of the allene. The reaction could be performed with cyclic and acyclic imines (not shown) with a surprising inversion of the stereocentre configuration. Interestingly, both configurations of allenes 371/372 could be obtained depending on the enantiomer of SegPhos used, always with good diastereoselectivity (3:1 to >20:1 dr) and enantioselectivity (87% to >99% ee), although (R)-L10 seemed to achieve better selectivity. Very recently, the authors extended this method with the same nucleophiles 370 to (3E,5Z)-5-bromo-1,3,5-trienes 373 electrophilic partners, allowing the stereodivergent formation of similar products 374 with an additional C=C double-bond between both stereogenic elements.<sup>162</sup>

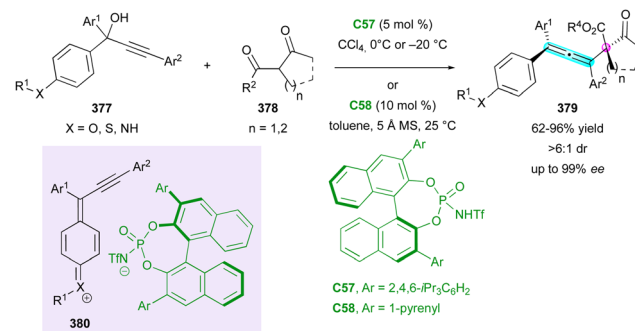
### Organocatalysed approaches

The organocatalysed enantioselective synthesis of chiral allenes featuring a stereocentre has been also the focus of interest in the last two decades.<sup>163</sup> One of the first examples of the organocatalytic approach was reported by the Tang group in 2010.<sup>164</sup> They proposed a synthetic way to perform bromolactonisation of conjugated (Z)-enyne-carboxylic acids 375 using an electrophilic brominating agent such as *N*-bromosuccinimide (NBS), promoted by chiral urea catalyst C56 (Scheme 108). This reaction exclusively gave chiral allenic lactones 376 in generally high yield (44–88%) and stereoselectivity (>10:1 dr, up to 99% ee), but was only compatible with (Z)-enye isomers 375, where the other double bond geometry giving rise to a racemic mixture. A very broad range of substrates could be used, containing electron-withdrawing or electron-donating group, with different linkers ( $n = 0, 1$ ), leading either to mono-6-membered ring or fused bicyclic seven-membered ring lactones, respectively.

Following their interest in the organocatalytic synthesis of chiral allenoates by formal  $S_N2'$  nucleophilic substitutions of propargylic derivatives,<sup>165</sup> the Sun group became interested more recently in the stereocontrolled synthesis of tetrasubstituted allenes 379 endowed with a quaternary stereocentre (Scheme 109).<sup>166</sup> Their strategy is based on the ability of racemic propargylic alcohols 377 to generate highly reactive propargylic cation intermediate 380, which is prone to participate in an efficient intermolecular C–C bond formation with 1,3-dicarbonyl pronucleophiles 378 in the presence of CPA catalyst C57 or C58. The presence of a 4-heteroatom ( $X = O, S, NH$ )



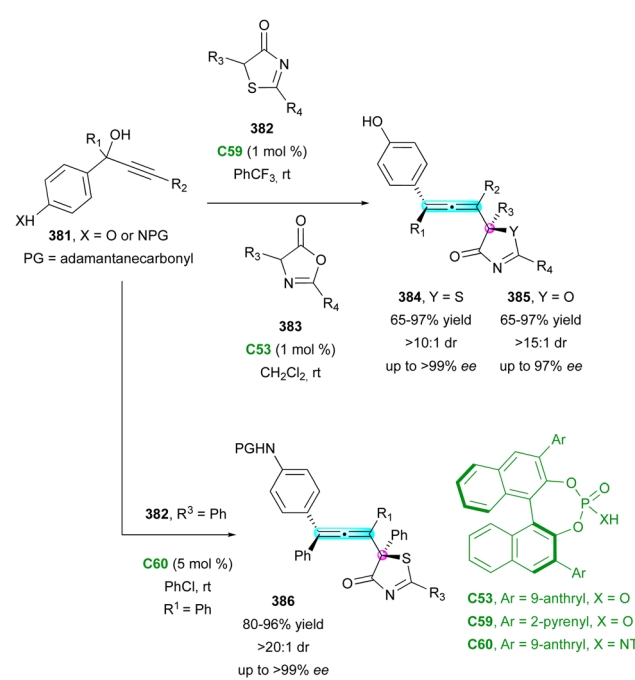
Scheme 108 Enantioselective bromolactonisation of conjugated (Z)-enynes.



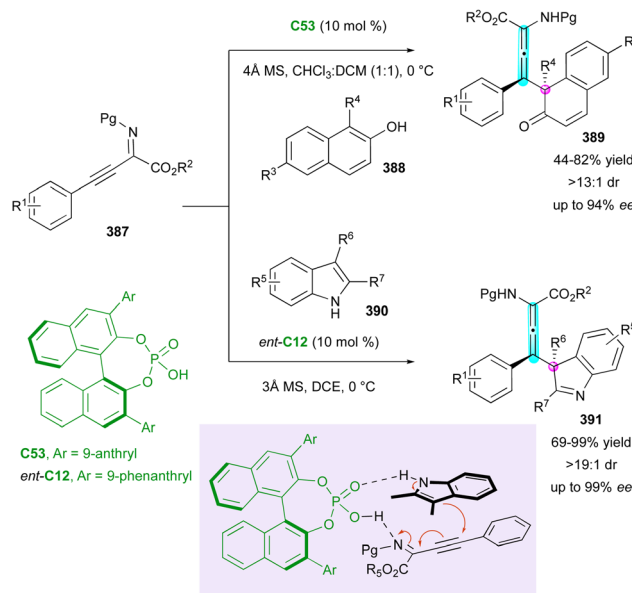
Scheme 109 Organocatalytic synthesis of chiral tetrasubstituted allenes from racemic propargylic alcohols and 1,3-dicarbonyls.

S) in propargylic alcohol 377 is mandatory to assist the generation and stabilisation of the key propargylic *para*-quinone methide (*p*-QM) cation 380 associated with its chiral counter anion, which tolerates a broad variety of electron-rich, electron-neutral, and electron-deficient aryl moieties ( $Ar^1, Ar^2$ ), leading to tetrasubstituted allenes 379 with good yield (62–96%) and good enantio- and diastereoselectivity (up to 97% ee, >6:1 dr). In 2019, the same group extended the reaction to generateaza-*p*-quinone methides as key intermediates ( $X = NH$ ) with comparable efficiency.<sup>167</sup>

A similar work was simultaneously achieved by the Li group, reporting the synthesis of vicinal axially chiral tetrasubstituted allenes 384–385 bearing a heteroatom-functionalised quaternary carbon stereocentre.<sup>168</sup> This was accomplished through the organocatalytic stereocontrolled addition of thiazolones 382 and azalactones 383 as nucleophiles to propargylic alcohols 381 ( $X = O$ ) catalysed by various CPA C59 and C53 (Scheme 110).



Scheme 110 Organocatalytic synthesis of chiral tetrasubstituted allenes featuring a heteroatom-functionalised quaternary carbon stereocentre.

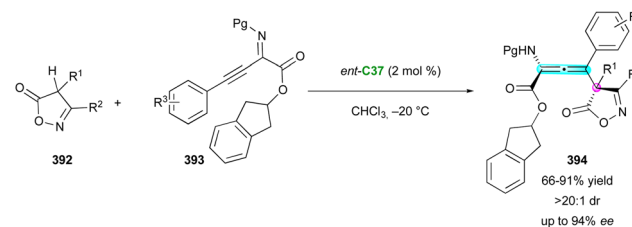


**Scheme 111** Organocatalytic enantioselective dearomatisation reaction for the synthesis of axial chiral allenoates.

The developed optimisation led to the use of non-standard conditions, such as  $\text{PhCF}_3$  as the solvent for thiazolone nucleophiles **382**, but provided excellent yields (65–97%) for a large extended scope with high enantio- and diastereoselectivity (up to >99% ee, >10:1 dr). In their following article, the authors extended this method to *para*-amino-substituted propargylic alcohols **381** ( $\text{X}=\text{NH}$ ) with a comparable efficiency only when an adamantane carbonyl is used as the *N*-protecting group,<sup>169</sup> leading to analogous centrally and axially chiral allenoates **386**.

In 2020, alternative contributions were proposed independently by the Wang<sup>170</sup> and Lin groups,<sup>171</sup> who developed the CPA-catalysed enantioselective synthesis of  $\alpha$ -tetrasubstituted  $\alpha$ -amino allenoates **389** and **391** bearing a quaternary stereogenic centre (Scheme 111). Electrophilic  $\beta,\gamma$ -alkynyl- $\alpha$ -imino esters **387** in combination with C-nucleophilic heterocycles such as 2,3-disubstituted indoles **390** and 1-substituted 2-naphthols **388**, in the presence of molecular sieves as a crucial dehydrating agent, allowed high efficiency to be achieved both in terms of yield and stereoselectivity. It was shown that the chiral backbone and the steric environment of the CPA-catalyst were the most influent parameters to ensure good stereocontrol because of the planar approach of both partners, directed by the hydrogen bond network created by CPA.

One year later, the Li group extended the reactivity of these electrophilic  $\beta,\gamma$ -alkynyl- $\alpha$ -imino esters **393** (Scheme 112).<sup>172</sup> They studied the stereoselective transformation of isoxazol-5(4*H*)-one derivatives **392** as pro-nucleophiles for regio- and stereoselective addition, leading to the corresponding  $\alpha$ -amino allenoates **394** with both axial and central chirality in good yields (66–91%) under similar conditions with CPA-catalyst (*S*)-TRIP *ent*-C37. However, in this case, no dehydrating agent was needed to preserve a high diastereo- and enantioselectivity (up to 94% ee, >20:1 dr) and the reaction was limited to the N-Boc

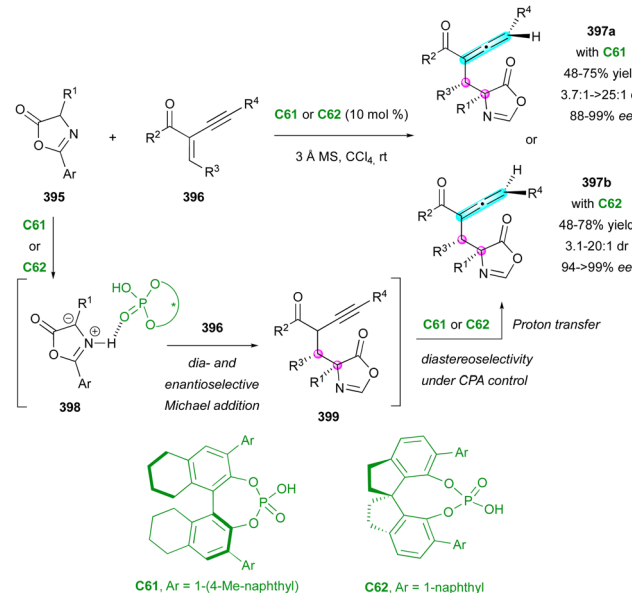


**Scheme 112** Organocatalytic enantioselective  $\gamma$ -additions of isoxazole-5(4*H*)-ones to access to axially and centrally chiral tetrasubstituted amino allenoates.

function as the protecting group, and 3-aryl substituted isoxazolones.

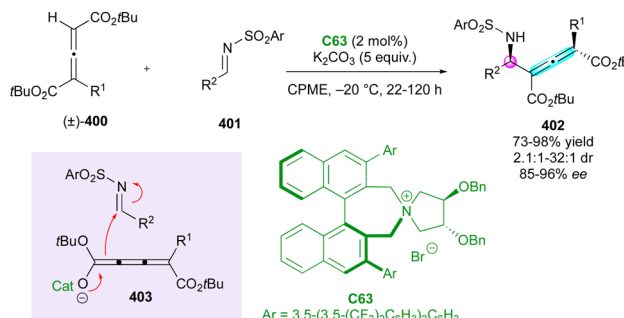
Related oxazolones **395** were used by Peng and Yang as nucleophilic partners with activated 1,3-enynes **396** under CPA catalysis for enantioselective and diastereodivergent access to axially chiral allenes **397a** and **b** bearing two stereogenic carbon atoms (Scheme 113).<sup>173</sup> Both catalysts **C61** and **C62** could catalyse the first Michael addition with oxazolones **395** activated as their Münchnone-type intermediate **398**, affording the same major stereoisomer for Michael adduct **399**, regardless of the structure of the organocatalyst. Then, the proton transfer generates the allene function, simultaneously creating the axial chirality and with diastereodivergency whose origin presumably comes from the difference in the rigidity between the Binol (more flexible) and the Spinol (more rigid) backbones of the catalyst. This was supported by DFT calculations.

In 2013, Maruoka's group made a step forward, demonstrating the feasibility of synthesising stereodefined tetrasubstituted allenes **402** featuring a stereogenic centre by the diastereo- and enantioselective alleno-Mannich-type reaction of racemic allenyl dicarboxylates ( $\pm$ )-**400** with tosylimines **401**



**Scheme 113** CPA-Catalysed stereodivergent synthesis of trisubstituted allenes.

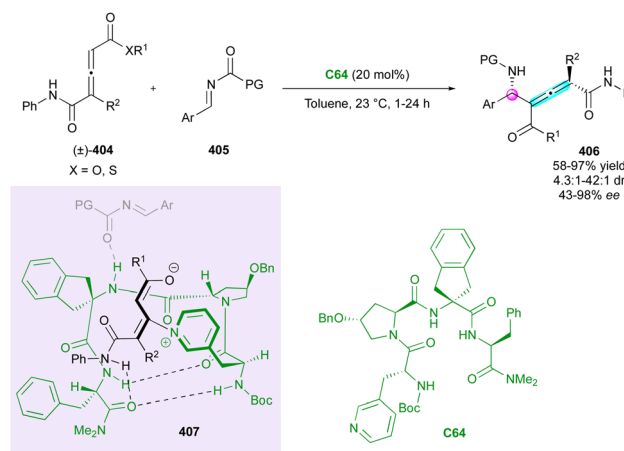




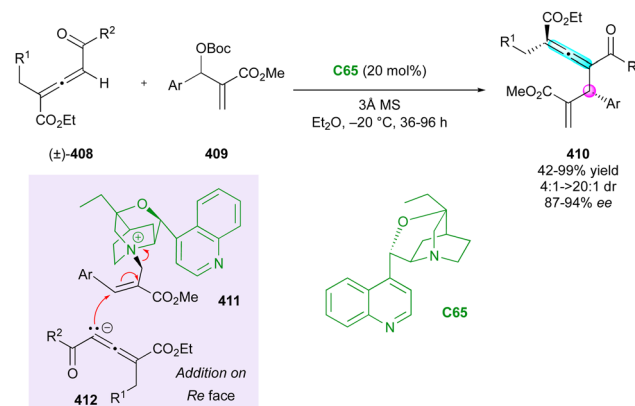
**Scheme 114** Enantioselective PTC for the synthesis of tetrasubstituted allenes.

under phase transfer catalysis (PTC).<sup>174</sup> Chiral cumulenolate key intermediate **403** is generated through the utilisation of chiral ammonium bromide **C63**, triggering nucleophilic addition to sulfonyl imine **396** (Scheme 114). The only limitation is the absence of reactivity for *p*-NO<sub>2</sub>-phenyl imines and the poor to moderate diastereocontrol in some cases, but the constant elevated enantiomeric excess is impressive for the first example reported in the literature.

Miller and co-workers disclosed a similar reaction employing pyridylalanine-based peptide catalyst **C64** with racemic allenyl amido esters or thioesters (±)-**404** (X = O, S) and *N*-acylimines **405**. In this case, the deep mechanistic study clearly demonstrated the intervention of an addition mechanism through chiral pyridinium dienolate intermediate **407** rather than the formation of a cumulenolate (Scheme 115).<sup>175</sup> Within this system, the presence of the anilide substituent in **404** as a hydrogen donor significantly improved the diastereoselectivity by participating in the H-bonding network compared to an ester function. The catalyst also controls the enantioselectivity of the reaction by creating hydrogen bonding interactions with the imine protecting group of **405**. Both the diastereo- and enantioselectivity were improved compared to the previous Maruoka's method (up to 42:1 dr and up to 98% ee).



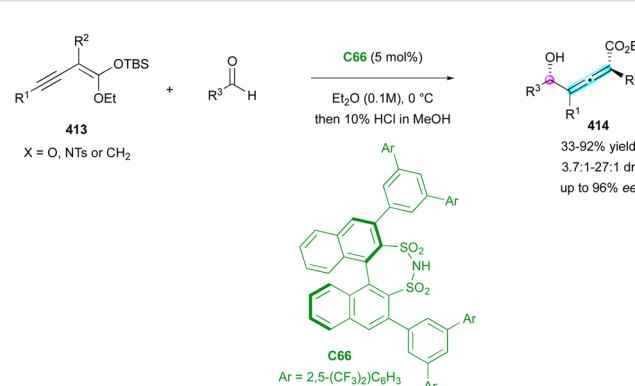
**Scheme 115** Pyridylalanine-based peptide-catalysed enantioselective addition of allenoates to *N*-acylimines.



**Scheme 116** Organocatalytic enantioselective C(sp<sup>2</sup>)-H allylic alkylation.

Guo and collaborators proposed a related approach *via* the enantioselective allylic alkylation of trisubstituted racemic allenoates (±)-**408** performed by a tertiary amine catalyst to simultaneously control the axial and central chirality (Scheme 116).<sup>176</sup> The use of β-isocinchonine **C65** as the catalyst resulted in aza-Michael addition to Morita–Baylis–Hillman carbonates (MBH) **409**, leading to electrophilic intermediates **411** with the simultaneous generation of *tert*-butoxide, which deprotonated the trisubstituted allenoates to transient allenic anions **412**. This triggered a diastereofacial nucleophilic addition by the Re face, leading to tetrasubstituted allenes **410** and release of the catalyst. For most examples, the diastereoselectivity was excellent (dr > 20:1), but the introduction of a nitro substituent in the *ortho* position of the aryl group of the MBH carbonate resulted in a diminished diastereomeric ratio (dr = 4:1).

The pioneering contribution by the List group for the development of enantioselective synthesis<sup>177</sup> was reported in 2016 with the proposal of a new alkynylous Mukaiyama aldol reaction, allowing enantioselective control of the two different stereogenic elements of α-hydroxy allenoates **414** (Scheme 117).<sup>178</sup> Silyl alkynyl ketene acetals **413** were selected as pro-nucleophiles towards simple aromatic aldehydes, using their previously developed silylated disulfonimide (DSI)-catalyst **C66** as a chiral Lewis acid. After a challenging optimisation,



**Scheme 117** Catalytic enantioselective alkynylous Mukaiyama aldol reaction.

they could perform the regio- ( $>20:1$ ), enantio- (up to 96% ee) and diastereoselective ( $3.7:1$  to  $27:1$  dr) transformation, proceeding with moderate to good yield (33–96%) (Schemes 116 and 117).

## Conclusions

In conclusion, the enantioselective synthesis of molecules bearing different multiple stereogenic elements represents a significant recent advancement in the field of organic chemistry. The reviewed studies emphasise the importance of developing efficient and selective methodologies for constructing complex chiral molecules in enantioenriched form, given that they already play a crucial role in catalyst/ligand design, drug discovery, natural product synthesis, materials science, and various other applications. However, although this field has undoubtedly made remarkable progress in last years, there are still challenges to be addressed, such as scalability, substrate scope, and broader applicability, in particular for molecules displaying helical and/or planar chirality in combination with other stereogenic elements. Also, the enantioselective synthesis of molecules bearing more than two different stereogenic elements is in its infancy and still represents a formidable challenge. The reviewed literature not only sheds light on the current state of the art but also paves the way for future research directions in the pursuit of more eco-compatible, selective, and broadly applicable methods for producing complex chiral molecular architectures.

## Data availability

No primary research results, software or code has been included and no new data were generated or analysed as part of this review.

## Conflicts of interest

There are no conflicts to declare.

## Acknowledgements

Financial support from the Agence Nationale pour la Recherche (ANR-21-CE07-0036), Aix-Marseille Université, the Centre National de la Recherche Scientifique (CNRS), and Centrale Marseille is gratefully acknowledged.

## Notes and references

- For a review, see: G. Bringmann, T. Gulder, T. A. M. Gulder and M. Breuning, *Chem. Rev.*, 2011, **111**, 563.
- (a) G. Bringmann, M. Rübenacker, P. Vogt, H. Busse, L. Aké Assi, K. Peters and H. G. von Schnerring, *Phytochem.*, 1991, **30**, 1691; (b) S. Fayez, T. Bruhn, D. Feineis, L. A. Assi, P. P. Kushwah, S. Kumar and G. Bringmann, *RSC Adv.*, 2022, **12**, 28916.
- A. Richieu, P. A. Peixoto, L. Pouységu, D. Deffieux and S. Quideau, *Angew. Chem., Int. Ed.*, 2017, **56**, 13833.
- (a) M. Isaka, M. Tanticharoen, P. Kongsaeree and Y. Thebtaranonth, *J. Org. Chem.*, 2001, **66**, 4803; (b) I. L. Jones, F. K. Moore and C. L. L. Chai, *Org. Lett.*, 2009, **11**, 5526.
- S. Obermaier, W. Thiele, L. Fürtges and M. Müller, *Angew. Chem., Int. Ed.*, 2019, **58**, 9125.
- (a) J. Kohno, Y. Koguchi, M. Nishio, K. Nakao, M. Kuroda, R. Shimizu, T. Ohnuki and S. Komatsubara, *J. Org. Chem.*, 2000, **65**, 990; (b) A. Coste, A. Bayle, J. Marrot and G. Evano, *Org. Lett.*, 2014, **16**, 1306.
- L. D. Fader, E. Malenfant, M. Parisien, R. Carson, F. Bilodeau, S. Landry, M. Pesant, C. Brochu, S. Morin, C. Chabot, T. Halmos, Y. Bousquet, M. D. Bailey, S. H. Kawai, R. Coulombe, S. LaPlante, A. Jakalian, P. K. Bhardwaj, D. Wernic, P. Schroeder, M. Amad, P. Edwards, M. Garneau, J. Duan, M. Cordingley, R. Bethell, S. W. Mason, M. Bös, P. Bonneau, M.-A. Poupart, A.-M. Faucher, B. Simoneau, C. Fenwick, C. Yoakim and Y. Tsantrizos, *ACS Med. Chem. Lett.*, 2014, **5**, 422.
- Y. Ikeura, T. Doi, A. Fujishima and H. Natsugari, *Chem. Commun.*, 1998, 2141.
- B. A. Lanman, A. T. Parsons and S. G. Zech, *Acc. Chem. Res.*, 2022, **55**, 2892.
- (a) M. Omote, Y. Nishimura, K. Sato, A. Ando and I. Kumadaki, *Tetrahedron Lett.*, 2005, **46**, 319; (b) L.-S. Zheng, K.-Z. Jiang, Y. Deng, X.-F. Bai, G. Gao, F.-L. Gu and L.-W. Xu, *Eur. J. Org. Chem.*, 2013, 748; (c) R. Oost, J. Rong, A. J. Minnaard and S. R. Harutyunyan, *Catal. Sci. Technol.*, 2014, **4**, 1997; (d) S. Kitagaki, K. Sugisaka and C. Mukai, *Org. Biomol. Chem.*, 2015, **13**, 4833; (e) X.-F. Bai, T. Song, Z. Xu, C.-G. Xia, W.-S. Huang and L.-W. Xu, *Angew. Chem., Int. Ed.*, 2015, **54**, 5255; (f) Y. Zhang, S.-Z. Nie, J.-J. Ye, J.-P. Wang, M.-M. Zhou, C.-Q. Zhao and Q. Li, *J. Org. Chem.*, 2019, **84**, 8423; (g) L. Ling, Z. Song, H. Shan, C. Wang, S. Li, Y. Wang, J. Hu, Q. Chen, H. Zhang and Y. Yang, *Chem. Commun.*, 2023, **59**, 2739.
- Y. Hao, Z.-H. Li, Z.-G. Ma, R.-X. Liu, R.-T. Ge, Q.-Z. Li, T.-M. Ding and S.-Y. Zhang, *Chem. Sci.*, 2023, **14**, 9496.
- (a) M. Hasegawa, Y. Nojima, Y. Nagata, K. Usui, K.-I. Sugiura and Y. Mazaki, *Eur. J. Org. Chem.*, 2023, e202300656; (b) S. F. Pizzolato, P. Štacko, J. C. M. Kistemaker, T. van Leeuwen, E. Otten and B. L. Feringa, *J. Am. Chem. Soc.*, 2018, **140**, 17278.
- (a) T. M. T. Tuyet, T. Harada, K. Hashimoto, M. Hatsuda and A. Oku, *J. Org. Chem.*, 2000, **65**, 1335; (b) R. S. Ward and D. D. Hughes, *Tetrahedron*, 2001, **57**, 4015; (c) M. Penhoat, V. Levacher and G. Dupas, *J. Org. Chem.*, 2003, **68**, 9517; (d) I. G. Stará, Z. Alexandrová, F. Teply, P. Sehnal, I. Starý, D. Šaman, M. Buděšínský and J. Cvačka, *Org. Lett.*, 2005, **7**, 2547; (e) W. Zhang, H. Xu, H. Xu and W. Tang, *J. Am. Chem. Soc.*, 2009, **131**, 3832; (f) S. Postikova, M. Sabbah, D. Wightman, I. T. Nguyen, M. Sanselme, T. Besson, J.-F. Brière, S. Oudeyer and V. Levacher, *J. Org. Chem.*, 2013, **78**, 8191; (g) R. Raghunathan, E. Kumarasamy, A. Iyer, A. Ugrinova and J. Sivaguru, *Chem. Commun.*, 2013, **49**, 8713;



(h) P. Aillard, P. Retailleau, A. Voituriez and A. Marinetti, *Chem. Commun.*, 2014, **50**, 2199; (i) Z. Zuo, J. Liu, J. Nan, L. Fan, W. Sun, Y. Wang and X. Luan, *Angew. Chem., Int. Ed.*, 2015, **54**, 15385; (j) M. Šámal, S. Chercheja, J. Rybáček, J. V. Chocholoušová, J. Vacek, L. Bednárová, D. Šaman, I. G. Stará and I. Starý, *J. Am. Chem. Soc.*, 2015, **137**, 8469; (k) D. Waghray, G. Bagdziunas, J. Jacobs, L. Van Meervelt, J. V. Grazulevicius and W. Dehaen, *Chem. – Eur. J.*, 2015, **21**, 18791; (l) X. Xue and Z. Gu, *Org. Lett.*, 2019, **21**, 3942; (m) J. Nejedlý, M. Šámal, J. Rybáček, I. G. Sánchez, V. Houska, T. Warzecha, J. Vacek, L. Sieger, M. Buděšínský, L. Bednárová, P. Fiedler, I. Císařová, I. Starý and I. G. Stará, *J. Org. Chem.*, 2020, **85**, 248.

14 (a) B. H. Lipshutz, F. Kayser and Z.-P. Liu, *Angew. Chem., Int. Ed. Engl.*, 1994, **33**, 1842; (b) G. Brigmann, P. A. Keller and K. Rölfing, *Synlett*, 1994, 423; (c) O. Kitagawa, H. Izawa, K. Sato, A. Dobashi, T. Taguchi and M. Shiro, *J. Org. Chem.*, 1998, **63**, 2634; (d) A. Fürstner and M. Méndez, *Angew. Chem., Int. Ed.*, 2003, **42**, 5355; (e) P.-E. Broutin and F. Colobert, *Org. Lett.*, 2003, **5**, 3281; (f) A. I. Meyers, T. D. Nelson, H. Moorlag, D. J. Rawson and A. Meier, *Tetrahedron*, 2004, **60**, 4459; (g) C. G. Newton, E. Braconi, J. Kuziola, M. D. Wodrich and N. Cramer, *Angew. Chem., Int. Ed.*, 2018, **57**, 11040; (h) D. Meidlinger, L. Marx, C. Bordeianu, S. Choppin and F. Colobert, *Angew. Chem., Int. Ed.*, 2018, **57**, 9160; (i) A. Urbano, A. M. del Hoyo, A. Martínez-Carrión and M. C. Carreño, *Org. Lett.*, 2019, **21**, 4623; (j) S. Jin, J.-Y. Wang, Y. Tang, H. Rouh, S. Zhang, T. Xu, Y. Wang, Q. Yuan, D. Chen, D. Unruh and G. Li, *Front. Chem.*, 2022, **10**, 860398; (k) A. Mondal, N. O. Thiel, R. Dorel and B. L. Feringa, *Nat. Catal.*, 2022, **5**, 10.

15 (a) B. D. Sherry and F. D. Toste, *J. Am. Chem. Soc.*, 2004, **126**, 15978; (b) G. Gao, F.-L. Gu, J.-X. Jiang, K. Jiang, C.-Q. Sheng, G.-Q. Lai and L.-W. Xu, *Chem. – Eur. J.*, 2011, **17**, 2698.

16 (a) C. K. Hazra, Q. Dherbassy, J. Wencel-Delord and F. Colobert, *Angew. Chem., Int. Ed.*, 2014, **53**, 13871; (b) L.-J. Li, J.-J. Chen, C.-F. Feng, H.-Y. Li, X. Wang, H. Xu and H.-X. Dai, *Org. Lett.*, 2020, **22**, 9169.

17 (a) A. Alexakis, I. Marek, P. Mangeney and J. F. Normant, *Tetrahedron*, 1991, **47**, 1677; (b) G. Bringmann, M. Breuning, S. Tasler, H. Endress, C. L. J. Ewers, L. Göbel, K. Peters and E.-M. Peters, *Chem. – Eur. J.*, 1999, **5**, 3029; (c) G. Bringmann, M. Breuning, S. Tasler, H. Endress, C. L. J. Ewers, L. Göbel, K. Peters and E.-M. Peters, *Chem. – Eur. J.*, 1999, **5**, 3029; (d) K. Kamikawa, M. Furusyo, T. Uno, Y. Sato, A. Konoo, G. Bringmann and M. Uemura, *Org. Lett.*, 2001, **3**, 3667; (e) V. Chan, J. G. Kim, C. Jimeno, P. J. Carroll and P. J. Walsh, *Org. Lett.*, 2004, **6**, 2051; (f) A. Yubuta, A. Tsurusaki and K. Kamikawa, *Chem. Commun.*, 2021, **57**, 6600; (g) D. Enders, S. Nolla and J. W. Bats, *Synlett*, 2005, 2679; (h) R. Senda, Y. Watanabe, S. Miwa, A. Sato and O. Kitagawa, *J. Org. Chem.*, 2023, **88**, 9579; (i) B. Yang, X. Tan, Y. Ge, Y. Lia and C. He, *Org. Chem. Front.*, 2023, **10**, 4862.

18 H. Yang, W.-L. Xu, X.-Y. Zeng, J. Chen, L. Yu and L. Zhou, *Org. Lett.*, 2021, **23**, 9315; J. Dong, A. Ostertag and C. Sparr, *Angew. Chem., Int. Ed.*, 2022, **61**, e202212627; Q. Ni, Z. Zhu, Y. Fan, X. Chen and X. Song, *Org. Lett.*, 2021, **23**, 9548; H. Homma, S. Harada, T. Ito, A. Kanda and T. Nemoto, *Org. Lett.*, 2020, **22**, 8132; Y. Kwon, A. J. Chinn, B. Kim and S. J. Miller, *Angew. Chem., Int. Ed.*, 2018, **57**, 6251.

19 X.-F. Bai, Y.-M. Cui, J. Cao and L.-W. Xu, *Acc. Chem. Res.*, 2022, **55**, 2545.

20 In the following excellent review, Zhang and Shi summarised only examples of atropisomers bearing one other stereogenic element (central, planar, helical chirality). H.-H. Zhang, T.-Z. Li, S.-J. Liu and F. Shi, *Angew. Chem., Int. Ed.*, 2023, **63**, e202311053.

21 During the evaluation process of this manuscript, several methodologies have been released in the literature: (a) P. Wu, W.-T. Zhang, J.-X. Yang, X.-Y. Yu, S.-F. Ni, W. Tan and F. Shi, *Angew. Chem., Int. Ed.*, 2024, **63**, e202410581; (b) Y. Wu, Z. Wang, Y. Shan, Y. Ma, T. Li, C. Yuan, H. Guo and B. Mao, *Chem. Sci.*, 2024, **15**, 9703; (c) X. Hu, Y. Zhao, T. He, C. Niu, F. Liu, W. Jia, Y. Mu, X. Li and Z.-Q. Rong, *Chem. Sci.*, 2024, **15**, 13541; (d) J. Hou, W. Hao, Y. Chen, Z. Wang and W. Yao, *J. Org. Chem.*, 2024, **89**, 9068; (e) T.-T. Wang, J. Cao and X. Li, *Org. Lett.*, 2024, **26**, 6179; (f) T. von Münchow, Y.-R. Liu, R. Parmar, S. E. Peters, S. Trienes and L. Ackermann, *Angew. Chem., Int. Ed.*, 2024, **63**, e202405423; (g) X. Wang, S.-J. Wang, X. Xin, H. An, Z. Tu, H. Yang, M. W. Wong and S. Lu, *Chem. Sci.*, 2024, **15**, 13240; (h) X. Wang, S.-J. Wang, X. Xin, H. An, Z. Tu, H. Yang, M. W. Wong and S. Lu, *Chem. Sci.*, 2024, **15**, 13240; (i) Q. Liu, K. Teng, Y. Zhang, Y. Lv, Y. Robin Chi and Z. Jin, *Angew. Chem., Int. Ed.*, 2024, **63**, e202406386.

22 D. Leow, S. Lin, S. K. Chittimalla, X. Fu and C.-H. Tan, *Angew. Chem., Int. Ed.*, 2008, **47**, 5641.

23 P. Dorizon, C. Martin, J.-C. Daran, J.-C. Fiaud and H. B. Kagan, *Tetrahedron: Asymmetry*, 2001, **12**, 2625.

24 K. Akagawa, N. Nishi, I. Yoshikawa and K. Kudo, *Eur. J. Org. Chem.*, 2015, 5055.

25 Y. Zhao, H. Wang, B. Wua and Y.-G. Zhou, *Org. Chem. Front.*, 2019, **6**, 3956.

26 Y. Zhao, X.-Q. Wang, Y.-J. Yu and Y.-G. Zhou, *J. Org. Chem.*, 2021, **86**, 1262.

27 A.-N. Alba, P. Gómez-Sal, R. Rios and A. Moyano, *Tetrahedron: Asymmetry*, 2009, **20**, 1314.

28 M. Akiyama, K. Akagawa, H. Seinob and K. Kudo, *Chem. Commun.*, 2014, **50**, 7893.

29 G. Yang, Y. He, T. Wang, Z. Li and J. Wang, *Angew. Chem., Int. Ed.*, 2024, **63**, e202316739.

30 J. Bie, M. Lang and J. Wang, *Org. Lett.*, 2018, **20**, 5866.

31 (a) S. Barik, R. C. Das, K. Balanna and A. T. Biju, *Org. Lett.*, 2022, **24**, 5456; (b) For an isolated example of a closely related C–N axially chiral fused-dihydropyridinone, see: Y. Chu, M. Wu, F. Hu, P. Zhou, Z. Cao and X.-P. Hui, *Org. Lett.*, 2022, **24**, 3884.

32 R. Mi, Z. Ding, S. Yu, R. H. Crabtree and X. Li, *J. Am. Chem. Soc.*, 2023, **145**, 8150.

33 L. Cui, Y. Wang, Z. Fan, Z. Li and Z. Zhou, *Adv. Synth. Catal.*, 2019, **361**, 3575.



34 C. Ma, F.-T. Sheng, H.-Q. Wang, S. Deng, Y.-C. Zhang, Y. Jiao, W. Tan and F. Shi, *J. Am. Chem. Soc.*, 2020, **142**, 15686.

35 Q. Shi, F. Fang and D.-J. Cheng, *Adv. Synth. Catal.*, 2024, **366**, 1.

36 J. Clayden and L. W. Lai, *Angew. Chem., Int. Ed.*, 1999, **38**, 2556.

37 V. Chan, J. G. Kim, C. Jimeno, P. J. Carroll and P. J. Walsh, *Org. Lett.*, 2004, **6**, 2051.

38 Z. Gao, J. Qian, H. Yang, X.-C. Hang, J. Zhang and G. Jiang, *Chem. Commun.*, 2020, **56**, 7265.

39 S.-L. Li, Q. Wu, C. Yang, X. Li and J.-P. Cheng, *Org. Lett.*, 2019, **21**, 5495.

40 X. Li, J.-P. Cheng and G. Zheng, *Org. Lett.*, 2021, **23**, 3997.

41 F. Jiang, K.-W. Chen, P. Wu, Y.-C. Zhang, Y. Jiao and F. Shi, *Angew. Chem., Int. Ed.*, 2019, **58**, 15104.

42 S. Yang, J.-B. Huang, D.-H. Wang, N.-Y. Wang, Y.-Y. Chen, X.-Y. Ke, H. Chen, S.-F. Ni, Y.-C. Zhang and F. Shi, *Precis. Chem.*, 2024, **2**, 208.

43 X. Yuan, X. Wu, F. Peng, H. Yang, C. Zhu and H. Fu, *Chem. Commun.*, 2020, **56**, 12648.

44 C. Ma, F. Jiang, F.-T. Sheng, Y. Jiao, G.-J. Mei and F. Shi, *Angew. Chem., Int. Ed.*, 2019, **58**, 3014.

45 F.-T. Sheng, Z.-M. Li, Y.-Z. Zhang, L.-X. Sun, Y.-C. Zhang, W. Tan and F. Shi, *Chin. J. Chem.*, 2020, **38**, 583.

46 J.-Y. Wang, C.-H. Gao, C. Ma, X.-Y. Wu, S.-F. Ni, W. Tan and F. Shi, *Angew. Chem., Int. Ed.*, 2023, e202316454.

47 (a) V. S. Raut, M. Jean, N. Vanthuyne, C. Roussel, T. Constantieux, C. Bressy, X. Bugaut, D. Bonne and J. Rodriguez, *J. Am. Chem. Soc.*, 2017, **139**, 2140; (b) S. Shaaban, H. Li, F. Otte, C. Strohmann, A. P. Antonchick and H. Waldmann, *Org. Lett.*, 2020, **22**, 9199; (c) For a recent review, see: W. Tan, X.-Y. Wu and F. Shi, *ChemCatChem*, 2024, **16**, e202401022.

48 P. Wu, L. Yu, C.-H. Gao, Q. Cheng, S. Deng, Y. Jiao, W. Tan and F. Shi, *Fundam. Res.*, 2023, **10**, 237.

49 Y. Xia, M. Liu, C. Qian, P. Li, M. Dong and W. Li, *Org. Chem. Front.*, 2023, **10**, 30.

50 H.-Q. Wang, S.-F. Wu, J.-R. Yang, Y.-C. Zhang and F. Shi, *J. Org. Chem.*, 2023, **88**(12), 7684.

51 A. Kim, A. Kim, S. Park, S. Kim, H. Jo, K. M. Ok, S. K. Lee, J. Song and Y. Kwon, *Angew. Chem., Int. Ed.*, 2021, **60**, 12279.

52 A. Kim, C. Lee, J. Song, S. K. Lee and Y. Kwon, *Nat. Commun.*, 2023, **14**, 5502.

53 C.-X. Hu, L. Chen, D. Hu, X. Song, Z.-C. Chen, W. Du and Y.-C. Chen, *Org. Lett.*, 2020, **22**, 8973.

54 (a) G. T. Wong, D. Manfra, F. M. Poulet, Q. Zhang, H. Josien, T. Bara, L. Engstrom, M. Pinzon-Ortiz, J. S. Fine, H. J. Lee, L. Zhang, G. A. Higgins and E. M. Parker, *J. Biol. Chem.*, 2004, **279**, 12876; (b) I. H. Hall, A. R. K. Murthy and S. D. Wyrick, *J. Pharm. Sci.*, 1986, **75**, 622; (c) H. J. Lee and K. Maruoka, *Chem. Rec.*, 2022, **22**, e202200004.

55 Y. Liu, Y.-L. S. Tse, F. Y. Kwong and Y.-Y. Yeung, *ACS Catal.*, 2017, **7**, 4435.

56 J. Liu, X. Yang, Z. Zuo, J. Nan, Y. Wang and X. Luan, *Org. Lett.*, 2018, **20**, 244.

57 X. Wang, Y. Luo, J. Zhao and S. Luo, *Org. Biomol. Chem.*, 2023, **21**, 6697.

58 J.-Y. Du, T. Balan, T. D. W. Claridge and M. D. Smith, *J. Am. Chem. Soc.*, 2022, **144**, 14790.

59 N. Kotwal, Tamanna, A. Changotra and P. Chauhan, *Org. Lett.*, 2023, **25**, 7523.

60 Y. Wang, Y. Huang, X. Bao, X. Wei, S. Wei, J. Qu and B. Wang, *Chem. Sci.*, 2024, **15**, 8880.

61 J.-H. Wu, S. Fang, X. Zheng, J. He, Y. Ma, Z. Su and T. Wang, *Angew. Chem., Int. Ed.*, 2023, **62**, e202309515.

62 J. A. Carmona, V. Hornillos, P. Ramírez-López, A. Ros, J. Iglesias-Sigüenza, E. Gómez-Bengoa, R. Fernández and J. M. Lassaletta, *J. Am. Chem. Soc.*, 2018, **140**, 11067.

63 V. Hornillos, J. A. Carmona, A. Ros, J. Iglesias-Sigüenza, J. López-Serrano, R. Fernández and J. M. Lassaletta, *Angew. Chem., Int. Ed.*, 2018, **57**, 3777.

64 J. A. Carmona, P. Rodriguez-Salamanca, R. Fernandez, J. M. Lassaletta and V. Hornillos, *Angew. Chem., Int. Ed.*, 2023, **62**, e202306981.

65 C. Rodríguez-Franco, A. Ros, P. Merino, R. Fernández, J. M. Lassaletta and V. Hornillos, *ACS Catal.*, 2023, **13**, 12134.

66 A. Romero-Arenas, V. Hornillos, J. Iglesias-Sigüenza, R. Fernández, J. López-Serrano, A. Ros and J. M. Lassaletta, *J. Am. Chem. Soc.*, 2020, **142**, 2628.

67 M. Xiong, Z. Yan, S.-C. Chen, J. Tang, F. Yang and D. Xing, *ACS Catal.*, 2024, **14**, 7243.

68 Y. Li, Y.-C. Liou, J. C. A. Oliveira and L. Ackermann, *Angew. Chem., Int. Ed.*, 2022, **61**, e202212595.

69 Z.-J. Zhang, N. Jacob, S. Bhatia, P. Boos, X. Chen, J. C. DeMuth, A. M. Messinis, B. Bongsuiru Jei, J. C. A. Oliveira, A. Radović, M. L. Neidig, J. Wencel-Delord and L. Ackermann, *Nat. Commun.*, 2024, **15**, 3503.

70 Z.-J. Zhang, M. M. Simon, S. Yu, S.-W. Li, X. Chen, S. Cattani, X. Hong and L. Ackermann, *J. Am. Chem. Soc.*, 2024, **146**, 9172.

71 T. Bhattacharya, S. Ghosh, S. Dutta, S. Guin, A. Ghosh, H. Ge, R. B. Sunoj and D. Maiti, *Angew. Chem., Int. Ed.*, 2024, **63**, e202310112.

72 S. H. Jang, H. W. Kim, W. Jeong, D. Moon and Y. H. Rhee, *Org. Lett.*, 2018, **20**, 1248.

73 Z. Gao, C.-X. Yan, J. Qian, H. Yang, P. Zhou, J. Zhang and G. Jiang, *ACS Catal.*, 2021, **11**, 6931.

74 Y. Zhang, Y.-Q. Liu, L. Hu, X. Zhang and Q. Yin, *Org. Lett.*, 2020, **22**, 6479.

75 H. Hu, Y. Peng, T. Yu, S. Cheng, S. Luo and Q. Zhu, *Org. Lett.*, 2021, **23**, 3636.

76 D. Ji, J. Jing, Y. Wang, Z. Qi, F. Wang, X. Zhang, Y. Wang and X. Li, *Chem.*, 2022, **8**, 3346.

77 Q. Ren, M. Lang, H. Liu, X. Li, D. Wu, J. Wu, M. Yang, J. Wei, Z. Ren and L. Wang, *Org. Lett.*, 2023, **25**, 7745.

78 E. García-Urdiales, I. Alfonso and V. Gotor, *Chem. Rev.*, 2011, **111**, PR110.

79 C. Nájera, F. Foubelo, J. M. Sansano and M. Yus, *Tetrahedron*, 2022, **106–107**, 132629.

80 J. Bennett, P. L. Pickering and N. S. Simpkins, *Chem. Commun.*, 2004, 1392.



81 D. P. Curran, H. Qi, S. J. Geib and N. C. DeMello, *J. Am. Chem. Soc.*, 1994, **116**, 3131.

82 (a) W.-L. Duan, Y. Imazaki, R. Shintani and T. Hayashi, *Tetrahedron*, 2007, **63**, 8529; (b) for the utilisation of a *N,N*-bidentate ligand, see: J. Lai, J. Yang, C. Yang, R. Csuk, B. Song and S. Li, *Org. Chem. Front.*, 2022, **9**, 183.

83 For a personal account, see: N. Di Iorio, S. Crotti and G. Bencivenni, *Chem. Rec.*, 2019, **19**, 2095.

84 N. Di Iorio, P. Righi, A. Mazzanti, M. Mancinelli, A. Ciogli and G. Bencivenni, *J. Am. Chem. Soc.*, 2014, **136**, 10250.

85 (a) N. Di Iorio, F. Champavert, A. Erice, P. Righi, A. Mazzanti and G. Bencivenni, *Tetrahedron*, 2016, **72**, 5191; (b) N. Di Iorio, L. Soprani, S. Crotti, E. Marotta, A. Mazzanti, P. Righi and G. Bencivenni, *Synthesis*, 2017, 1519.

86 F. Eudier, P. Righi, A. Mazzanti, A. Ciogli and G. Bencivenni, *Org. Lett.*, 2015, **17**, 1728.

87 Desymmetrization of *N*-pyrazolyl maleimides via organo enantioselective Michael addition of pyrazolones was also reported, albeit with no diastereoselectivity: J. Geng, X. Wei, B. He, Y. Hao, J. Qu and B. Wang, *Molecules*, 2023, **28**, 4279.

88 J. Zhang, Y. Zhang, L. Lin, Q. Yao, X. Liua and X. Feng, *Chem. Commun.*, 2015, **51**, 10554.

89 J. Wang, H. Chen, L. Kong, F. Wang, Y. Lan and X. Li, *ACS Catal.*, 2021, **11**, 9151.

90 For recent reviews, see: (a) Y. He, J. Chen, X. Jiang and S. Zhu, *Chin. J. Chem.*, 2022, **40**, 651; (b) X. Yin, S. Li, K. Guo, L. Song and X. Wang, *Eur. J. Org. Chem.*, 2023, e202300783; (c) X.-Y. Sun, B.-Y. Yao, B. Xuan, L.-J. Xiao and Q.-L. Zhou, *Chem. Catal.*, 2022, **2**, 3140.

91 X.-W. Gu, Y.-L. Sun, J.-L. Xie, X.-B. Wang, Z. Xu, G.-W. Yin, L. Li, K.-F. Yang and L.-W. Xu, *Nat. Commun.*, 2020, **11**, 2904.

92 F. Sun, T. Wang, G.-J. Cheng and X. Fang, *ACS Catal.*, 2021, **11**, 7578.

93 S. Barik, S. Shee, S. Das, R. G. Gonnade, G. Jindal, S. Mukherjee and A. T. Biju, *Angew. Chem., Int. Ed.*, 2021, **60**, 12264.

94 H.-C. Liu, H.-Y. Tao, H. Cong and C.-J. Wang, *J. Org. Chem.*, 2016, **81**, 3752.

95 Y. Wu, B. Xu, B. Liu, Z.-M. Zhang and Y. Liu, *Org. Biomol. Chem.*, 2019, **17**, 1395.

96 S. Zhang, Z.-H. Luo, W.-T. Wang, L. Qian and J.-Y. Liao, *Org. Lett.*, 2022, **24**, 4645.

97 H. Wang, Y. Wei, Y. Li, S. Long, L.-J. Sun, S. Li and Y.-W. Lin, *Org. Lett.*, 2022, **24**(36), 6494.

98 W.-T. Wang, S. Zhang, W. Lin, Z.-H. Luo, D. Hu, F. Huang, R. Bai, Y. Lan, L. Qian and J.-Y. Liao, *Org. Chem. Front.*, 2024, **11**, 3308.

99 (a) E. J. Corey, S. Sarshar and D.-H. Lee, *J. Am. Chem. Soc.*, 1994, **116**, 12089; (b) K. Uemae, S. Masuda and Y. Yamamoto, *J. Chem. Soc., Perkin Trans. 1*, 2001, 1002.

100 M. Barday, J. Rodrigues, P. Bouillac, J. Rodriguez, M. Amatore and T. Constantieux, *Adv. Synth. Catal.*, 2023, **365**, 148.

101 J. W. Zhang, J.-H. Xu, D.-J. Cheng, C. Shi, X.-Y. Liu and B. Tan, *Nat. Commun.*, 2016, **7**, 10677.

102 L.-L. Zhang, J.-W. Zhang, S.-H. Xiang, Z. Guo and B. Tan, *Org. Lett.*, 2018, **19**, 6022.

103 C. Parida, S. K. Dave, K. Das and S. C. Pan, *Adv. Synth. Catal.*, 2023, **365**, 1185.

104 D. Liang, J.-R. Chen, L.-P. Tan, Z.-W. He and W.-J. Xiao, *J. Am. Chem. Soc.*, 2022, **144**, 6040.

105 F. Huang, L.-F. Tao, J. Liu, L. Qian and J.-Y. Liao, *Chem. Commun.*, 2023, **59**, 4487.

106 H. Jiang, X.-K. He, X. Jiang, W. Zhao, L.-Q. Lu, Y. Cheng and W.-J. Xiao, *J. Am. Chem. Soc.*, 2023, **145**, 6944.

107 T. Liang, Y. Wu, J. Sun, M. Li, H. Zhao, J. Zhang, G. Zheng and Q. Zhang, *Chin. J. Chem.*, 2023, **41**, 3253.

108 Y. Wang, R. Mi, S. Yu and X. Li, *ACS Catal.*, 2024, **14**, 4638.

109 Y. Liu, L. Yuan, L. Dai, Q. Zhu, G. Zhong and X. Zeng, *J. Org. Chem.*, 2024, **11**, 7630.

110 Y.-D. Shao, D.-D. Han, W.-Y. Maa and D.-J. Cheng, *Org. Chem. Front.*, 2020, **7**, 2255.

111 S. Lu, J.-Y. Ong, H. Yang, S. B. Poh, X. Liew, C. S. D. Seow, M. W. Wong and Y. Zhao, *J. Am. Chem. Soc.*, 2019, **141**, 17062.

112 Y.-S. Jang, Ł. Woźniak, J. Pedroni and N. Cramer, *Angew. Chem., Int. Ed.*, 2018, **57**, 12901.

113 L. Pang, Q. Sun, Z. Huang, G. Li, J. Liu, J. Guo, C. Yao, J. Yu and Q. Li, *Angew. Chem., Int. Ed.*, 2022, **61**, e202211710.

114 L. Pang, C. Wang, C. Ma, J. Liu, M. Shi, C. Yao, J. Yu and Q. Li, *Org. Lett.*, 2023, **25**, 7705.

115 J. Li, Y. Yan, X. Chen, Z. Huang and Y. Huang, *Chem. Sci.*, 2024, **15**, 6943.

116 X. Bi, J. Feng, X. Xue and Z. Gu, *Org. Lett.*, 2021, **23**, 3201.

117 Y. Guo, M.-M. Liu, X. Zhu, L. Zhu and C. He, *Angew. Chem., Int. Ed.*, 2021, **60**, 13887.

118 C. Li, S.-Z. Cai, J. Ye and X. Fang, *Org. Lett.*, 2024, **18**, 3867.

119 H. Koide, T. Hata and M. Uemura, *J. Org. Chem.*, 2002, **67**, 1929.

120 K. Kamikawa, S. Arae, W.-Y. Wu, C. Nakamura, T. Takahashi and M. Ogasawara, *Chem. – Eur. J.*, 2015, **21**, 4954.

121 P.-C. Zhang, Y.-L. Li, J. He, H.-H. Wu, Z. Li and J. Zhang, *Nat. Commun.*, 2021, **12**, 4609.

122 Y. An, X.-Y. Zhang, Y.-N. Ding, Y. Li, X.-Y. Liu and X.-Y. Liu, *Org. Lett.*, 2022, **24**, 7294.

123 J. Ye, L. Li, Y. You, C. Jiao, Z. Cui, Y. Zhang, S. Jia, H. Cong, S. Liu, H.-G. Cheng and Q. Zhou, *JACS Au*, 2023, **3**, 384.

124 (a) V. Dočekal, F. Koucký, I. Císařová and J. Veselý, *Nat. Commun.*, 2024, **15**, 3090; (b) M.-L. Delcourt, S. Felder, E. Benedetti and L. Micouin, *ACS Catal.*, 2018, **8**, 6612–6616.

125 D. Ly, J. Basca and H. M. L. Davies, *ACS Catal.*, 2024, **14**, 6423–6431.

126 L. Wang, S. Li, M. Blümel, A. R. Philipps, A. Wang, R. Puttreddy, K. Rissanen and D. Enders, *Angew. Chem., Int. Ed.*, 2016, **55**, 11110.

127 C. Min, Y. Lin and D. Seidel, *Angew. Chem., Int. Ed.*, 2017, **56**, 15353.

128 Y. Li, X.-Y. Duan, C. Yang, Y. Wei, J. Li, X. Ren and J. Qi, *J. Org. Chem.*, 2023, **88**, 11299.

129 S. S. Ranganathappa, B. S. Dehury, G. K. Singh, S. Shee and A. T. Biju, *ACS Catal.*, 2024, **14**, 6965.



130 S.-J. Wang, X. Wang, X. Xin, S. Zhang, H. Yang, M. W. Wong and S. Lu, *Nat. Commun.*, 2024, **15**, 518.

131 (a) J. Rodriguez and D. Bonne, *Chem. Commun.*, 2019, **55**, 11168; (b) W. Qin, Y. Liu and H. Yan, *Acc. Chem. Res.*, 2022, **55**, 2780.

132 for a pioneer contribution, see: M. Furusawa, K. Arita, T. Imahori, K. Igawa, K. Tomooka and R. Irie, *Tetrahedron Lett.*, 2013, **54**, 7107.

133 A. Huang, L. Zhang, D. Li, Y. Liu, H. Yan and W. Li, *Org. Lett.*, 2019, **21**, 95.

134 W. Zhang, S. Wei, W. Wang, J. Qu and B. Wang, *Chem. Commun.*, 2021, **57**, 6550.

135 S. Huang, H. Wen, Y. Tian, P. Wang, W. Qin and H. Yan, *Angew. Chem., Int. Ed.*, 2021, **60**, 21486.

136 S. Xu, A. Huang, Y. Yang, Y. Wang, M. Zhang, Z. Sun, M. Zhao, Y. Wei, G. Li and L. Hong, *Org. Lett.*, 2022, **24**, 2978.

137 B.-B. Gou, Y. Tang, Y.-H. Lin, L. Yu, Q.-S. Jian, H.-R. Sun, J. Chen and L. Zhou, *Angew. Chem., Int. Ed.*, 2022, **61**, e202208174.

138 (a) S.-G. Li, Y.-T. Wang, Q. Zhang, K.-B. Wang, J.-J. Xue, D.-H. Li, Y.-K. Jing, B. Lin and H.-M. Hua, *Org. Lett.*, 2020, **22**, 7522; (b) Q.-F. He, Z.-L. Wu, X.-J. Huang, T.-Q. Xia, G. Tang, W. Tang, L. Shi, W.-C. Ye and Y. Wang, *J. Org. Chem.*, 2021, **86**, 5870.

139 (a) N. Di Iorio, G. Filippini, A. Mazzanti, P. Righi and G. Bencivenni, *Org. Lett.*, 2017, **19**, 6692; (b) For a pioneer observation of a dynamic equilibration in C(sp<sup>2</sup>)-C(sp<sup>3</sup>) stereogenic dihydropyridines, see: O. Quinonero, M. Jean, N. Vanthuyne, C. Roussel, D. Bonne, C. Constantieux, C. Bressy, X. Bugaut and J. Rodriguez, *Angew. Chem., Int. Ed.*, 2016, **55**, 1401.

140 G. Bertuzzi, V. Corti, J. A. Izzo, S. Ričko, N. I. Jessen and K. A. Jørgensen, *J. Am. Chem. Soc.*, 2022, **144**, 1056.

141 P. Liu, X. Bao, J.-V. Naubron, S. Chentouf, S. Humbel, N. Vanthuyne, M. Jean, L. Giordano, J. Rodriguez and D. Bonne, *J. Am. Chem. Soc.*, 2020, **142**, 16199.

142 V. S. Raut, M. Jean, N. Vanthuyne, C. Roussel, T. Constantieux, C. Bressy, X. Bugaut, D. Bonne and J. Rodriguez, *J. Am. Chem. Soc.*, 2017, **139**, 2140.

143 A. Gaucherand, E. Yen-Pon, D. García-López, J.-V. Naubron, S. Chentouf, M. Giorgi, S. Humbel, M. Jean, J. Rodriguez and D. Bonne, *Chem. Sci.*, 2024, **15**, 7300.

144 C. Li, Y.-B. Shao, X. Gao, Z. Ren, C. Guo, M. Li and X. Li, *Nat. Commun.*, 2023, **14**, 3380.

145 W. Liu, T. Qin, W. Xie, J. Zhou, Z. Ye and X. Yang, *Angew. Chem., Int. Ed.*, 2023, **62**, e202303430.

146 S. Jia, S. Li, Y. Liu, W. Qin and H. Yan, *Angew. Chem., Int. Ed.*, 2019, **58**, 18496.

147 X. Liu, B. Zhu, X. Zhang, H. Zhu, J. Zhang, A. Chu, F. Wang and R. Wang, *Nat. Commun.*, 2024, **15**, 732.

148 T. Shibata, M. Otomo, Y.-K. Tahara and K. Endo, *Org. Biomol. Chem.*, 2008, **6**, 4296.

149 For reviews on CA-RE of alkynes with alkenes: (a) S.-I. Kato and F. Diederich, *Chem. Commun.*, 2010, **46**, 1994; (b) T. Michinobu and F. Diederich, *Angew. Chem., Int. Ed.*, 2018, **57**, 3552.

150 W. Xiao, F. Li, X. Liu, W. Cao and X. Feng, *Org. Lett.*, 2023, **25**, 8005.

151 F. Wang, J. Jing, Y. Zhao, X. Zhu, X.-P. Zhang, L. Zhao, P. Hu, W.-Q. Deng and X. Li, *Angew. Chem., Int. Ed.*, 2021, **60**, 16628.

152 For a recent review, see: S. Du, A.-X. Zhou, R. Yang, X.-R. Song and Q. Xiao, *Org. Chem. Front.*, 2021, **8**, 6760.

153 Z. Li, V. Boyarskikh, J. H. Hansen, J. Autschbach, D. G. Musaev and H. M. L. Davies, *J. Am. Chem. Soc.*, 2012, **134**, 15497.

154 Y. Liu, X. Liu, H. Hu, J. Guo, Y. Xia, L. Lin and X. Feng, *Angew. Chem., Int. Ed.*, 2016, **55**, 4054.

155 G. Xu, Z. Wang, Y. Shao and J. Sun, *Org. Lett.*, 2021, **23**, 5175.

156 S.-Q. Yang, Y.-F. Wang, W.-C. Zhao, G.-Q. Lin and Z.-T. He, *J. Am. Chem. Soc.*, 2021, **143**, 7285.

157 F.-H. Zhang, X. Guo, X. Zeng and Z. Wang, *Nat. Commun.*, 2022, **13**, 5036.

158 A. Hossain, R. L. Anderson, C. S. Zhang, P.-J. Chen and G. C. Fu, *J. Am. Chem. Soc.*, 2024, **146**, 7173.

159 Z. Wang, H. Yin and G. C. Fu, *Nature*, 2018, **563**, 379.

160 G. Wang, X. Liu, Y. Chen, J. Yang, J. Li, L. Lin and X. Feng, *ACS Catal.*, 2016, **6**, 2482.

161 J. Zhang, X. Huo, J. Xiao, L. Zhao, S. Ma and W. Zhang, *J. Am. Chem. Soc.*, 2021, **143**, 12622.

162 J. Zhang, Y. Luo, E. Zheng, X. Huo, S. Ma and W. Zhang, *J. Am. Chem. Soc.*, 2024, **146**, 9241.

163 For a recent review, see: T. T. Nguyen, *Org. Biomol. Chem.*, 2023, **21**, 252.

164 W. Zhang, S. Zheng, N. Liu, J. B. Werness, I. A. Guzei and W. Tang, *J. Am. Chem. Soc.*, 2010, **132**, 3664.

165 H. Qian, X. Yu, J. Zhang and J. Sun, *J. Am. Chem. Soc.*, 2013, **135**, 18020.

166 D. Qian, L. Wu, Z. Lin and J. Sun, *Nat. Commun.*, 2017, **8**, 567.

167 M. Chen, D. Qian and J. Sun, *Org. Lett.*, 2019, **21**, 8127.

168 P. Zhang, Q. Huang, Y. Cheng, R. Li, P. Li and W. Li, *Org. Lett.*, 2019, **21**, 503.

169 L. Zhang, Y. Han, A. Huang, P. Zhang, P. Li and W. Li, *Org. Lett.*, 2019, **21**, 7415.

170 J. Yang, Z. Wang, Z. He, G. Li, L. Hong, W. Sun and R. Wang, *Angew. Chem., Int. Ed.*, 2020, **59**, 642.

171 A. G. Woldegiorgis, Z. Han and X. Lin, *Org. Lett.*, 2021, **23**, 6606.

172 F. Li, S. Liang, Y. Luan, X. Chen, H. Zhao, A. Huang, P. Li and W. Li, *Org. Chem. Front.*, 2021, **8**, 1243.

173 J. Wang, S. Zheng, S. Rajkumar, J. Xie, N. Yu, Q. Peng and X. Yang, *Nat. Commun.*, 2020, **11**, 5527.

174 T. Hashimoto, K. Sakata, F. Tamakuni, M. J. Dutton and K. Maruoka, *Nat. Chem.*, 2013, **5**, 240.

175 C. T. Mbofana and S. J. Miller, *J. Am. Chem. Soc.*, 2014, **136**, 3285.

176 Y. Hu, W. Shi, B. Zheng, J. Liao, W. Wang, Y. Wu and H. Guo, *Angew. Chem., Int. Ed.*, 2020, **59**, 19820.

177 J. Seayad and B. List, *Org. Biomol. Chem.*, 2005, **3**, 719.

178 A. Tap, A. Blond, V. N. Wakchaure and B. List, *Angew. Chem., Int. Ed.*, 2016, **55**, 8962.

